

A NUMERICAL SIMULATION OF NEARLY INCOMPRESSIBLE,  
STABLY STRATIFIED ATMOSPHERIC TURBULENT DIFFUSION

A THESIS

Presented to

The Faculty of the Graduate Division

by

James Edward Hicks

In Partial Fulfillment

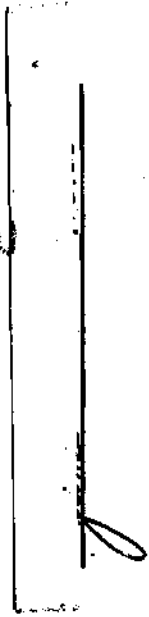
of the Requirements for the Degree

Doctor of Philosophy in the School of Aerospace Engineering

Georgia Institute of Technology

September 1971

In presenting the dissertation as a partial fulfillment of the requirements for an advanced degree from the Georgia Institute of Technology, I agree that the Library of the Institute shall make it available for inspection and circulation in accordance with its regulations governing materials of this type. I agree that permission to copy from, or to publish from, this dissertation may be granted by the professor under whose direction it was written, or, in his absence, by the Dean of the Graduate Division when such copying or publication is solely for scholarly purposes and does not involve potential financial gain. It is understood that any copying from, or publication of, this dissertation which involves potential financial gain will not be allowed without written permission.

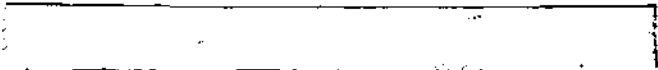




7/25/68

A NUMERICAL SIMULATION OF NEARLY INCOMPRESSIBLE,  
STABLY STRATIFIED ATMOSPHERIC TURBULENT DIFFUSION

Approved:

  
Chairman *J*

  
  
  
Date approved by Chairman: 8/18/71

## ACKNOWLEDGMENTS

I wish to express my deepest appreciation to Dr. C. G. Justus, my thesis advisor, for his suggestion of the problem and his continued interest in it, as well as his invaluable counsel and guidance during the course of the research. The interest of Dr. R. G. Roper is also gratefully acknowledged. Dr. Justus, Dr. Roper and Dr. L. H. Bangert are due special thanks for their careful reading of the manuscript.

This work was supported by the National Aeronautics and Space Administration through Grant NGL-11-002-004 and the National Science Foundation through Grant GA-29213. The assistance of Dr. H. D. Edwards and Dr. C. G. Justus, directors of these projects at Georgia Institute of Technology, is appreciated. The financial assistance of the U. S. Department of Health, Education and Welfare, through an NDEA Title IV Fellowship, is also acknowledged.

## TABLE OF CONTENTS

	Page
ACKNOWLEDGMENTS . . . . .	ii
LIST OF TABLES . . . . .	v
LIST OF FIGURES . . . . .	vi
LIST OF SYMBOLS . . . . .	viii
SUMMARY . . . . .	xi
Chapter	
I. INTRODUCTION . . . . .	1
Description of Turbulent Diffusion	
Methods of Previous Research	
Purposes and Methods of Present Research	
II. DYNAMICS OF TURBULENT DIFFUSION MODEL . . . . .	12
III. ANALYSIS OF SPACE-TIME CORRELATED TURBULENT ACCELERATION FIELD . . . . .	25
Analysis of the Relative Motion of Two Fluid Points	
Analysis of the Motion of a Single Fluid Point	
Explicit Correlation Over One Time Interval	
Explicit Correlation Over Two Time Intervals	
Analysis of the Eulerian Correlations	
IV. OBSERVED CHARACTERISTICS OF THE DIFFUSION SIMULATION AND COMPARISON WITH PREVIOUS RESULTS . . . . .	37
Simulation of One and Two Dimensional Eddy Diffusion	
Simulation of Three-Dimensional Turbulent Diffusion	
Single Fluid Point Analysis	
Neutral Density Stratification ( $\Gamma = 0$ )	
Stable Density Stratification ( $\Gamma > 0$ )	
Unstable Density Stratification ( $\Gamma < 0$ )	
Analysis Maintaining Explicit Eulerian Correlations Over Two Time Step Increments	

Chapter	Page
IV. (continued)	
Point Pair Analysis	
Neutrally Stratified Atmospheres	
Stably Stratified Atmospheres	
Unstable Stratified Atmospheres	
V. CONCLUSION AND RECOMMENDATIONS . . . . .	96
BIBLIOGRAPHY . . . . .	100
VITA . . . . .	103

## LIST OF TABLES

Table		Page
1.	Statistical Properties of the Diffusion of a Single Fluid Point . . . . .	53
2.	Lagrangian Velocity Characteristics of the Diffusion of a Single Fluid Point . . . . .	61
3.	Comparison of the Statistical Characteristics of the Diffusion of a Single Fluid Point for $CI = 1$ and $CI = 2$ ( $\Gamma = 10^{-2}$ , $K_x = 1$ ) . . . . .	74
4.	Statistical Properties of the Relative Diffusion of Two Fluid Points . . . . .	81
5.	Lagrangian Velocity Characteristics of the Relative Diffusion of Two Fluid Points . . . . .	87

## LIST OF FIGURES

Figure		Page
1.	Eulerian Acceleration Correlation Function . . . . .	34
2.	Fluid Point Dispersion Through Background Acceleration Field with Zero Length and Time Correlation Scales . . . . .	46
3.	Fluid Point Dispersion Through Acceleration Field with Finite Correlation Scales . . . . .	48
4.	Lagrangian Velocity Time Correlation, Finite Eulerian Correlation Scales . . . . .	49
5.	Fluid Point Dispersion Through a Field with Moderate Mean Wind Shear . . . . .	51
6.	Variation of $C_x^3$ with Shear . . . . .	52
7.	Variation of $D_y$ with Shear and Temperature Stratification <sup>y</sup> . . . . .	57
8.	Influence of Mean Wind Shears and Temperature Stratifications on Anisotropy of Turbulent Velocity Field . . . . .	59
9.	Fluid Point Dispersion Through Field with Moderately Stable Temperature Stratification . . . . .	60



Figure	Page
10. Fluid Point Dispersion Through a Field with Moderate Shear and Stable Temperature Stratification . . . . .	65
11. Lagrangian Velocity Time Correlations, Moderate Shear and Temperature Stratification . . . . .	66
12. Variation of $C_x^2$ with Shear . . . . .	68
13. Fluid Point Dispersion Through an Unsteady Stratified Field . . . . .	70
14. Fluid Point Dispersion Through Field with Moderate Shear and Stable Temperature Stratification, Maintaining Explicit Eulerian Correlations over 2 Time Steps . . .	72
15. Lagrangian Time Correlation, $CI = 2$ . . . . .	73
16. Point Pair Dispersion Through Acceleration Field with Finite Length and Time Correlation Scales . . . .	77
17. Lagrangian Space-Time Correlations ( $\tau = 0$ ) . . . . .	80
18. Point Pair Dispersion Through Field with Moderate Shear . . . . .	85
19. Variation of $C_x^3$ with Shear, Point Pair Analysis . . .	86
20. Point Pair Dispersion Through Field with Moderate Shear and Stable Temperature Stratification . . . . .	91
21. Variation of $C_x^2$ with Shear, Point Analysis . . . . .	93
22. Point Pair Dispersion with Initial Separation in Direction of Shear . . . . .	95

## LIST OF SYMBOLS

$a_{ij}$	space-time correlated turbulent pressure acceleration component
$c$	r-m-s turbulent acceleration component magnitude
$C_x^2, C_x^3$	coefficients in second and third power law dependences, respectively, of shear-dominated fluid point dispersion
CI	number of time steps over which Eulerian acceleration correlations are explicitly maintained
D	eddy diffusivity
g	acceleration of gravity
K	$(k-1)/k$ , where $k$ is the ratio of specific heats $c_p/c_v$
$K_i$	mean wind shear ( $\partial \bar{U}_i / \partial z$ )
L	number of initial separations (point pair analysis) or characteristic lengths (single particle analysis) per Eulerian length scale
$L_e$	integral length scale of the (Eulerian) turbulent acceleration correlations
p	thermodynamic pressure
$R_i$	relative point pair separation component
$\hat{w}_i$	Lagrangian velocity correlation
$t, t_k$	time, time step level
T	thermodynamic temperature
$T_e$	integral time scale of the (Eulerian) turbulent acceleration correlations

$T_L$	integral time scale of the Lagrangian turbulent velocity correlations
TL	number of time steps per Eulerian time scale
$u_i$	Lagrangian turbulent velocity component
$U_i$	Lagrangian total velocity component
w	vertical component of turbulent velocity
$X_i$	fluid point separation component
$y_i, z_i$	pseudo-random numbers drawn from a normal distribution
$\alpha_{ij}, \beta_{ij}$	coefficients of turbulent acceleration correlation equations
$\gamma$	atmospheric lapse rate
$\Gamma$	logarithmic potential temperature gradient
$\Gamma_d$	dry adiabatic lapse rate ( $9.8^\circ \text{ C/km}$ )
$\epsilon$	viscous dissipation
$\theta$	potential temperature
$\nu$	kinematic viscosity
$\nu_{ij}$	space-time correlated turbulent pressure acceleration component
$\rho_{ij}$	Eulerian space-time acceleration correlation component
$\rho_{uw}, \rho_{vw}$	turbulent velocity cross correlations
$\rho_{zw}$	temperature-velocity cross correlations
$\sigma$	standard deviation of a statistical average
$\omega$	viscous damping coefficient

$D/Dt$	total derivative operator
$\nabla$	gradient operator
$\nabla^2$	Laplacian operator
$(\sim)$	denotes a vector
$(\bar{\quad}) , (\quad)_0$	denotes a mean component
$(\quad)'$	denotes a perturbation component
$\langle (\quad) \rangle$	denotes an ensemble average

## SUMMARY

A numerical simulation of atmospheric turbulent diffusion is presented in which marked fluid points and point pairs are followed as they undergo three dimensional random walks in a background field of space-time correlated turbulent accelerations. A hybrid Eulerian-Lagrangian technique is employed in which fluid accelerations at each time step are evaluated at the position of the fluid point using an Eulerian analysis; the fluid point trajectory and position coordinates for the subsequent time interval are then evaluated in Lagrangian coordinates. Included in the fluid point equations of motion are the effects of a linear mean wind shear and potential temperature gradient and a Stokes type viscous damping. The correlated random accelerations are taken to represent the turbulent pressure force terms of these equations of motion and are determined from a stationary, homogeneous, isotropic Eulerian space-time correlation function with Gaussian time and longitudinal spatial correlations. The distribution function of the random accelerations is taken to be Gaussian. Cross correlations between different acceleration components at the same time are neglected.

Various statistical characteristics of the resulting particle dispersion are presented and compared with corresponding characteristics of turbulent diffusion as proposed by previous researchers.

Observed results indicate that the technique successfully simulates stably-stratified shear-dependent atmospheric turbulent diffusion and should prove to be a useful tool for studying the dispersal

of pollutants in the earth's atmosphere as well as the general problem of the relation between Lagrangian and Eulerian statistics.

Evidence is presented regarding the effects of vertical gradients of the horizontal mean winds, temperature stratification, initial separation (for the point pair studies) and the space and time scale of the acceleration correlations upon the characteristics of the modeled diffusion. Several major conclusions are drawn.

1. Both the short and the long time behavior of the fluid point displacements in a neutrally stratified atmosphere with uniform mean winds were successfully modeled. The turbulent velocity components were observed to have a Lagrangian time correlation scale somewhat greater than the Eulerian time correlation scale of the acceleration field and to be stationary for appropriate choices for the viscous damping parameter and the mean square initial velocity component magnitude. The influence of the initial conditions did not appear to extend as far in time for the relative dispersal of two fluid points as for the single fluid point. This effect is due to the influence of the initial correlation between the two fluid points. An intermediate time transition period was evident in these studies which appeared to be the result of the combination of the influences of Lagrangian acceleration correlations (tending to result in mean-square particle separations varying as the fourth power of the time) and a Richardson-type diffusion (tending to result in mean-square separations varying as the cube of the time).

2. Mean wind shears tended to increase the diffusion in the direction controlled by shear such that the mean square particle displacements in that direction varied as the cube of the time for times after release longer than the correlation time scale.

3. Stable temperature stratifications resulted in decreased diffusion in the vertical. Sufficiently stable stratifications were observed to completely inhibit the vertical diffusion and led to a "leveling off" of the vertical mean square particle displacements at values which decreased with further increases in stability. This buoyancy-induced effect was also evident in the vertical component of the mean square turbulent velocity and appeared to result in decreased diffusion in the direction dominated by shear and increased cross shear diffusion. Sufficiently stable temperature stratifications appeared to reduce the  $t^3$  dependence of these components back toward the eddy diffusion otherwise expected.

4. The inhibited vertical dispersion due to stable stratification and the enhanced horizontal dispersion due to mean wind shears thus both contribute to a highly anisotropic diffusion, despite the model assumption of an isotropic turbulent pressure acceleration field.

## CHAPTER I

## INTRODUCTION

Description of Turbulent Diffusion

Turbulent fluid flows are characterized generally by unsteady, dissipative, rotational motions, which may be considered as a superposition of eddies of widely varying scales. The turbulent velocity field exhibits random yet continuous variations which have derivatives in both space and time and correlations over length and time scales comparable with the characteristic lengths and times of the flow. This wide continuous variation of scale, or spectrum, of turbulent motions gives rise to a diffusion of mixing process which appears to be the result of a continuum phenomenon, in contrast to the Brownian motion underlying molecular diffusion, and which is much more vigorous and effective than molecular diffusion.

Now, a complete solution of the full non-linear equations of motion for turbulent flow has never been obtained; and the turbulent velocity and pressure fields of no laboratory experiment have ever been described in detail. For these reasons and because for most purposes one does not require detailed information of the flow, one relies on statistical methods of description. Thus, any discussion of turbulence would involve statistical averages of pertinent fluid flow parameters. To be most meaningful, these should be ensemble averages, taken over a number of realizations of the flow field with identical macroscopic



conditions.

There are various ways of categorizing turbulent flows. One system is based on the way the turbulence is generated. Turbulence can be generated in shear layers, either along solid boundaries or between layers of fluid with different velocities. These would be called, respectively, wall, shear turbulence and free, shear turbulence. Turbulence may also be generated through unstable fluid stratification, called instability turbulence, and through the flow of a stream through a grid of bars, called grid turbulence. Only shear-induced turbulence can sustain itself.

Another meaningful method of categorizing turbulence is through the statistical properties of the turbulent velocity field. Turbulent flow fields in which the statistical properties are independent of the particular position in the field are called homogeneous. If the statistical field properties are independent of direction, the turbulence is isotropic. If the mean velocity field has a gradient, a mean shear stress is produced and the turbulence cannot be strictly isotropic; but, if the mean shear is constant, the turbulence may be homogeneous. If the statistical properties are independent of time, the turbulence is stationary.

Turbulence occurring in the atmosphere is generally non-stationary, nonhomogeneous, nonisotropic, free, shear turbulence.

The statistical properties of the turbulent mixing which results from a particular field of turbulence should depend on the statistical properties of the turbulence and may also depend on certain properties

of the mean flow, for example, gradients in the mean velocity; in this case in particular mean wind shears could stretch parcels of fluid and contribute significantly to the dispersion. This double action is a commonly observed characteristic of turbulent dispersion and has been noticed since Reynolds original observations of turbulent pipe flow. In the atmosphere other phenomena, such as the density stratification, may also significantly alter the observed turbulent diffusion. Since these phenomena generally have a preferred direction associated with them, it is to be expected that one of their most significant effects would be to contribute to the anisotropy of the diffusion.

Any fluid flow field is most simply analyzed in an Eulerian coordinate system, in which flow properties are considered at fixed points in space. Eulerian time correlations describe changes at a fixed point with time, and Eulerian space correlations relate changes at two fixed points in the field. The most straightforward analysis of diffusion, however, uses a Lagrangian approach, in which a marked fluid element is followed in its wandering through the flow field. Lagrangian time correlations describe changes in the fluid element velocity with time as the fluid element travels along its trajectory. Lagrangian space-time correlations would describe changes with time in the correlations of the velocities of two fluid elements as each wandered along its streamline. Both the Lagrangian time and space-time correlations apparently combine features of the Eulerian space and time correlations. However, no general relation linking Eulerian and Lagrangian correlations has ever been deduced, nor is it intuitively obvious that such a relation

should exist in the general case of non-stationary, nonhomogeneous turbulence.

Recent interest in environmental pollution control has made a basic knowledge of turbulent atmospheric dispersion a critical need. In particular, information is needed on such parameters as the space and time scales for transition between various modes of diffusion, the Lagrangian velocity correlations, and large scale eddy diffusion coefficients. The dependence of these parameters on such characteristics of the turbulent field as its space and time scales and such mean flow characteristics as the density stratification and mean wind profile need clarification.

#### Methods of Previous Research

The inherent three-dimensional, unsteady, non-linear nature of the equations of motion of a turbulent fluid has prompted previous research into the simple examples of turbulence. However, even in the case of stationary homogeneous isotropic turbulence in an incompressible fluid, complete solutions have not been obtained for the correlation and energy spectrum functions, nor for their variations with time.

Taylor [1920] developed a fundamental approach to the statistical theory of turbulent diffusion and derived relations for the mean square particle displacements in the limiting cases of very small and very large times after release. Taylor considered the turbulent velocity correlations of a single fluid point, released with some initial velocity into a homogeneous isotropic medium and found that the mean square displacement should increase with the square of the time for

small times after release and with the first power of time for times after release larger than an integral time scale  $T_L$  of the velocity correlation  $R_\xi$ ,

$$T_L = \lim_{t \rightarrow \infty} \int_0^t R_\xi d\xi \quad (1.1)$$

and found that an eddy diffusion coefficient  $D$  could be defined by

$$\langle X^2 \rangle = 2 D t \quad (t \gg T_L) \quad (1.2)$$

where

$$D = \langle u^2 \rangle T_L \quad (1.3)$$

with  $\langle u^2 \rangle$  the mean square fluid point velocity.

Batchelor [1950] applied the similarity theory of Kolmogorov [1941] to the problem of the relative dispersion of two fluid points released a distance  $l_0$  apart in a field of homogeneous isotropic turbulence and found that in a suitably intermediate range of eddy sizes and times after release, the mean square particle separation should vary as the product of the viscous dissipation with the cube of the time, or, alternatively that the relative diffusion coefficient should vary as the 4/3 power of the scale of diffusion. This relation has been known as Richardson's law of dispersion since Richardson [1926] deduced it from several sets of empirical observations of atmospheric diffusion.

This statistical analysis, begun by Taylor, provides some

insight into the problem, but provides no information about the effects of many important mean flow characteristics on the diffusion, such as mean velocity and temperature gradients.

Recent attempts have been made to analyze the diffusion problem which include some of these mean flow characteristics by numerically integrating the full nonlinear Navier-Stokes equations; e.g., Harlow and Amsden [1968]. However, because of size and time limitations of even the largest and fastest computers now available, it appears that fully-developed turbulence cannot be calculated without the introduction of constitutive relations, which relate averages of the turbulent quantities to mean flow quantities [Harlow and Nakayama, 1967; Amsden and Harlow, 1968].

A different but more promising approach is that of recent attempts at simulating certain aspects of the turbulent field. One of the earlier attempts was that of Brier [1950] who considered the correlations between two particles undergoing discrete motion in one dimension. Both Lumley and Corrsin [1959] and Patterson and Corrsin [1965] have described computer simulations of diffusion in one dimension in which a binary random velocity field (i.e., velocity components =  $\pm 1$ ) was constructed on a grid in two dimensional x-space. Kraichnan [1970] simulated divergenceless, stationary, homogeneous, isotropic turbulent diffusion of two fluid particles with velocity fields determined from assumed spectrum functions.

Deardorff and Peskin [1970] have described a method which seems to combine features of the above simulation attempts with some of the techniques of the aforementioned integration of the Navier-Stokes

equations for the case of two fluid points difusing in a large Reynolds number shear flow. A semiempirical exponential form was constructed for the two point velocity correlations, and sub-grid scale Reynolds stresses were simulated by spatially and temporally variable eddy coefficients. Results indicated a  $t^3$  or steeper dependence for downstream mean square separation in the case of strong shear and Reynolds stress:

$$\langle (x_a - x_b)^2 \rangle = C t^3 \quad (1.4)$$

where the coefficient  $C$  appeared to obey

$$C \propto \left( \frac{\partial \bar{u}}{\partial x} \right)^2 \langle w^2 \rangle T_L \quad (1.5)$$

The single point and point pair velocity correlations were also computed; results indicated that the relationship between the single point Lagrangian time scale and downstream Eulerian length scale was (using Taylor's hypothesis) in good agreement with the ratio of Lagrangian time scale to Eulerian fixed point time scale ( $\beta = 4$ ) found by Hay and Pasquill [1959]. Results also indicated that the two particle velocity correlations for the same time decayed very slowly, with a time constant at least five times the Lagrangian single particle time scale. A point of possible criticism of this method is the exponential form of the assumed Eulerian velocity correlation function, which would appear to lead to infinite fluid point accelerations. (This would follow from the relation between the mean square turbulent acceleration and the

correlation microscale [Lumley and Panofsky, 1964] and the fact that the exponential correlation function would have no definable microscale).

A quite similar analysis [Lilly, 1966] considered the dispersion of fluid points in a field of large scale turbulence, such as might be encountered in the atmosphere. As a first-order approximation, the sub-grid scale Reynold's stresses were simulated, through an eddy viscosity hypothesis, by a product of the strain of the mean flow with a coefficient of eddy viscosity. The hypothesis is analogous to that in the mixing length theories, for the case of constant eddy viscosity.

Another similar theoretical analysis was that of Kao [1968] who considered the dispersion of particles in stratified atmospheres. The viscous force terms in the equations of motion were approximated by a Stokes frictional damping, and the buoyancy force terms were approximated by products of the vertical particle displacement with the negative of the (assumed constant) logarithmic potential temperature gradient  $\Gamma = (g/\theta) \partial\theta/\partial z$ . The Boussinesq approximation was used in that density fluctuations were assumed important only in the buoyancy force terms. Kao found that the temperature stratification was very important for the long time vertical diffusion. He found that the stratification effect leads to constant mean square particle displacements ("zero diffusion") for the stably stratified atmosphere ( $\Gamma > 0$ ), produces displacements proportional to time after release in the neutrally-stratified case ( $\Gamma = 0$ ), and makes for exponentially-increasing displacements in the unstable case ( $\Gamma < 0$ ).

A different approach to the statistical analysis begun by Taylor has been described by Lin [1960 a,b], who considered the correlated

turbulent accelerations of fluid points in homogeneous turbulence, in a manner similar to Taylor's work with correlated velocities. Lin's results indicated that, for the relative diffusion of two fluid points released with zero initial velocity, the mean square relative displacement was zero for very small times after release; and varied as the cube of the time for suitably intermediate times after release, or, alternatively, that the relative diffusion coefficient varied as the  $4/3$  power of the scale of diffusion in these intermediate times, essentially obeying Richardson's law of dispersion. The negligible diffusion at very small times after release appears to be directly attributable to the fact that non-zero initial fluid point velocities could not be considered in Lin's analysis.

#### Purposes and Methods of Present Research

It was recognized from the analysis of Richardson [1926] that certain similarities exist between the random motions of molecules and random fluctuations in turbulence, even though turbulent diffusion is several factors of ten more effective than molecular diffusion. Attempts to analyze turbulence by considering the similarities with molecular processes and by the use of eddy parameters (e.g., Prandtl [1926]) suggest that a model of turbulent diffusion might be constructed which is based on the model of molecular diffusion. One of the basic differences in the two models, however, would be the non-zero correlations of the turbulent velocity fluctuations over time and length scales comparable to the characteristic times and lengths of the modeled turbulent flow.



Now, there is a striking similarity between Lin's work and pioneering work in Brownian motion theory by Einstein [1905] who considered the random walk of molecules subjected to a completely random (uncorrelated) fluctuating force  $F(t)$  described by the equation

$$m \frac{Du}{Dt} = F(t) - fu \quad (1.6)$$

where  $u$  is the fluctuating velocity of the molecule of mass  $m$  and where  $-fu$  is a frictional damping term proportional to the molecular velocity.

It would appear, then, that a model of turbulent diffusion might be constructed, in a manner similar to that in Brownian motion, if the motions of certain marked fluid elements were considered to be described by equations analogous to the above. The term corresponding to  $F(t)$  would then be taken as the correlated fluctuating turbulent pressure force. Single fluid points or point pairs could then be followed as they undergo three dimensional random walks in a background field of space-time correlated turbulent accelerations for which an Eulerian correlation has been modeled.

If shear-induced convective accelerations and buoyancy forces were included in the fluid point equations of motion, the model could be used to evaluate the effects upon the diffusion properties of various profiles and magnitudes of wind shears and potential temperature gradients, and the results of this study could prove useful in developing better models for dispersal of atmospheric pollutants in the earth's atmosphere. This study should also provide information on the effects

on the diffusion of the space and time scales of the acceleration correlations, the initial separation of the particle pairs, and the magnitude of viscous damping. The study should also be useful in the general problem of the relation between the Lagrangian and Eulerian correlations.

## CHAPTER II

## DYNAMICS OF TURBULENT DIFFUSION MODEL

In a Lagrangian analysis of diffusion, we consider the motions of clusters of marked fluid points. We shall assume that the marked fluid points are dynamically indistinguishable from the surrounding fluid. According to a classical theorem of mechanics, the motion of such a cluster of marked fluid points may be resolved into the motion of the center of mass of the system of particles and the motion of individual particles relative to the center of mass. It is evident that the motion of the center of mass describes the motion of the cloud of particles as a whole, while the relative motion of the fluid points determines the change in shape of the cloud. The change of shape of the cluster is independent of the motion of its centroid.

To illustrate how the motion of a marked cluster could be resolved into the motion of its centroid plus the motion of particles relative to the centroid, consider for the moment the simple case of the one-dimensional motion of a cloud of  $N$  fluid points in a field of uniform flow with mean velocity  $U$ . Let the velocity of the  $i$ -th particle during the  $r$ -th time interval be given by

$$U_{ri} = U + u_{ri} \quad (i = 1, 2, \dots, N) \quad (2.1)$$

The total distance  $X_{ni}$  traveled by the  $i$ -th particle in  $n$  intervals is given by

$$X_{ni} = nU + u_{1i} + u_{2i} + u_{3i} + \dots + u_{ni} \quad (2.2)$$

where, for convenience, the time interval has been taken as unity.

At the end of  $n$  unit time intervals, define the standard deviation  $\sigma_n$  of the  $N$  particles by

$$\sigma_n^2 = \frac{1}{N-1} \sum_{i=1}^N (X_{ni} - \langle X_n \rangle)^2 \quad (2.3)$$

where

$$\langle X_n \rangle = \frac{1}{N} \sum_{i=1}^N X_{ni} \quad (2.4)$$

It may be easily shown that Equation (2.3) may be written as

$$\sigma_n^2 = \frac{1}{2N(N-1)} \sum_{i=1}^N \sum_{j=1}^N (X_{ni} - X_{nj})^2 \quad (2.5)$$

Thus, if any two particles  $i$  and  $j$  have a relative separation

$R_n = X_{ni} - X_{nj}$  from each other at the end of  $n$  time intervals, the quantity

$$R_n^2 = \left( X_{ni} - X_{nj} \right)^2 \quad (2.6)$$

can be used as an estimate of  $\sigma_n^2$ . Study of the change of  $\sigma_n^2$  with time is identical with study of how the mean square particle separation  $R_n^2$  changes with time.

Thus it is evident that the motion of the cluster of  $N$  particles may be resolved into the motion of the centroid, described by  $\langle X_n \rangle$ , and the motions of particles relative to the centroid, described by  $\sigma_n$ . It should also be evident that the motion of the centroid may be studied by analyzing the motion of a single fluid point, while the relative motions may be studied by analyzing the relative behavior of two fluid points.

Consider the trajectories of small elements of fluid ("fluid points") through a statistically stationary, homogeneous, isotropic, Eulerian space-time correlation acceleration field. Fluid point positions and velocities will be computed relative to a rectangular coordinate system translating with the mean wind velocity at the point of release. The coordinate system is assumed to be oriented such that the mean wind velocity lies in the x-y plane. The fluid is assumed to be "nearly incompressible" and to have constant vertical gradients of the potential temperature and horizontal mean wind components. The term "nearly incompressible" is taken here to characterize a flow having a divergenceless velocity field but a mean vertical density gradient such that wandering fluid elements may experience buoyancy accelerations. This approach is related to the Boussinesq approximation discussed by

Dutton and Fichtl [1969]. The velocity of each fluid point will vary according to

$$\rho \frac{DU}{Dt} = \tilde{F} \quad (2.7)$$

where  $\tilde{F}$  is the sum of the forces acting on the fluid point, which may include pressure, viscous damping and gravity. Thus

$$\frac{DU}{Dt} = -\frac{1}{\rho} \nabla p + \nu \nabla^2 \tilde{U} - g\hat{k} \quad (2.8)$$

Since the mean wind  $\bar{U}$  is assumed to have a linear variation, the mean components of the viscous term are zero. We assume, in a manner similar to that of Kao [1968], that the turbulent viscous term may be adequately modeled by a Stokes friction damping, i.e., assume that the wandering of each fluid point from the surrounding mean wind is resisted by a force proportional to the fluid point's velocity relative to the surrounding mean wind velocity:

$$\nu \nabla^2 \tilde{U} = \nu \nabla^2 \tilde{u} = -\omega (\tilde{U} - \bar{U}) = -\omega \tilde{u} \quad (2.9)$$

The use of the Stokes-type hypothesis for the viscous term, which may appear to be plausible as a first approximation, is, in the final analysis, a mathematical convenience and an aid to the solution of the equation of motion. However, the magnitude of the coefficient  $\omega$  is fixed by the

magnitude of the viscous dissipation  $\epsilon$  as  $\omega = \epsilon / \langle u^2 \rangle$ . Then by writing the velocity, pressure and density as sums of mean plus fluctuating parts, and expanding the substantial derivative, we may show that Equation (2.8) becomes (assuming  $\rho' \ll \rho_0$ )

$$\begin{aligned} \frac{\partial}{\partial t} (\bar{u} + \tilde{u}) + (\bar{u}_j + u_j) \frac{\partial}{\partial x_j} (\bar{u} + \tilde{u}) = & \quad (2.10) \\ & - \frac{1}{\rho_0} \left(1 - \frac{\rho'}{\rho_0}\right) \nabla (p_0 + p') - \omega \tilde{u} - g\hat{k} \end{aligned}$$

Now, if we take the mean of Equation (2.10), we have

$$\frac{\partial \bar{u}}{\partial t} + \bar{u}_j \frac{\partial \bar{u}}{\partial x_j} + \langle u_j \frac{\partial \tilde{u}}{\partial x_j} \rangle = - \frac{1}{\rho_0} \nabla p_0 - g\hat{k} \quad (2.11)$$

The last term on the left can be written, in the case of divergenceless flow, as the gradient of the Reynolds stresses, which are spatially invariant for homogeneous turbulent fields. Then, the vertical component of Equation (2.11) becomes (if we assume the vertical to be the only non-zero shear component):

$$\frac{\partial \bar{u}_3}{\partial t} + \bar{u}_3 \frac{\partial \bar{u}_3}{\partial x_3} = - \frac{1}{\rho_0} \frac{\partial p_0}{\partial x_3} - g \quad (2.12)$$

If we assume hydrostatic equilibrium for the mean state, the right

hand side of Equation (2.12) is zero. Thus,

$$\frac{\partial \bar{u}_3}{\partial t} + \bar{u}_3 \frac{\partial \bar{u}_3}{\partial x_3} = 0 \quad (2.13)$$

The general solution to Equation (2.13) is

$$\bar{u}_3(x_3, t) = \frac{Kx_3 + A}{Kt + B} \quad (2.14)$$

where  $K$  is some constant of separation and where  $A$  and  $B$  are constants of integration. Since we assume

$$\bar{u}_3(x_3, t_0) = 0 \quad (2.15)$$

then  $\bar{u}_3$  must remain zero for all time. Equation (2.11), for zero horizontal mean pressure gradients, is then

$$\frac{\partial \bar{u}_j}{\partial t} = 0 \quad (j = 1, 2) \quad (2.16)$$

Then, from Equations (2.15) and (2.16)

$$\frac{D\bar{u}}{Dt} = \frac{\partial \bar{u}}{\partial t} + U_j \frac{\partial \bar{u}}{\partial x_j} = u_3 \frac{\partial \bar{u}}{\partial x_3} \quad (2.17)$$

Then, subtracting Equations (2.11) from (2.10) gives an equation for



the turbulent velocities:

$$\frac{Du}{\partial t} + u_3 \frac{\partial \bar{u}}{\partial x_3} + u_3 \frac{\partial u}{\partial x_3} = - \frac{\rho'}{\rho_0} g \hat{k} - \frac{1}{\rho_0} \nabla p' - \omega u \quad (2.18)$$

or

$$\frac{Du}{Dt} = - u_3 \frac{\partial \bar{u}}{\partial x_3} - \frac{1}{\rho_0} \nabla p' - \frac{\rho'}{\rho_0} g \hat{k} - \omega u \quad (2.19)$$

If use is made of the perfect gas equation of state and classical assumptions with regard to the pressure fluctuations (see, e.g., p. 60 of Lumley and Panofsky [1959]), the buoyancy acceleration of Equation (2.19) becomes

$$- \frac{\rho'}{\rho_0} g \hat{k} = \frac{T'}{T_0} g \hat{k} \quad (2.20)$$

Now, the rate of increase with altitude of the difference  $T'$  between the temperature of a wandering fluid parcel and the temperature of the surrounding medium is equal to the lapse rate  $\gamma$  of the ambient temperature  $T$  minus the rate of decrease of the parcel temperature. For small temperature fluctuations, the fluid parcel will move in a nearly dry adiabatic fashion with lapse rate  $\Gamma_d = g/c_p$ . Then

$$\frac{dT'}{dx_3} = \gamma - \Gamma_d \quad (2.21)$$

Now the potential temperature  $\theta$  is defined as

$$\theta = T \left( \frac{p}{p_0} \right)^{-K} \quad (2.22)$$

where  $p_0$  is a reference pressure. Therefore,

$$\frac{1}{\theta} \frac{d\theta}{dx_3} = \frac{1}{T} \frac{dT}{dx_3} - \frac{K}{p} \frac{dp}{dx_3} \quad (2.23)$$

where  $\theta$ ,  $T$ , and  $p$  are the mean (altitude-dependent) properties of the atmosphere. For an atmosphere in hydrostatic equilibrium

$$\begin{aligned} \frac{1}{\theta} \frac{d\theta}{dx_3} &= \frac{1}{T} \left( \frac{dT}{dx_3} + \frac{g}{c_p} \right) \\ &= -\frac{1}{T} (\gamma - \Gamma_d) \end{aligned} \quad (2.24)$$

Thus, we have

$$\begin{aligned} -\frac{\rho'}{\rho_0} g &= g \frac{T'}{T} = g \frac{1}{T} \left( \frac{dT'}{dx_3} \right) \Delta x_3 \\ &= g \frac{1}{T} (\gamma - \Gamma_d) \Delta x_3 \\ &= -\frac{g}{\theta} \frac{d\theta}{dx_3} \Delta x_3 \end{aligned} \quad (2.25)$$

Take  $\frac{g}{\theta} \frac{d\theta}{dx_3}$  as a constant logarithmic vertical potential temperature gradient  $\Gamma$ , an assumption which is not entirely unrealistic and which is commonly used in the literature [e.g., Kao, 1968]. It may be seen from Equation (2.24) that this corresponds to assuming a logarithmic temperature profile for the atmosphere. Then

$$-g \frac{\rho'}{\rho_0} = -\Gamma [X_3(t) - X_3(t_0)] \quad (2.26)$$

The assumption  $\rho' \ll \rho_0$  limits the range of validity of the buoyancy acceleration model of Equation (2.26) to atmospheres having small potential temperature gradients; i.e., we require

$$\Gamma \ll g / < (\Delta x_3)^2 >^{\frac{1}{2}} \quad (2.27)$$

The pressure force components of Equation (2.19) are modeled by random space-time correlated accelerations  $a_i$ , assumed constant over each time step. The mean wind shears  $\partial \bar{u}_i / \partial x_3$  are taken constant and equal to  $K_i$ . Equation (2.19) thus is

$$\frac{Du_i}{Dt} = a_i - K_i u_3 - \Gamma_i [X_3(t) - X_3(t_0)] - \omega u_i \quad (2.28)$$

which, when summed with the mean velocity equation from (2.17),

$$\frac{D\bar{u}_i}{Dt} = K_i u_3 \quad (2.29)$$

gives an equation for the total acceleration on the fluid element,

$$A_i = \frac{DU_i}{Dt} = a_i - \Gamma_i [X_3(t) - X_3(t_0)] - \omega u_i \quad (2.30)$$

The shear terms have important influence, however, on the variation of the particle velocity through the viscous terms in this equation; the viscous terms provide a link between the shear effects and the particle trajectory. Therefore, the consideration of a finite fluid viscosity is necessary for an understanding of the physically meaningful characteristics of the diffusion model. Furthermore, since the shear effects would have a length scale of the order of the characteristic lengths of the flow, it may be concluded that the effects of these viscous terms would not be restricted to any inertial range of eddies. These conclusions regarding the importance and length scales of the viscous terms are in contrast to the minor role given the fluid viscosity in much of the literature on the dynamical theories of turbulent diffusion.

Now, Equations (2.28), (2.29) and (2.30) may be solved for the turbulent, mean and total fluid point velocity components, and hence the particle separation components, by expanding the accelerations on the right hand sides of the three equations in Taylor series and integrating with a finite difference approximation technique, which would yield infinite series solutions in the time step. We should, in general, require that the orders of the approximations to the quantities of most physical significance, namely the fluid point displacement and total velocity components, all be equal, say to order  $n$ .

Also, we require that the fluid point mean velocity be equal to the velocity of the surrounding mean wind, whose value is the product of the constant mean wind shear with the vertical component of the fluid point displacement. Thus, the series approximation of the mean velocity should also be of order  $n$ . But, from Equation (2.29)

$$\bar{U}_i(t_{k+1}) = \bar{U}_i(t_k) + K_i \int_{t_k}^{t_{k+1}} u_3(t') dt' \quad (2.31)$$

Thus, we see that for the approximation of  $\bar{U}_i(t)$  be of order  $n$ , the series expansion of  $u_3(t)$  should be of order  $(n-1)$ . No such special conditions are evident, however, on the horizontal turbulent velocity components.

Thus, for example, if it were desired to include terms of second order in the displacement and total velocity approximations, it would be necessary to include second order terms in the mean and turbulent horizontal velocity approximations. But the requirement that the mean fluid point velocity be equal to the velocity of the surrounding mean wind would require that the series expansion for the vertical turbulent velocity be truncated at first order. This is equivalent to assuming a constant acceleration on the right hand side for the vertical component of Equation (2.28)

Expansion of the accelerations of Equations (2.28), (2.29) and (2.30) and integration, keeping terms in the total velocity of second order, yields

$$u_i(t_{k+1}) = u_i(t_k) + \left\{ a_i(t_k) - K_i u_3(t_k) - \omega u_i(t_k) \right\} (t_{k+1} - t_k) \quad (2.32)$$

$$- \frac{1}{2} K_i A_3(t_k) (t_{k+1} - t_k)^2 \quad (i = 1,2)$$

$$u_3(t_{k+1}) = u_3(t_k) + A_3(t_k) (t_{k+1} - t_k) \quad (2.33)$$

$$\bar{u}_i(t_{k+1}) = \bar{u}_i(t_k) + K_i u_3(t_k) (t_{k+1} - t_k) \quad (2.34)$$

$$+ \frac{1}{2} K_i A_3(t_k) (t_{k+1} - t_k)^2 \quad (i = 1,2)$$

$$\bar{u}_3(t_{k+1}) = 0 \quad (2.35)$$

$$U_i(t_{k+1}) = U_i(t_k) + A_i(t_k) (t_{k+1} - t_k) \quad (i = 1,2) \quad (2.36)$$

$$U_3(t_{k+1}) = U_3(t_k) + A_3(t_k) (t_{k+1} - t_k) \quad (2.37)$$

where  $A_i$  may be found from Equation (2.30).

That Equations (2.32) through (2.37) are a consistent set of relations may be seen by addition of Equations (2.32) and (2.34) to arrive at the total horizontal velocities of Equation (2.36), and by addition of Equations (2.33) and (2.35) to arrive at the total vertical velocity of Equation (2.37). Also, we note that Equation (2.31) is satisfied exactly, as we required.

Integration of the total Lagrangian velocity from Equations (2.36) and (2.37) yields

$$x_i(t_{k+1}) = x_i(t_k) + U_i(t_k) (t_{k+1} - t_k) \quad (2.38)$$

$$+ \frac{1}{2} A_i(t_k) (t_{k+1} - t_k)^2 \quad (i = 1,2)$$

$$x_3(t_{k+1}) = x_3(t_k) + u_3(t_k) (t_{k+1} - t_k) \quad (2.39)$$

$$+ \frac{1}{2} A_3(t_k) (t_{k+1} - t_k)^2$$

Again, we note that Equation (2.34) is the same as Equation (2.39) multiplied through by  $K_i$ , as it must if the mean Lagrangian velocity is to be equal to the velocity of the surrounding mean wind.

Equations (2.32) through (2.39) constitute the working set of equations from which the fluid point displacement and Lagrangian velocity correlation characteristics are found.

## CHAPTER III

## ANALYSIS OF SPACE-TIME CORRELATED TURBULENT ACCELERATION FIELD

Analysis of the Relative Motion of Two Fluid Points

At the time of release, assume that one fluid point is at the origin of an n-dimensional ( $n = 1, 2$  or  $3$ ) orthogonal coordinate system which moves with the mean wind velocity at the point of release. The second fluid point is assumed to be located one (non-dimensional) unit distance from the first, with the (initial) separation vector  $\underline{r}_0$ . We assume that the (constant, turbulent) fluid point acceleration components  $v_{ij}$  during each unit (non-dimensional) time interval may be written in terms of previous components  $a_{ij}$  as

$$v_{i1} = \alpha_{i1} a_{i1} + \alpha_{i2} a_{i2} + \alpha_{i3} y_i \quad (3.1)$$

$$v_{i2} = \beta_{i1} a_{i1} + \beta_{i2} a_{i2} + \beta_{i3} y_i + \beta_{i4} z_i$$

where  $y_i$  and  $z_i$  are random (uncorrelated) numbers drawn from a normal distribution with zero mean and standard deviation  $c$ , and the  $a_{ij}$ 's are the previous turbulent acceleration components for the two particles, and the  $\alpha_{ij}$ 's and  $\beta_{ij}$ 's are to be determined. The numbers  $y_i$  and  $z_i$  were computed using a pseudo-random normal deviate generator employing the "chi-squared projection" technique [Bell, 1968].



We assume that the fluid point acceleration components  $v_{i1}$  and  $v_{i2}$  are correlated with each other and previous components as

$$\begin{aligned}
 \langle a_{i1} a_{i2} \rangle &= \rho_{i0} \left( \langle a_{i1}^2 \rangle \langle a_{i2}^2 \rangle \right)^{\frac{1}{2}} & (3.2) \\
 \langle v_{i1} a_{i1} \rangle &= \rho_{i1} \left( \langle v_{i1}^2 \rangle \langle a_{i1}^2 \rangle \right)^{\frac{1}{2}} \\
 \langle v_{i1} a_{i2} \rangle &= \rho_{i2} \left( \langle v_{i1}^2 \rangle \langle a_{i2}^2 \rangle \right)^{\frac{1}{2}} \\
 \langle v_{i2} a_{i2} \rangle &= \rho_{i3} \left( \langle v_{i2}^2 \rangle \langle a_{i2}^2 \rangle \right)^{\frac{1}{2}} \\
 \langle v_{i2} a_{i1} \rangle &= \rho_{i4} \left( \langle v_{i2}^2 \rangle \langle a_{i1}^2 \rangle \right)^{\frac{1}{2}} \\
 \langle v_{i1} v_{i2} \rangle &= \rho_{i5} \left( \langle v_{i1}^2 \rangle \langle v_{i2}^2 \rangle \right)^{\frac{1}{2}}
 \end{aligned}$$

where the  $\rho_{ij}$ 's are the Eulerian auto-correlations between the  $i$ -th components of the respective accelerations and where, for homogeneous, isotropic, stationary turbulent acceleration fields, we assume

$$\langle v_{ij}^2 \rangle = \langle a_{ij}^2 \rangle = c^2 \quad (3.3)$$

In these studies, the cross correlations between different acceleration components are neglected. This is partially justified by the fact that cross correlations between different components at the same time are zero in the isotropic case. The major effect of the assumption of isotropy for the turbulent acceleration field and the neglect of the

cross correlations is to reduce the coefficients  $\alpha_{ij}$  of Equation (3.1) from tensor to vector quantities.

Thus,

$$\langle a_{i1} a_{i2} \rangle = \rho_{i0} c^2 \quad (3.4)$$

$$\langle v_{i1} a_{i1} \rangle = \rho_{i1} c^2$$

$$\langle v_{i1} a_{i2} \rangle = \rho_{i2} c^2$$

$$\langle v_{i2} a_{i2} \rangle = \rho_{i3} c^2$$

$$\langle v_{i2} a_{i1} \rangle = \rho_{i4} c^2$$

$$\langle v_{i1} v_{i2} \rangle = \rho_{i5} c^2$$

where the magnitude of the  $\rho$ 's will depend on the particular space-time separation concerned and may be computed from an assumed form for the Eulerian correlation function as discussed later.

Performing the multiplications and averaging required by (3.4), with conditions (3.3), noting that

$$\langle y_1 z_1 \rangle = 0 \quad (3.5)$$

gives seven requirements on the seven  $\alpha$ 's and  $\beta$ 's

$$\alpha_{i1}^2 + \alpha_{i2}^2 + 2 \alpha_{i1} \alpha_{i2} \rho_{i3}^2 = 1 \quad (3.6)$$

$$\beta_{i1}^2 + \beta_{i2}^2 + 2 \beta_{i1} \beta_{i2} \rho_{i0} + \beta_{i3}^2 + \beta_{i4}^2 = 1 \quad (3.7)$$

$$\alpha_{i1} + \alpha_{i2} \rho_{i0} = \rho_{i1} \quad (3.8)$$

$$\alpha_{i1} \rho_{i0} + \alpha_{i2} = \rho_{i2} \quad (3.9)$$

$$\beta_{i1} + \beta_{i2} \rho_{i0} = \rho_{i3} \quad (3.10)$$

$$\beta_{i1} \rho_{i0} + \beta_{i2} = \rho_{i4} \quad (3.11)$$

$$\alpha_{i1} \beta_{i1} + (\alpha_{i1} \beta_{i2} + \alpha_{i2} \beta_{i1}) \rho_{i0} + \alpha_{i2} \beta_{i2} + \alpha_{i3} \beta_{i3} = \rho_{i5} \quad (3.12)$$

Equations (3.8) and (3.9) may then be used to find  $\alpha_{i1}$  and  $\alpha_{i2}$  as

$$\alpha_{i1} = \frac{\rho_{i1} - \rho_{i0} \rho_{i2}}{1 - \rho_{i0}^2} \quad (3.13)$$

$$\alpha_{i2} = \frac{\rho_{i2} - \rho_{i0} \rho_{i1}}{1 - \rho_{i0}^2} \quad (3.14)$$

and Equations (3.10) and (3.11) used to find  $\beta_{i1}$  and  $\beta_{i2}$  as

$$\beta_{i1} = \frac{\rho_{i3} - \rho_{i0} \rho_{i4}}{1 - \rho_{i0}^2} \quad (3.15)$$

$$\beta_{i2} = \frac{\rho_{i4} - \rho_{i0} \rho_{i3}}{1 - \rho_{i0}^2} \quad (3.16)$$

Then, with  $\alpha_{i1}$ ,  $\alpha_{i2}$ ,  $\beta_{i1}$ ,  $\beta_{i2}$  considered known, the remaining parameters may be found from Equations (3.6), (3.7) and (3.12) as

$$\alpha_{i3} = \left(1 - \alpha_{i1}^2 - \alpha_{i2}^2 - 2\alpha_{i1}\alpha_{i2}\rho_{i0}\right)^{\frac{1}{2}} \quad (3.17)$$

$$\beta_{i3} = \frac{\rho_{i5} - \alpha_{i1}\beta_{i1} - (\alpha_{i1}\beta_{i2} + \alpha_{i2}\beta_{i1})\rho_{i0} - \alpha_{i2}\beta_{i2}}{\alpha_{i3}} \quad (3.18)$$

$$\beta_{i4} = \left(1 - \beta_{i1}^2 - \beta_{i2}^2 - 2\beta_{i1}\beta_{i2}\rho_{i0} - \beta_{i3}^2\right)^{\frac{1}{2}} \quad (3.19)$$

Thus, the "new" turbulent acceleration components, assumed constant over the next unit interval, are given by (3.1) with the  $\alpha$ 's and the  $\beta$ 's given by Equations (3.13) through (3.19).

To compute the turbulent acceleration components for the initial time step, assume that the coefficients  $\alpha_{i1}$ ,  $\alpha_{i2}$ ,  $\beta_{i1}$ , and  $\beta_{i2}$  are zero.

#### Analysis of the Motion of a Single Fluid Point

The general technique implemented in the computer programs permits consideration of cases where the instantaneous fluid point

acceleration is assumed to be a linear combination of either the immediately preceding acceleration or of the two immediately preceding accelerations (plus random fluctuations). These two cases are discussed separately below.

We may assume that at time  $t = 0$  the single fluid point is at the origin of an  $n$ -dimensional ( $n \leq 3$ ) orthogonal coordinate system which translates at a speed equal to the average fluid velocity at the point of release.

#### Explicit Correlation Over One Time Interval

The  $n$  turbulent acceleration components  $v_i$  are assumed to be given by

$$v_i = \alpha_{i1} a_i + \alpha_{i2} y_i \quad (3.20)$$

where  $a_i$  is the immediately preceding  $i$ -th acceleration component and  $y_i$  is a random number drawn from a normal distribution with zero mean and standard deviation  $c$ .

Assuming stationary, homogeneous turbulent acceleration fields, we write

$$\langle v_i^2 \rangle = \langle a_i^2 \rangle = c^2 \quad (3.21)$$

$$\langle v_i a_i \rangle = \rho_i \left( \langle v_i^2 \rangle \langle a_i^2 \rangle \right)^{\frac{1}{2}}$$

We will have two conditions on the two unknowns  $\alpha_{i1}$ , and  $\alpha_{i2}$ :

$$\alpha_{i1}^2 + \alpha_{i2}^2 = 1 \quad (3.22)$$

$$\alpha_{i1} = \rho_i$$

which require that the instantaneous fluid point acceleration be written as

$$v_i = \rho_i a_i + \left(1 - \rho_i^2\right)^{\frac{1}{2}} y_i \quad (3.23)$$

The correlations  $\rho_i$  may be computed from an assumed form for the Eulerian correlation field and previously computed fluid point separations. The acceleration components during the first time step are entirely random and are equal to  $y_i$ .

#### Explicit Correlation Over Two Time Intervals

The  $n$  turbulent acceleration components at time  $t + \Delta t$  in terms of the preceding accelerations (at times  $t$  and  $t - \Delta t$ ) are assumed to be

$$v_i(t + \Delta t) = \alpha_{i1} a_i(t - \Delta t) + \alpha_{i2} a_i(t) + \alpha_{i3} y_i \quad (3.24)$$

Again, assume homogeneous, stationary acceleration fields; the correlations among the acceleration components may be written as

$$\langle a_i(t - \Delta t) a_i(t) \rangle = \rho_{i0} c^2 \quad (3.25)$$

$$\langle a_i(t - \Delta t) v_i(t + \Delta t) \rangle = \rho_{i1} c^2$$

$$\langle a_i(t) v_i(t + \Delta t) \rangle = \rho_{i2} c^2$$

where  $c^2$  is the mean square turbulent acceleration component magnitude,

$$\langle a_i^2 \rangle = \langle v_i^2 \rangle = c^2 \quad (3.26)$$

Equations (4.25) and (4.26) yield three conditions on the three unknowns  $\alpha$ 's. These may be solved to give

$$\alpha_{i1} = \frac{\rho_{i1} - \rho_{i0} \rho_{i2}}{1 - \rho_{i0}^2} \quad (3.27)$$

$$\alpha_{i2} = \frac{\rho_{i2} - \rho_{i0} \rho_{i1}}{1 - \rho_{i0}^2}$$

$$\alpha_{i3} = \left(1 - \rho_{i0}^2 - \rho_{i1}^2 - \rho_{i2}^2 + 2 \rho_{i0} \rho_{i1} \rho_{i2}\right) / \left(1 - \rho_{i0}^2\right)$$

Again, the correlations  $\rho_{ij}$  may be computed from an assumed form for the Eulerian correlation function and the particular space-time separation concerned.

For the calculation of the acceleration components during the initial time intervals, assume that the coefficients  $\alpha_{i1}$  and  $\alpha_{i2}$

are zero; for the second time interval, assume that  $\alpha_{i1}$  is zero.

Then, the "new" turbulent acceleration components are given by (3.24) and the  $\alpha$ 's found from (3.27).

#### Analysis of the Eulerian Correlations

The  $\rho_{ij}$ 's of the preceding discussion are the Eulerian correlations between the components of the respective accelerations and are determined from a stationary, homogeneous, isotropic Eulerian space-time correlation function. The acceleration correlations between two points are basically characterized by the directions of the acceleration components relative to the vector joining the two points, since there is no preferred direction of coordinate system in the isotropic case. Therefore, it is convenient to consider a longitudinal correlation  $f_1$  defined by (see Figure 1).

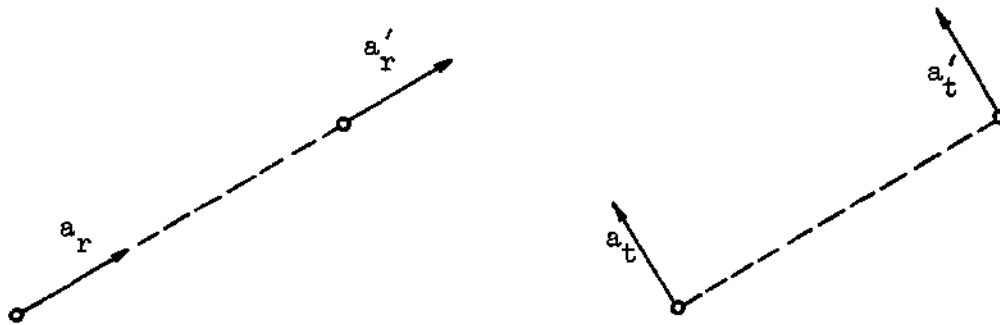
$$\langle a^2 \rangle f_1(r) = \langle a_r a_r' \rangle \quad (3.28)$$

and a transverse correlation  $f_2(r)$  defined by

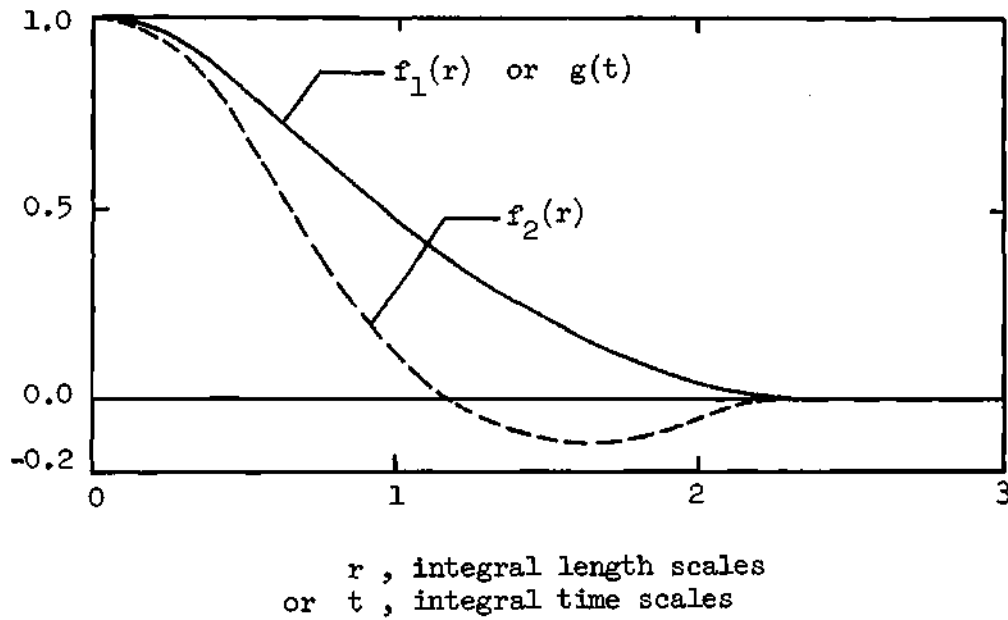
$$\langle a^2 \rangle f_2(r) = \langle a_t a_t' \rangle \quad (3.29)$$

for two parallel acceleration components perpendicular to the vector joining the points. Isotropy requires that this transverse correlation be independent of the particular pair of parallel components considered. An acceleration correlation tensor may be defined by the 9 correlations





Longitudinal and Transverse Displacements



Assumed Gaussian Form for the Longitudinal Correlation  $f_1(r)$  and Time Correlation  $g(t)$  and Corresponding Form of the Transverse Correlation  $f_2(r)$

Figure 1. Eulerian Acceleration Correlation Functions

between the 3 acceleration components at each point. Isotropy again would require that the cross correlation (e.g.,  $\langle a_r a_t' \rangle$ ) be zero. Arbitrary auto-correlations (i.e.,  $\langle a_i a_i' \rangle$ ) can then be expressed in terms of the two basic correlation  $f_1(r)$  and  $f_2(r)$  as

$$\rho_i(\underline{r}, \tau) = \left\{ \left[ f_1(r) - f_2(r) \right] \left( \frac{r_i}{r} \right)^2 + f_2(r) \right\} g(\tau) \quad (3.30)$$

Equation (3.30) is essentially the same as that derived by von Karman [1937] for velocity correlations but has in addition the provision for the consideration of time correlations  $g(\tau)$ . The longitudinal spatial correlation  $f_1(r)$  and the time correlation  $g(\tau)$  are taken as Gaussian. Batchelor [1953] shows that the transverse correlation may be found in terms of the longitudinal as

$$f_2(r) = f_1(r) + \frac{r}{2} \frac{df_1(r)}{dr} \quad (3.31)$$

Thus, if the longitudinal correlation is written as

$$f_1(r) = \exp(-\pi r^2 / 4L_e^2) \quad (3.32)$$

where  $L_e$  is the integral length scale

$$\int_0^{\infty} f_1(r) dr = L_e \quad (3.33)$$

then the transverse correlation may be written as

$$f_2(r) = \left(1 - \frac{\pi r^2}{4 L_e^2}\right) \exp(-\pi r^2/4 L_e^2) \quad (3.34)$$

It is noticed that the transverse correlation has a zero at  $2/\pi^{1/2}$  times the Eulerian length scale  $L_e$ . This fact is used later as a relatively simple determination of the Lagrangian integral scale. The time correlation may be written as

$$g(\tau) = \exp(-\pi \tau^2/4 T_e^2) \quad (3.35)$$

where  $T_e$  is the integral time scale

$$T_e = \int_0^{\infty} g(\tau) d\tau \quad (3.36)$$

In the study of the single particle, the displacement vector  $\underline{r}$  is the distance traveled over either one or two time steps and  $\tau$  can be either one or two time intervals. In the study of the particle pair, correlations are maintained over particle pair separation at the same time ( $\tau = 0$ ) and over displacement distances at the successive time steps ( $\tau = 1$  time step interval). The distribution function of the random accelerations is taken to be Gaussian.

## CHAPTER IV

OBSERVED CHARACTERISTICS OF THE DIFFUSION  
SIMULATION AND COMPARISON WITH PREVIOUS RESULTS

The finite difference numerical simulation technique, consisting essentially of Equations (2.32 - 2.39), has been used in digital computing machinery to investigate certain characteristics of the random walks of single fluid points and point pairs, whose motions describe certain aspects of the diffusion of a cluster of marked fluid particles which is both spreading about its centroid and "meandering" as a whole as discussed in Chapter II. These parcels were followed as they wandered through flow fields in which a turbulent pressure field was simulated by correlated random accelerations having some (stationary, isotropic, homogeneous) mean square magnitude  $c^2$  and space and time correlation integral scales  $L_e$  and  $T_e$ , in which buoyancy accelerations were analyzed through the use of a constant logarithmic vertical potential temperature gradient  $\Gamma$ , and in which the effects of velocity gradients were studied through the use of constant vertical shears  $K_i$  of the horizontal mean winds.

Now, parameters which were of primary interest in the consideration of the fluid point's random walk are the mean square displacement components (for the single fluid point analysis) and separation components (for the point pair analysis) as functions of the time  $t$  after release. Values for these parameters and a measure of their accuracy may be found

from the values  $X_{ij}$  of the separation components computed in each of the  $N$  runs through the mathematical program as

$$\langle X_i^2(t) \rangle = \frac{1}{N} \sum_{j=1}^N [X_{ij}(t)]^2 \quad (4.1)$$

$$\sigma_i^2(t) = \frac{1}{N-1} \left\{ \frac{1}{N} \sum_{j=1}^N [X_{ij}(t)]^4 - \frac{1}{N^2} \left( \sum_{j=1}^N [X_{ij}(t)]^2 \right)^2 \right\}$$

where  $X_{ij}(t)$  is the  $i$ -th component of particle displacement computed in the  $j$ -th run at arbitrary time  $t$ ,  $\sigma_i$  is the standard deviation of the  $i$ -th displacement components  $X_{ij}$  about the root mean square displacement component  $\langle X_i^2 \rangle^{\frac{1}{2}}$ , and  $N$  is the total number of runs (realizations) considered.

A parameter which plays an important role in molecular diffusion is the diffusivity  $D$ , as shown in the well-known formula

$$\langle s^2 \rangle = 2Dt \quad (4.2)$$

where  $s$  is the displacement of a particle due to molecular diffusion. In the mixing length approach to turbulence, the eddy diffusivity  $D$  plays a similar role. A measure of the eddy diffusivity was computed from the present investigation by considering the long time behavior of the fluid points. The diffusivity was computed as one half the factor of proportionality of the linear relationship asymptotically approached in the variation of the mean square point displacement versus

time. In the event that no line of unit slope could be fitted to the long time behavior of a particular run, it was surmised that other effects (e.g., a shear-induced effect) over-shadowed the eddy diffusion which would otherwise be exhibited at long times after release, and an attempt was made to explain the over-shadowing effect.

Other parameters of considerable interest are the Lagrangian velocity correlations exhibited by the particles as they move through the Eulerian acceleration correlation background. For the single fluid point analysis, the interesting parameters were the Lagrangian time correlations of the turbulent components at a particular time  $\tau$  with the corresponding components at later times  $\tau + k\Delta t$ . For stationary turbulent velocity fields, these correlations would not depend on the particular value of  $\tau$  but only on the time separation  $k\Delta t$ . These correlations were computed by storing the product of initial turbulent velocity components with subsequently computed velocity components; and by the use of

$$R_i(k\Delta t) = \langle u_i(\tau) u_i(\tau + k\Delta t) \rangle / \left\{ \langle u_i^2(\tau) \rangle \langle u_i^2(\tau + k\Delta t) \rangle \right\}^{\frac{1}{2}} \quad (4.3)$$

$$= \frac{\sum_{j=1}^N [u_{ij}(\tau) u_{ij}(\tau + k\Delta t)]}{\left\{ \sum_{j=1}^N u_{ij}^2(\tau) \sum_{j=1}^N u_{ij}^2(\tau + k\Delta t) \right\}^{\frac{1}{2}}}$$

where  $u_{ij}$  is the  $i$ -th velocity component computed in the  $j$ -th of  $N$  total runs. The assumed stationarity of the turbulent fields permits this to be written as

$$R_i(k\Delta t) = \frac{1}{N \langle u_i^2 \rangle} \sum_{j=1}^N [u_{ij}(0) u_{ij}(k\Delta t)] \quad (4.4)$$

For the two fluid point analysis, the Lagrangian space-time correlations between the turbulent velocity components of the two particles would also be interesting. These correlations could never be stationary, however, because of the inherent wandering apart of the two particles. Thus, these correlations should be computed for several interesting times after release. A prudent choice of the number of correlations studied would have to be made to keep the required computing time within limits. The two point Lagrangian space-time correlations were found from

$$R_i(\tau, k\Delta t) = \frac{1}{N \langle u_i^2 \rangle} \sum_{j=1}^N [u_{ij1}(\tau) u_{ij2}(\tau + k\Delta t)] \quad (4.5)$$

for only the single time  $\tau = 0$ .

The integral time scales of the Lagrangian correlations were estimated in those cases where the results permitted, from the initial zero crossing of the transverse components (cf. Equation (3.34)).

Following the fluid points through an  $n$ -dimensional random walk over the Eulerian correlation background corresponds to observing

one realization of the modeled turbulence. Significant insight into the characteristics of the diffusion were found from ensemble averages of the pertinent parameters, which were taken over a number of realizations with identical macroscopic initial conditions, both on the fluid point parameters (such as the initial separation and initial mean relative velocity) as well as on the fluid flow parameters (such as the level and scales of the turbulence, mean wind shears, and potential temperature gradients). Such identical initial conditions would be difficult to achieve in an actual turbulent flow experiment, and assumptions must be made as to the equivalence of averages over time and space to ensemble averages. In this "mathematical" experiment, however, identical initial conditions may be specified exactly, and averages of the pertinent parameters over several runs through the mathematical programs would truly be ensemble averages.

Reliability statistics indicate that the standard deviations of these averages would vary as the inverse square root of the number of realizations. This, to double the reliability of an estimate, i.e., halve its standard deviation, the number of realizations was roughly quadrupled. This reasoning, along with the fact that the necessary computing time was roughly proportional to the number of realizations, made a prudent choice of the statistical deviations that would be tolerated in the results an absolute necessity. Preliminary runs indicated that 15 realizations led to standard deviations in the mean square particle displacements of the order of 10% of the averages computed. To achieve comparable accuracy in the results for the Lagrangian velocity correlations, preliminary runs indicated that 150 realizations



would be necessary.

The number of time steps after release to be computed was another important consideration. Enough times had to be considered so that the true long-time characteristics of the diffusion were found; but again, the required computing time was roughly proportional to the number of times considered. Preliminary runs indicated that the time elapsed before the long-time behavior became clearly evident was strongly dependent on such parameters as the time and length scales of the turbulence, but it appeared that a time interval per run equal to 500 times the integral time scale was sufficient and not overly time consuming, when paired with the previously-mentioned 15 runs necessary to establish a reliable average. This combination of runs and time intervals considered required approximately one minute of computing time for the single fluid point analysis and two minutes for the point pair analysis.

Preliminary results also indicated that the Lagrangian velocity correlations fell to zero within approximately ten to fifteen integral time scales of the turbulent acceleration correlation function. Therefore, computing time was saved, in those cases where only information regarding the Lagrangian velocity correlations was desired, by considering only times out to twenty integral time scales after release. This permitted the consideration of the 150 realizations in the statistical averages of the velocity correlations which were necessary to achieve reasonable accuracy.

### Simulation of One and Two Dimensional Eddy Diffusion

The simulation of one-and two-dimensional diffusion would not include the full three-dimensional character of turbulence, nor would the analysis provide the opportunity to include the effects of mean wind shear or density stratification. The analysis did provide however the opportunity of checking out the basic technique and led to several interesting conclusions concerning it. In the case of fluid points released with zero velocity into a field of turbulent accelerations with small correlation length and time scales (i.e., when the characteristic lengths and times of the flow were taken as much larger than the correlation scales), it was found that the anticipated eddy diffusion could be successfully simulated if the characteristic viscous damping time were taken as approximately one integral time scale. This choice for the viscous damping coefficient led to approximately stationary mean square turbulent velocities after an initial period during which the velocities "built-up" from their zero initial values. This period in which the velocities built up was characterized by the mean square displacements varying as  $t^4$ , the result of the predominance of Lagrangian acceleration correlations. It was found that if the particles were released with some random initial velocity with mean square value equal to that observed at long times after release, the turbulent velocities remained approximately stationary from the point of release onward, while if the particles were released with initial velocities with mean square values larger than the value observed at long times, a period was observed in which the mean square turbulent velocities decayed from their initial value to the long time value, apparently as a result of

viscous effects. This period in which the mean square turbulent velocities either built up or decayed from their initial values to the long time behavior was also evident in the behavior of the particle displacements versus time. Finite initial particle velocities led to mean square displacements and separations proportional to the square of the time for very small times after release. A transition period, during which the proportionality changed to linear in time, was observed. The characteristic time to transition seemed to increase with increasing mean square initial velocity. This behavior was evidently due to the non-zero Lagrangian velocity correlations, which would result in these cases due to finite initial velocities in spite of the zero turbulent acceleration correlations. Even this simple analysis, then illustrates certain aspects of the relationship between the turbulent acceleration and Lagrangian velocity correlations.

These comments on the viscous damping coefficient and mean square initial velocity appeared to remain valid in the more complex cases of three-dimensional acceleration fields with finite length and time scales. Thus to simulate stationary turbulence velocity fields, the characteristic time of the viscous damping was held equal to one time integral scale for all of the cases considered, and the initial mean square turbulent velocity was set equal to the mean square value observed at long times.

"Trapping" effects, similar to those noted by Kraichnan [1970], were observed for one- and two-dimensional acceleration fields with finite correlation scales. These appeared to be related to the probability of both fluid points arriving at some point in the field at the

same time. Probability theory [Knapp, 1965] indicates that for infinite times of particle meandering this will happen infinitely many times in one or two dimensions. When this does happen, the basic technique of Equations (3.1), (3.20) and (3.24) evidently ceases to be valid; specifically, certain of the  $\alpha$ 's and  $\beta$ 's defined there become infinite. Probability theory indicates that in three-dimensions, the particles are most likely to wander apart permanently, and the trapping effects are not observed in the three-dimensional cases considered.

### Simulation of Three-Dimensional Turbulent Diffusion

#### Single Fluid Point Analysis

Neutral Density Stratification ( $\Gamma = 0$ ). The generalization of the aforementioned analysis, with zero length and time correlation scales, to the three dimensional random walk of a single particle resulted in the isotropic eddy diffusion of Figure 2. The range in which the influence of the initial velocity was felt is evident from the slopes of two at very small times after release. The isotropy of the diffusion was also evident in the mean square particle velocities, which in addition exhibited statistical stationarity throughout the time interval considered.

Cases in which the turbulent acceleration field exhibited finite Eulerian space-time correlations were then considered. The Eulerian length scale was taken as 10 times the characteristic length of the flow ( $L = 10$  in the tables below) while the Eulerian time scale was taken as 10 times the time step increment ( $TL = 10$ ). Eulerian correlations were explicitly maintained over one time step. The result-

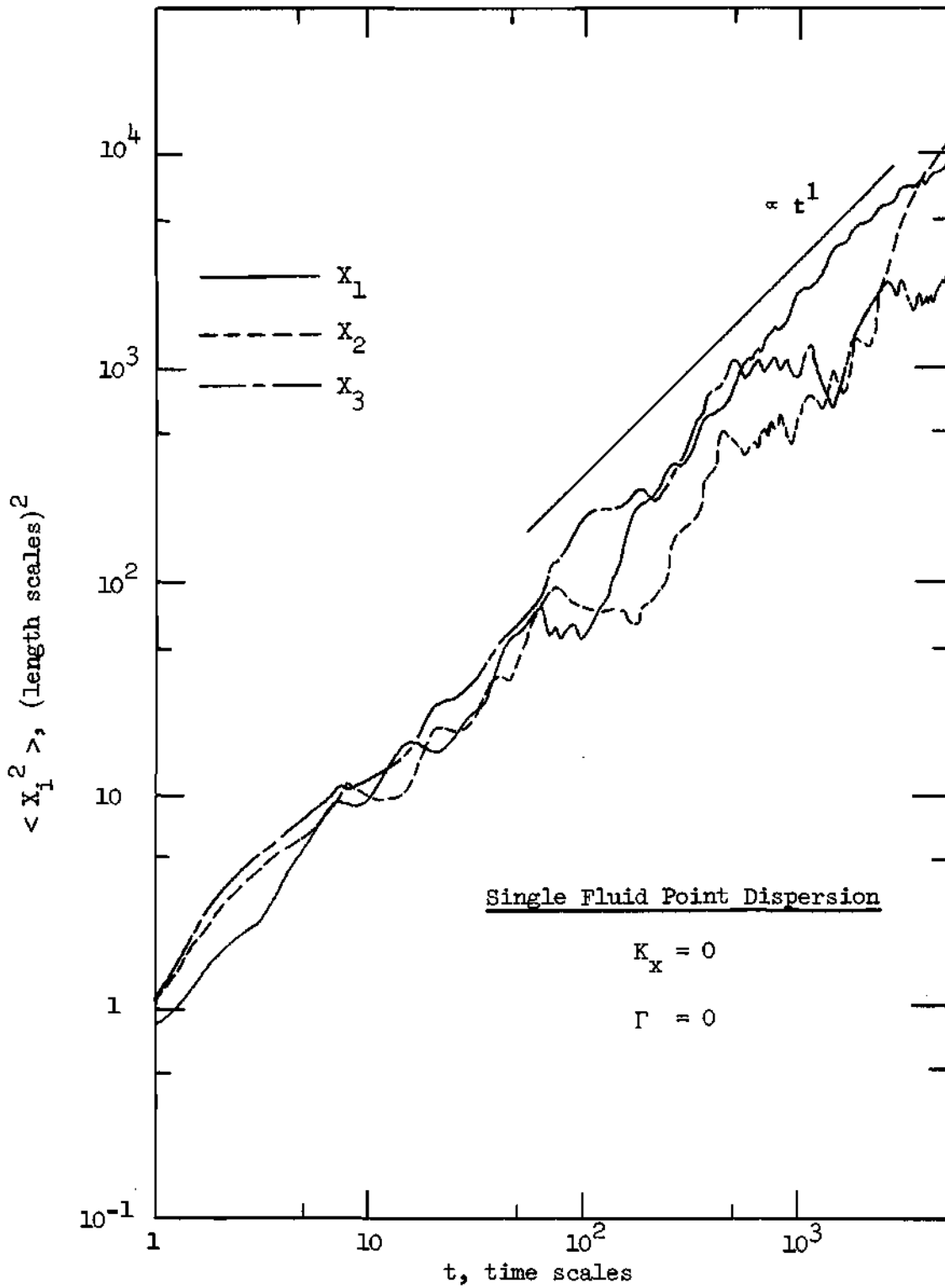


Figure 2. Fluid Point Dispersion Through Background Acceleration Field with Zero Length and Time Correlation Scales

ing three-dimensional, isotropic mean square particle separations versus time are shown in Figure 3. The initial time interval, over which the effects of the initial random velocity is felt, is clearly shown by the slopes of two (indicating  $\langle X_i^2 \rangle \propto t^2$ ) at small times after release. A transition to large scale eddy diffusion is seen at approximately 10 time scales (100 time step increments) after release, when the mean square particle separation is approximately 10 length scales. All of the eddy diffusivities  $D_i$  are approximately equal and appear to have an order of magnitude of 1 (length scale)<sup>2</sup> per time scale. This behavior was in agreement with the particle dispersion predicted for small and large times after release into a uniform, neutral atmosphere by Taylor [1920].

The Lagrangian time correlations of each of the three particle velocity components for this case are shown in Figure 4. Several interesting conclusions seem apparent. The isotropy of the diffusion is evidenced here in that all three correlations are approximately equal. The correlations do not appear to have a cusp at time  $t = 0$  and thus more closely obey a Gaussian than an exponential decay. In spite of relatively large random fluctuations at small correlation values, it appears that the correlations take on negative values approximately 10 time scales after release and thereafter decay to zero. From the analysis of Taylor [1920] and others, these negative correlation values appear to result in the transition from the initial behavior (as evidenced by slopes of 2 in Figure 3) to eddy diffusion (as evidenced by slopes of unity). The time interval of negative correlations and the time scale for transition to eddy diffusion appear to be in agree-

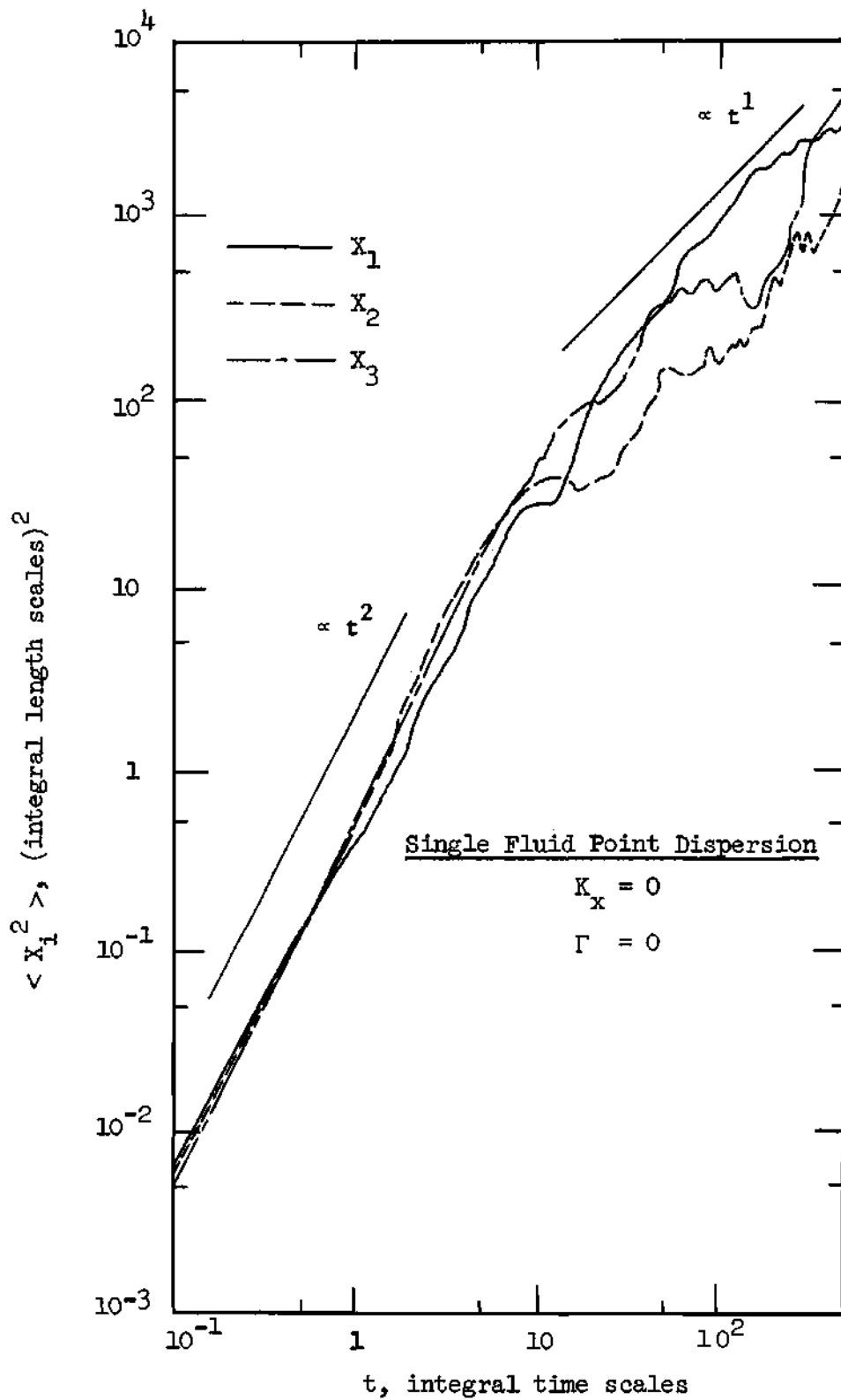


Figure 3. Fluid Point Dispersion Through Acceleration Field with Finite Correlation Scales

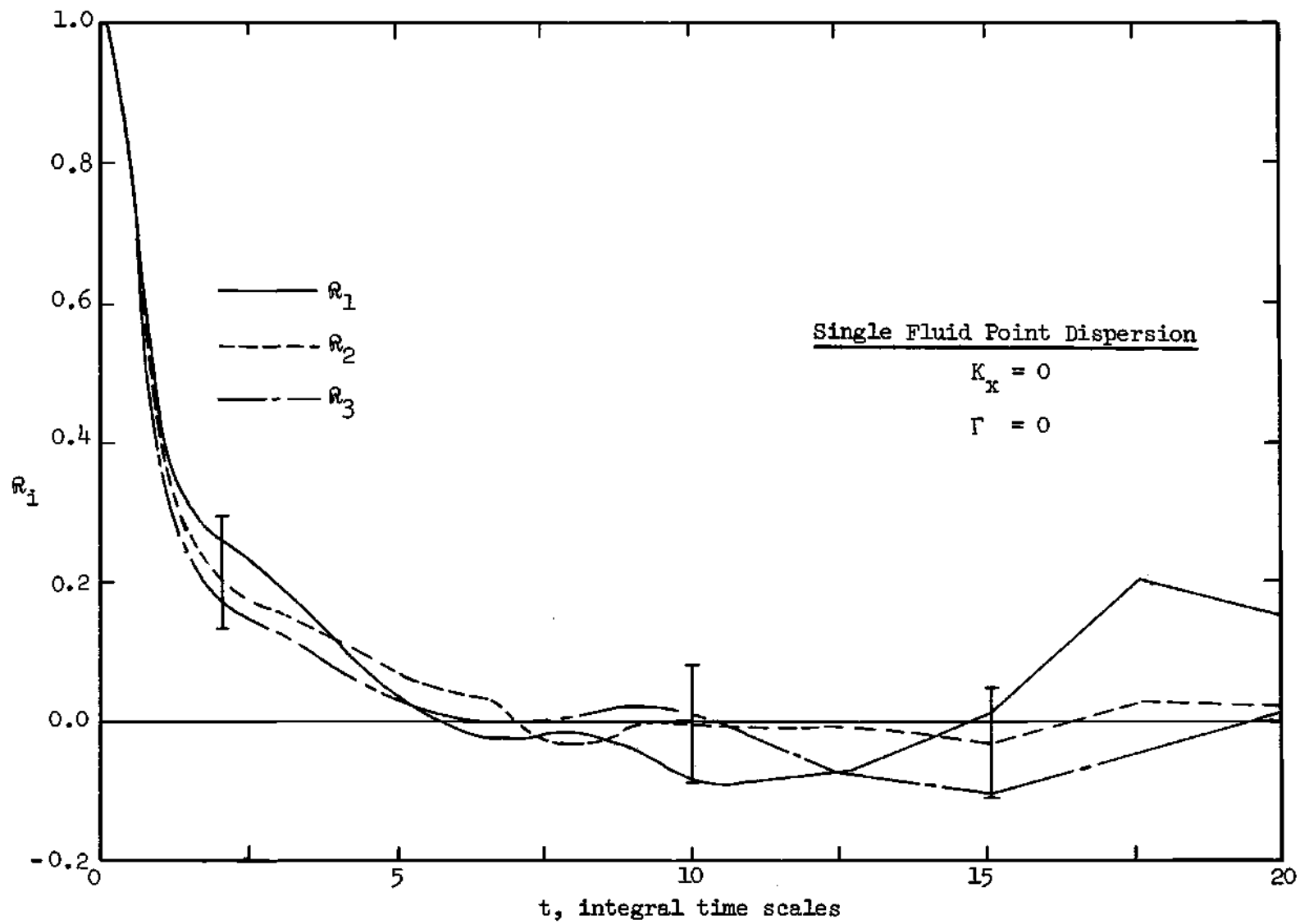


Figure 4. Lagrangian Velocity Time Correlations, Finite Eulerian Correlation Scales



ment.

Some typical effects of shears in the mean winds are evident from Figure 5, which is the result of including a moderate vertical shear of the x-component of the mean wind ( $K_x = 1.0$  (time scale)<sup>-1</sup>) in the aforementioned analysis. The major effect appears to be a  $t^3$  dependence at long times after release for the component dominated by shear, which leads to relatively large particle displacements in that direction. Indeed, the x-component of the mean square particle separation at time  $t = 500$  time scales ( $\langle X^2 \rangle_{500}$ ) has been increased by a factor of greater than  $10^4$  over what it was in the previous case of uniform mean wind. As could be anticipated from Equation (2.19), wherein is shown the direct effect of mean shear on the turbulent velocity components, the x-component of the mean square turbulent velocity is also increased in this analysis. Thus, the resulting diffusion is decidedly anisotropic in these cases. Both Riley and Corrsin [1971] and Thompson [1971] have noticed similar dependences for shear-dominated particle dispersion components in numerical simulations of turbulent shear flows.

The coefficient  $C_x^3$  of the  $t^3$  dependence, defined by

$$\langle X^2(t) \rangle = C_x^3 t^3, \quad t \rightarrow \infty \quad (4.6)$$

appears to increase with the magnitude of the shear, as shown in Figure 6 and Table 1. The variation appears to be well approximated by

$$C_x^3 \propto \langle w^2 \rangle \left( \frac{\partial \bar{U}}{\partial z} \right)^2 T_L \quad (4.7)$$

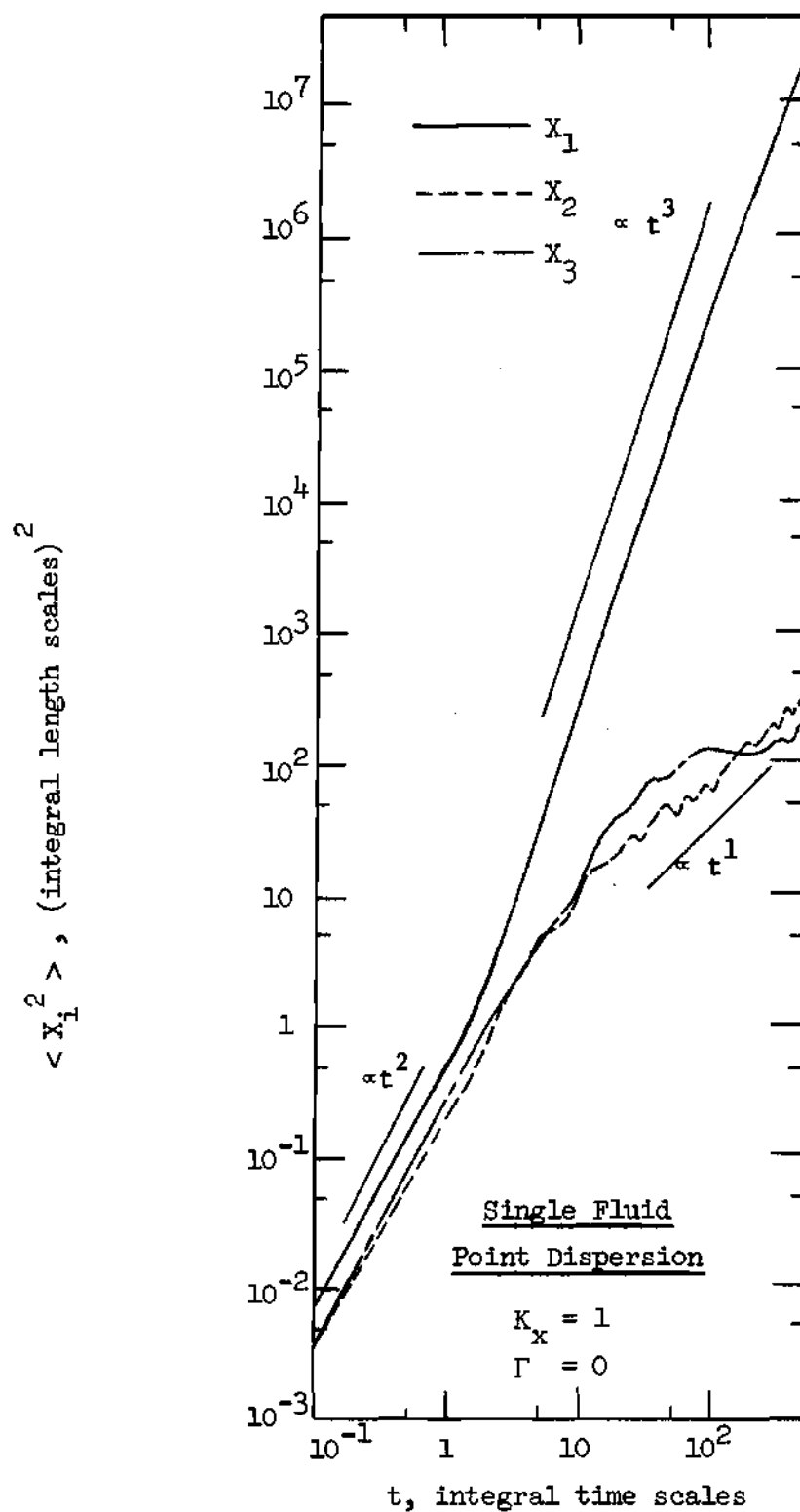


Figure 5. Fluid Point Dispersion Through a Field with Moderate Mean Wind Shear

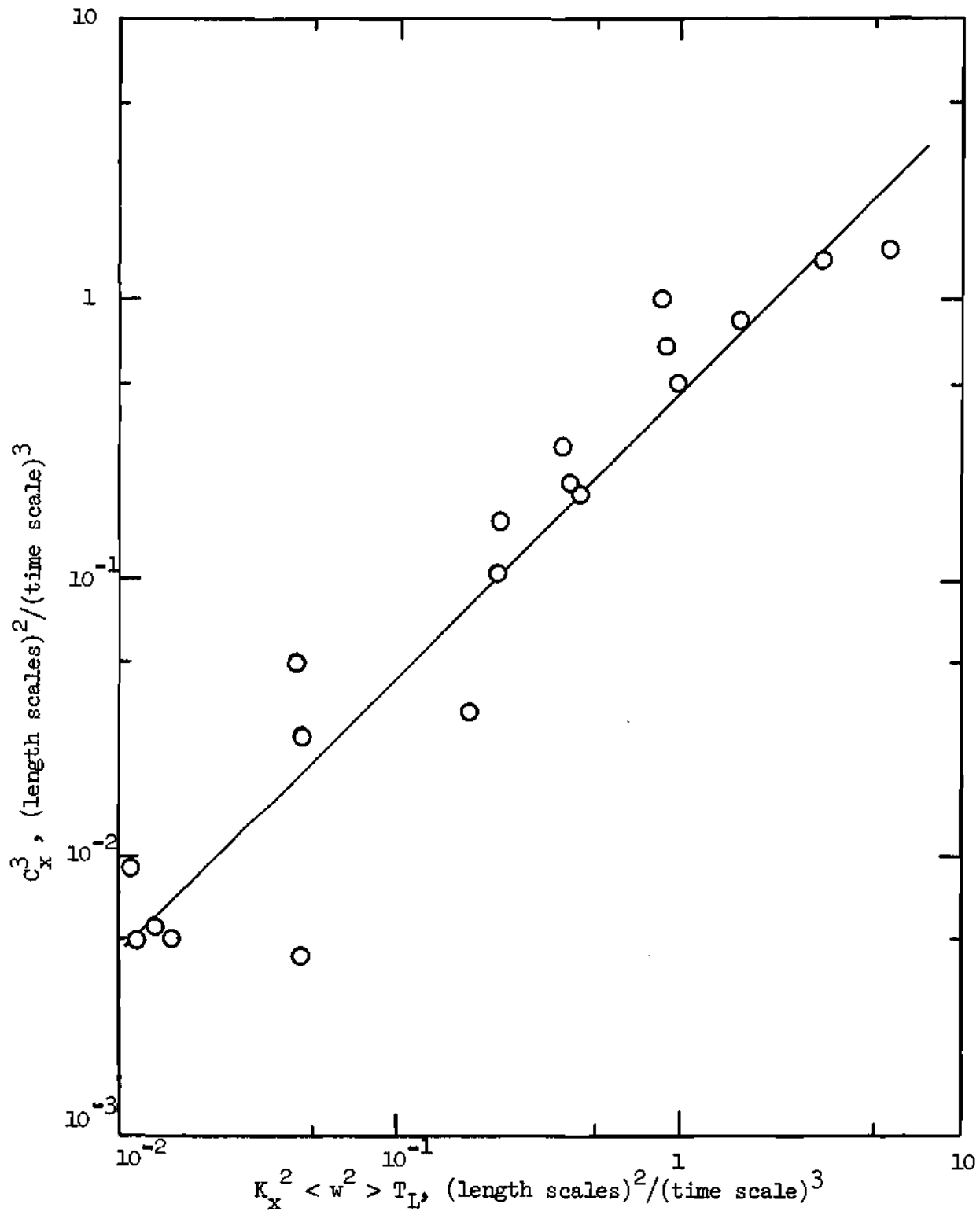


Figure 6. Variation of  $C_x^3$  with Shear

Table 1. Statistical Properties of the Diffusion of a Single Fluid Point

(L = 10, TL = 10,  $\omega = 1$ ,  $u_T = 0.7$ )

$\Gamma$ (TS <sup>-2</sup> )	$K_x$ (TS <sup>-1</sup> )	$P_x$	$C_x^P$ (LS <sup>2</sup> /TS <sup>P</sup> )	$\langle X^2 \rangle_{500}$ (LS <sup>2</sup> )	$D_y$ (LS <sup>2</sup> /TS)	$P_z$	$C_z^P$ (LS <sup>2</sup> /TS <sup>P</sup> )
0	0.0	1	9.6	$3.0 \times 10^3$	1.8	1	2.4
	0.1	3	$8.9 \times 10^{-3}$	$1.5 \times 10^6$	3.1	1	3.5
	0.2	3	$5.0 \times 10^{-2}$	$3.5 \times 10^6$	1.0	1	2.6
	0.5	3	$1.6 \times 10^{-1}$	$1.3 \times 10^7$	$5.6 \times 10^{-1}$	1	1.3
	1.0	3	$2.9 \times 10^{-1}$	$3.2 \times 10^7$	$4.3 \times 10^{-1}$	1	$8.7 \times 10^{-1}$
	2.0	3	$6.9 \times 10^{-1}$	$4.9 \times 10^7$	$1.6 \times 10^{-1}$	1	$3.3 \times 10^{-1}$
	5.0	3	1.5	$1.6 \times 10^8$	$1.0 \times 10^{-1}$	1	$2.0 \times 10^{-1}$
10 <sup>-4</sup>	1.0	3	$2.1 \times 10^{-1}$	$2.8 \times 10^7$	$5.0 \times 10^{-1}$	1	1.0
10 <sup>-3</sup>	0.0	1	4.5	$1.8 \times 10^3$	4.6	1	2.2
	0.1	3	$5.0 \times 10^{-3}$	$1.4 \times 10^6$	2.6	1	5.1
	0.2	3	$2.7 \times 10^{-2}$	$2.0 \times 10^6$	1.3	1	1.0
	0.5	3	$1.0 \times 10^{-1}$	$7.4 \times 10^6$	$5.5 \times 10^{-1}$	1	$6.8 \times 10^{-1}$
	1.0	3	$2.0 \times 10^{-1}$	$1.3 \times 10^7$	1.3	1	$4.1 \times 10^{-1}$
	2.0	3	$5.0 \times 10^{-1}$	$2.9 \times 10^7$	$5.5 \times 10^{-1}$	1	$2.6 \times 10^{-1}$
	5.0	3	1.32	$1.4 \times 10^8$	$2.4 \times 10^{-1}$	1	$1.5 \times 10^{-1}$

TS = Integral Time Scales of the Eulerian Acceleration Correlations

LS = Integral Length Scales of the Eulerian Acceleration Correlations

Table 1. Continued

$\Gamma$ (TS <sup>-2</sup> )	$K_x$ (TS <sup>-1</sup> )	$P_x$	$C_x^P$ (IS <sup>2</sup> /TS <sup>P</sup> )	$\langle X^2 \rangle_{500}$ (IS <sup>2</sup> )	$D_y$ (IS <sup>2</sup> /TS)	$P_z$	$C_z^P$ (IS <sup>2</sup> /TS <sup>P</sup> )	
$2 \times 10^{-3}$	0.0	1	$1.0 \times 10^1$	$3.0 \times 10^3$	3.5	1	2.7	
	0.1	3	$5.6 \times 10^{-3}$	$9.9 \times 10^5$	2.9	1	2.3	
	0.2	2	4.4	$1.4 \times 10^6$	1.1	0	$2.2 \times 10^2$	
	0.5	3	$3.4 \times 10^{-2}$	$4.7 \times 10^6$	2.4	1	$5.6 \times 10^{-1}$	
	1.0	2	$4.8 \times 10^1$	$1.3 \times 10^7$	$1.5 \times 10^{-1}$	0	$8.3 \times 10^1$	
	2.0	3	1.0	$3.6 \times 10^7$	$3.6 \times 10^{-1}$	1	$4.0 \times 10^{-1}$	
	5.0	3	$8.1 \times 10^{-1}$	$1.1 \times 10^8$	$2.5 \times 1.0^{-1}$	1	$1.3 \times 10^{-1}$	
	$5 \times 10^{-3}$	0.0	1	2.4	$3.1 \times 10^3$	2.1	1	2.5
		0.1	3	$5.0 \times 10^{-3}$	$4.5 \times 10^5$	2.5	1	1.9
		0.2	3	$4.2 \times 10^{-3}$	$8.3 \times 10^5$	3.7	1	$7.6 \times 10^{-1}$
0.5		2	$1.1 \times 10^1$	$2.6 \times 10^6$	$3.2 \times 10^{-1}$	0	$8.9 \times 10^1$	
1.0		2	$2.5 \times 10^1$	$6.6 \times 10^6$	$5.0 \times 10^{-1}$	0	$5.0 \times 10^1$	
2.0		2	$6.2 \times 10^1$	$3.9 \times 10^7$	$3.4 \times 10^{-1}$	0	$3.7 \times 10^1$	
5.0		2	$1.6 \times 10^2$	$7.7 \times 10^7$	$1.4 \times 10^{-1}$	0	$2.9 \times 10^1$	
$10^{-2}$		0.0	1	8.7	$2.9 \times 10^3$	2.0	0	$1.8 \times 10^2$
		0.1	2	$1.9 \times 10^{-1}$	$1.6 \times 10^5$	4.2	0	$1.3 \times 10^2$

Table 1. Continued

$\Gamma$	$K_x$	$P_x$	$C_x^P$	$\langle x^2 \rangle_{500}$	$D_y$	$P_z$	$C_z^P$
( $TS^{-2}$ )	( $TS^{-1}$ )		( $IS^2/TS^P$ )	( $IS^2$ )	( $IS^2/TS$ )		( $IS^2/TS^P$ )
$10^{-2}$	0.2	2	$7.6 \times 10^{-1}$	$2.6 \times 10^5$	3.1	0	$6.5 \times 10^1$
	0.5	2	2.2	$1.5 \times 10^6$	1.9	0	$5.0 \times 10^1$
	1.0	2	9.5	$3.1 \times 10^6$	1.1	0	$3.1 \times 10^1$
	2.0	2	$5.0 \times 10^1$	$7.0 \times 10^6$	$3.7 \times 10^{-1}$	0	$1.9 \times 10^1$
	5.0	2	$1.6 \times 10^2$	$2.0 \times 10^7$	$1.7 \times 10^{-1}$	0	8.6
$2 \times 10^{-2}$	0.0	1	2.7	$3.0 \times 10^3$	2.5	0	$2.3 \times 10^2$
	0.1	2	$1.5 \times 10^{-1}$	$6.9 \times 10^4$	4.1	0	$1.4 \times 10^2$
	0.2	1	$2.0 \times 10^2$	$9.8 \times 10^4$	1.1	0	$5.0 \times 10^1$
	0.5	1	$5.0 \times 10^2$	$2.0 \times 10^5$	1.3	0	$3.8 \times 10^1$
	1.0	1	$2.7 \times 10^3$	$1.3 \times 10^6$	$9.5 \times 10^{-1}$	0	$2.3 \times 10^1$
	2.0	1	$4.5 \times 10^3$	$2.2 \times 10^6$	$7.0 \times 10^{-1}$	0	$1.2 \times 10^1$
	5.0	1	$1.0 \times 10^4$	$5.5 \times 10^6$	$1.0 \times 10^{-1}$	0	6.2
$5 \times 10^{-2}$	1.0	1	$9.0 \times 10^2$	$3.4 \times 10^5$	1.1	0	$1.4 \times 10^1$
$10^{-1}$	1.0	1	$1.4 \times 10^2$	$4.7 \times 10^4$	$7.5 \times 10^{-1}$	0	7.6
$10^{-4}$	0.0	1	$1.0 \times 10^1$	$3.0 \times 10^3$	$9.5 \times 10^{-1}$	1	3.9
$10^{-2}$	1.0	(exponential)	(exponential)	$6.0 \times 10^9$	$2.5 \times 10^{-1}$	(exponential)	(exponential)

as suggested by Deardorff [1970].

It should be emphasized that even though this shear-induced effect appears to follow the same power law as the Richardson diffusion, it is not restricted to intermediate times after release nor is it the result of eddies in any apparent inertial range. In spite of this, Deardorff concluded that the coefficient of the shear-induced  $t^3$  dependence may be proportional to the viscous dissipation  $\epsilon$ , the coefficient of the Richardson law. Also, the coefficients of observed particle dispersions with  $t^3$  dependence have been used to evaluate viscous dissipation rates [e.g., Ball, 1961]. The viscous dissipation for the diffusion model would be equal to the product of the viscous damping coefficient  $\omega$  with the mean square turbulent velocity magnitude  $\langle u^2 \rangle$ . Preliminary studies indicated (for values of  $\omega$  for which the turbulent velocity field appeared relatively stationary) that  $\langle u^2 \rangle$  varied almost inversely with  $\omega$ , causing the viscous dissipation to remain relatively invariant. Thus, it appeared that the coefficient  $C_x^3$  was not directly related to  $\epsilon$ .

Secondary effects of the mean shear appear to include a decrease of the eddy diffusivities, in the directions not dominated by shear, as shown in Table 1 and Figure 7. This effect is evidently due to a complex interaction between displacement components coupled through the acceleration correlations. A possibly over-simplified statement of the effect would be that the mean shear tends to increase the total particle displacement which tends to decrease the Eulerian acceleration correlations. The decreased Eulerian acceleration correlations result in

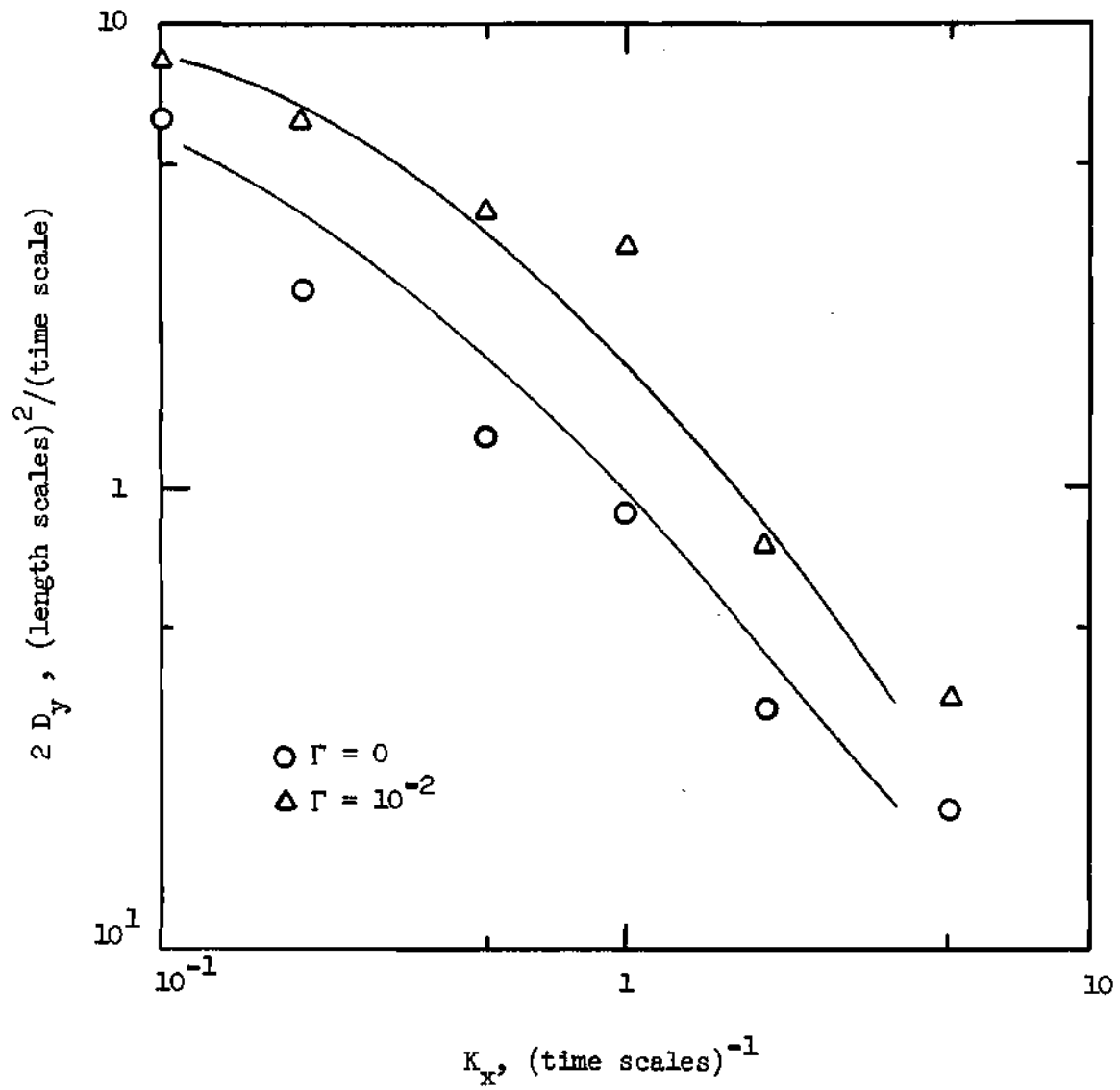


Figure 7. Variation of  $D_y$  with Shear and Temperature Stratification



decreases in the Lagrangian velocity correlation integral scale and hence the eddy diffusivity.

The anisotropy induced by the mean wind shear is evident in the turbulent velocity component ratios plotted versus the shear magnitude in Figure 8. The anisotropy is also evident in Table 2 where the velocity cross-correlation  $\rho_{uw}$  is shown. The relatively large negative values for this product indicate an increasingly large contribution to the turbulent energy by shear production.

Stable Density Stratification ( $\Gamma > 0$ ). The mean square particle displacements and turbulent velocities also showed a decidedly anisotropic behavior when stable density stratifications were considered.

The mean square particle displacement components for the case of uniform mean wind ( $K_x = 0$ ) and a moderately stable potential temperature gradient ( $\Gamma = 0.01$  (time scales)<sup>-2</sup>) are shown in Figure 9. The major effect of the buoyancy term appears as a "leveling off" of the vertical component of diffusion, somewhere near 100 (length scales)<sup>2</sup>. The horizontal particle displacements appear to be relatively unchanged from their corresponding values in the neutrally-stratified analysis; there does seem to be a very slight increase, however, in the horizontal eddy diffusivities with increasingly stable stratification, as illustrated for the y-component in Figure 7.

Effects of the buoyancy terms are also felt in the particle turbulent velocities. Table 2 illustrates a slight damping effect on the vertical mean square turbulent velocity magnitude with increasing  $\Gamma$ .

Table 2 also indicates the variation of the velocity temperature cross correlation  $\rho_{wz}$ , which indicate the importance of the buoyancy

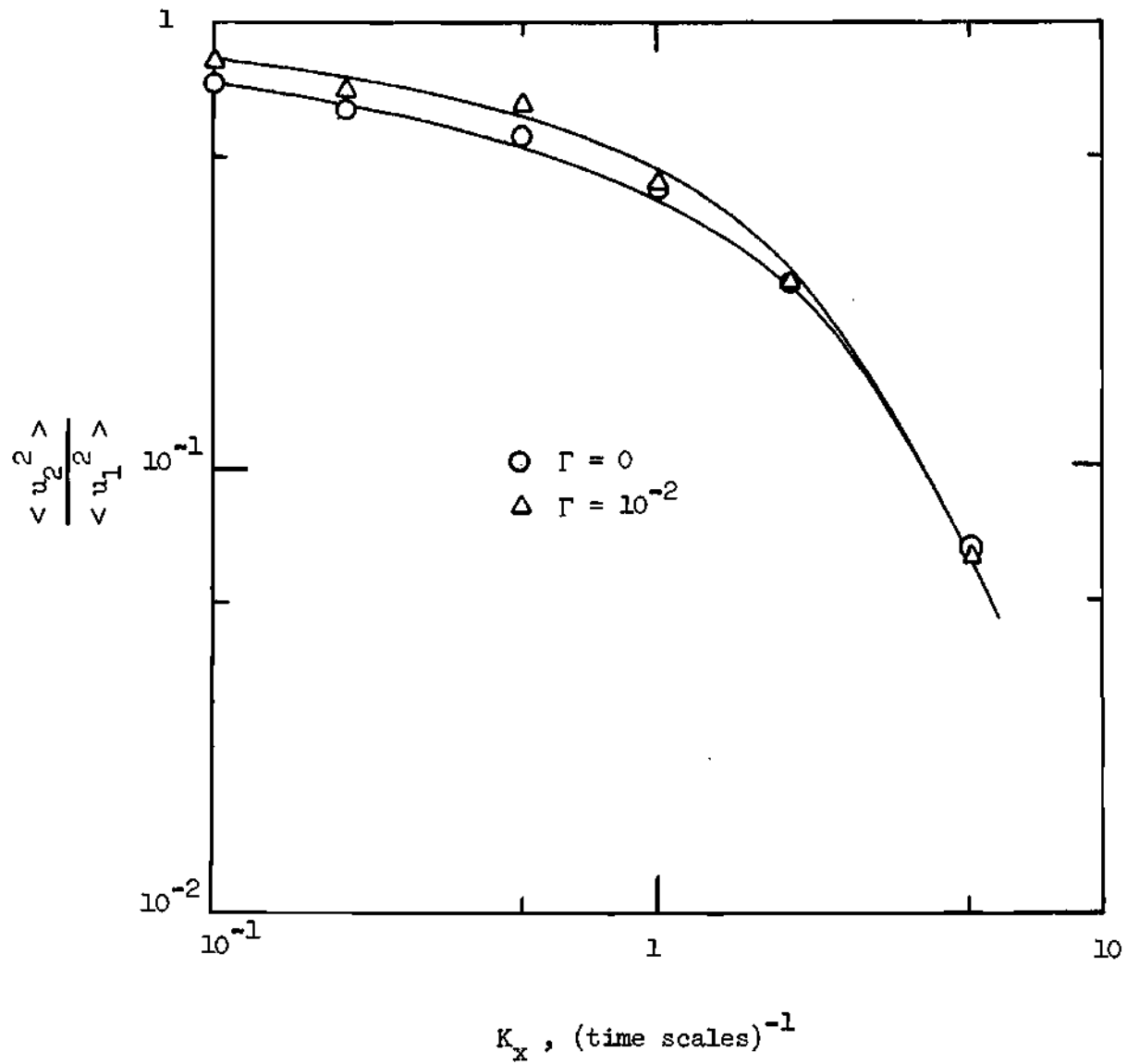


Figure 8. Influence of Mean Wind Shears and Temperature Stratifications on Anisotropy of Turbulent Velocity Field

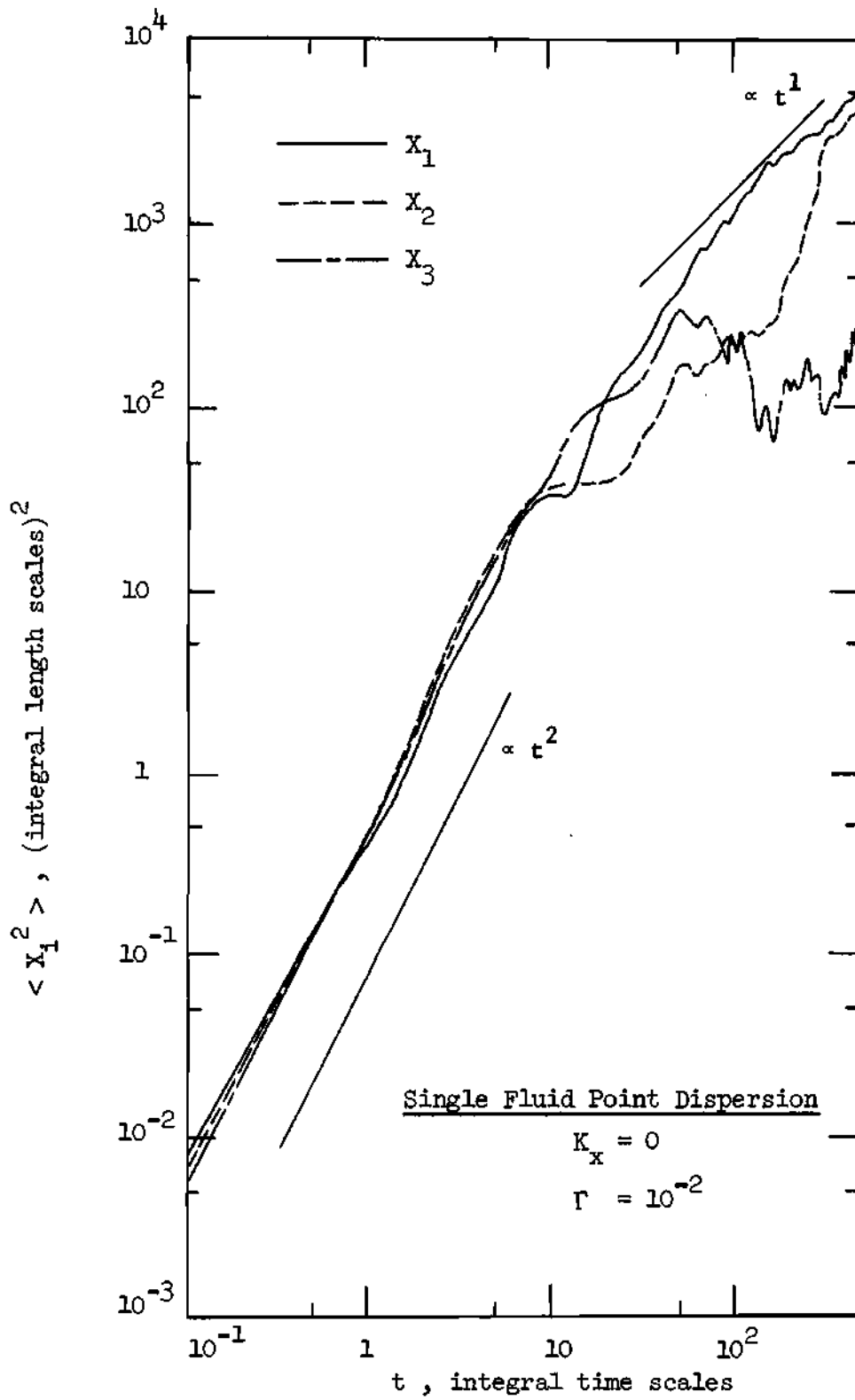


Figure 9. Fluid Point Dispersion Through Field with Moderately Stable Temperature Stratification

Table 2. Lagrangian Velocity Characteristics of the Diffusion of a Single Fluid Point  
 (L = 10, TL = 10, w = L, u<sub>I</sub> = 0.7)

$\Gamma$ (TS <sup>-2</sup> )	$K_x$ (TS <sup>-1</sup> )	$\langle u^2 \rangle$ (IS <sup>2</sup> /TS <sup>2</sup> )	$\langle v^2 \rangle$ (IS <sup>2</sup> /TS <sup>2</sup> )	$\langle w^2 \rangle$ (IS <sup>2</sup> /TS <sup>2</sup> )	$\tau$ (TS)	$\rho_{uw}$	$\rho_{vw}$	$\rho_{zw}$
0	0.0	6.04x10 <sup>-1</sup>	6.17x10 <sup>-1</sup>	6.00x10 <sup>-1</sup>	2.6	-3.07x10 <sup>-3</sup>	6.01x10 <sup>-3</sup>	3.99x10 <sup>-2</sup>
	0.1	7.99x10 <sup>-1</sup>	5.77x10 <sup>-1</sup>	5.56x10 <sup>-1</sup>	2.2	-7.73x10 <sup>-2</sup>	-2.03x10 <sup>-2</sup>	7.83x10 <sup>-2</sup>
	0.2	7.07x10 <sup>-1</sup>	4.52x10 <sup>-1</sup>	4.27x10 <sup>-1</sup>	2.6	-1.11x10 <sup>-1</sup>	-3.24x10 <sup>-2</sup>	4.63x10 <sup>-2</sup>
	0.5	4.24x10 <sup>-1</sup>	2.42x10 <sup>-1</sup>	2.31x10 <sup>-1</sup>	4.0	-2.88x10 <sup>-1</sup>	-2.57x10 <sup>-2</sup>	3.71x10 <sup>-2</sup>
	1.0	2.59x10 <sup>-1</sup>	1.05x10 <sup>-1</sup>	1.10x10 <sup>-1</sup>	3.1	-4.63x10 <sup>-1</sup>	-5.37x10 <sup>-2</sup>	5.71x10 <sup>-3</sup>
	2.0	2.86x10 <sup>-1</sup>	7.57x10 <sup>-2</sup>	7.63x10 <sup>-2</sup>	2.9	-6.69x10 <sup>-1</sup>	-2.78x10 <sup>-2</sup>	3.66x10 <sup>-2</sup>
	5.0	9.52x10 <sup>-1</sup>	6.37x10 <sup>-2</sup>	6.28x10 <sup>-2</sup>	2.7	-7.32x10 <sup>-1</sup>	7.57x10 <sup>-3</sup>	3.43x10 <sup>-2</sup>
10 <sup>-4</sup>	1.0	2.62x10 <sup>-1</sup>	1.06x10 <sup>-1</sup>	1.11x10 <sup>-1</sup>	3.7	-4.63x10 <sup>-1</sup>	-5.13x10 <sup>-2</sup>	5.44x10 <sup>-2</sup>
10 <sup>-3</sup>	0.0	6.05x10 <sup>-1</sup>	6.06x10 <sup>-1</sup>	6.06x10 <sup>-1</sup>	3.3	-2.96x10 <sup>-2</sup>	-2.41x10 <sup>-2</sup>	1.27x10 <sup>-2</sup>
	0.1	6.05x10 <sup>-1</sup>	4.64x10 <sup>-1</sup>	4.43x10 <sup>-1</sup>	5.3	-1.14x10 <sup>-1</sup>	-2.03x10 <sup>-2</sup>	5.75x10 <sup>-2</sup>
	0.2	5.66x10 <sup>-1</sup>	4.31x10 <sup>-1</sup>	4.08x10 <sup>-1</sup>	2.8	-1.33x10 <sup>-1</sup>	-5.73x10 <sup>-3</sup>	3.94x10 <sup>-2</sup>
	0.5	3.81x10 <sup>-1</sup>	2.22x10 <sup>-1</sup>	2.19x10 <sup>-1</sup>	3.9	-2.55x10 <sup>-1</sup>	-5.87x10 <sup>-3</sup>	3.03x10 <sup>-2</sup>
	1.0	3.43x10 <sup>-1</sup>	1.57x10 <sup>-1</sup>	1.46x10 <sup>-1</sup>	2.9	-4.29x10 <sup>-1</sup>	-1.80x10 <sup>-2</sup>	4.04x10 <sup>-2</sup>
	2.0	4.02x10 <sup>-1</sup>	9.97x10 <sup>-2</sup>	9.85x10 <sup>-2</sup>	2.5	-6.45x10 <sup>-1</sup>	-5.59x10 <sup>-2</sup>	4.14x10 <sup>-2</sup>
	5.0	1.01	6.57x10 <sup>-2</sup>	6.57x10 <sup>-2</sup>	3.1	-7.56x10 <sup>-1</sup>	-3.98x10 <sup>-2</sup>	5.34x10 <sup>-2</sup>

TS = Integral Time Scales of the Eulerian Acceleration Correlations  
 IS = Integral Length Scales of the Eulerian Acceleration Correlations

Table 2. Continued

$\Gamma$ (TS <sup>-2</sup> )	$K_x$ (TS <sup>-1</sup> )	$\langle u^2 \rangle$ (LS <sup>2</sup> /TS <sup>2</sup> )	$\langle v^2 \rangle$ (LS <sup>2</sup> /TS <sup>2</sup> )	$\langle w^2 \rangle$ (LS <sup>2</sup> /TS <sup>2</sup> )	T (TS)	$\rho_{uw}$	$\rho_{vw}$	$\rho_{zw}$
2x10 <sup>-3</sup>	0.0	6.05x10 <sup>-1</sup>	6.16x10 <sup>-1</sup>	5.96x10 <sup>-1</sup>	*	1.22x10 <sup>-2</sup>	-2.42x10 <sup>-2</sup>	4.52x10 <sup>-2</sup>
	0.1	6.28x10 <sup>-1</sup>	4.87x10 <sup>-1</sup>	4.68x10 <sup>-1</sup>	*	-1.03x10 <sup>-1</sup>	-1.69x10 <sup>-2</sup>	3.85x10 <sup>-2</sup>
	0.2	5.92x10 <sup>-1</sup>	4.69x10 <sup>-1</sup>	4.42x10 <sup>-1</sup>	*	-1.33x10 <sup>-1</sup>	-2.94x10 <sup>-3</sup>	3.13x10 <sup>-2</sup>
	0.5	4.48x10 <sup>-1</sup>	2.76x10 <sup>-1</sup>	2.56x10 <sup>-1</sup>	*	-2.73x10 <sup>-1</sup>	-1.58x10 <sup>-3</sup>	3.36x10 <sup>-2</sup>
	1.0	3.12x10 <sup>-1</sup>	1.23x10 <sup>-1</sup>	1.27x10 <sup>-1</sup>	*	-4.56x10 <sup>-1</sup>	-4.73x10 <sup>-2</sup>	2.26x10 <sup>-2</sup>
	2.0	3.61x10 <sup>-1</sup>	8.94x10 <sup>-2</sup>	8.65x10 <sup>-2</sup>	*	-6.56x10 <sup>-1</sup>	-4.40x10 <sup>-2</sup>	2.55x10 <sup>-2</sup>
	5.0	9.91x10 <sup>-1</sup>	6.58x10 <sup>-2</sup>	6.50x10 <sup>-2</sup>	*	-7.53x10 <sup>-1</sup>	-5.93x10 <sup>-2</sup>	4.00x10 <sup>-2</sup>
5x10 <sup>-3</sup>	0.0	6.03x10 <sup>-1</sup>	6.08x10 <sup>-1</sup>	5.94x10 <sup>-1</sup>	2.5	-2.21x10 <sup>-2</sup>	-7.24x10 <sup>-3</sup>	2.84x10 <sup>-2</sup>
	0.1	6.79x10 <sup>-1</sup>	5.41x10 <sup>-1</sup>	5.17x10 <sup>-1</sup>	*	-8.56x10 <sup>-2</sup>	-9.53x10 <sup>-4</sup>	1.29x10 <sup>-2</sup>
	0.2	6.48x10 <sup>-1</sup>	4.83x10 <sup>-1</sup>	4.61x10 <sup>-1</sup>	*	-1.44x10 <sup>-1</sup>	-5.18x10 <sup>-3</sup>	2.43x10 <sup>-2</sup>
	0.5	4.83x10 <sup>-1</sup>	2.90x10 <sup>-1</sup>	3.15x10 <sup>-1</sup>	*	-2.94x10 <sup>-1</sup>	-8.09x10 <sup>-3</sup>	7.65x10 <sup>-3</sup>
	1.0	4.48x10 <sup>-1</sup>	1.98x10 <sup>-1</sup>	1.97x10 <sup>-1</sup>	*	-4.61x10 <sup>-1</sup>	-4.05x10 <sup>-2</sup>	1.08x10 <sup>-2</sup>
	2.0	4.62x10 <sup>-1</sup>	1.11x10 <sup>-1</sup>	1.05x10 <sup>-1</sup>	*	-6.60x10 <sup>-1</sup>	-3.12x10 <sup>-2</sup>	8.40x10 <sup>-3</sup>
	5.0	1.04	7.08x10 <sup>-2</sup>	6.60x10 <sup>-2</sup>	*	-7.54x10 <sup>-1</sup>	-4.38x10 <sup>-2</sup>	7.71x10 <sup>-3</sup>
10 <sup>-2</sup>	0.0	6.04x10 <sup>-1</sup>	6.16x10 <sup>-1</sup>	5.92x10 <sup>-1</sup>	4.0	4.37x10 <sup>-3</sup>	-2.86x10 <sup>-2</sup>	2.32x10 <sup>-2</sup>
	0.1	6.72x10 <sup>-1</sup>	5.72x10 <sup>-1</sup>	5.49x10 <sup>-1</sup>	3.2	-9.12x10 <sup>-2</sup>	-3.18x10 <sup>-2</sup>	1.88x10 <sup>-2</sup>

\* Value not computed

Table 2. Continued

$\Gamma$ (TS <sup>-2</sup> )	$K_x$ (TS <sup>-1</sup> )	$\langle u^2 \rangle$ (LS <sup>2</sup> /TS <sup>2</sup> )	$\langle v^2 \rangle$ (LS <sup>2</sup> /TS <sup>2</sup> )	$\langle w^2 \rangle$ (LS <sup>2</sup> /TS <sup>2</sup> )	T (TS)	$\rho_{uw}$	$\rho_{vw}$	$\rho_{zw}$
10 <sup>-2</sup>	0.2	6.57x10 <sup>-1</sup>	5.36x10 <sup>-1</sup>	5.32x10 <sup>-1</sup>	3.4	-1.31x10 <sup>-1</sup>	-3.72x10 <sup>-3</sup>	1.88x10 <sup>-3</sup>
	0.5	5.75x10 <sup>-1</sup>	3.73x10 <sup>-1</sup>	3.75x10 <sup>-1</sup>	3.0	-3.42x10 <sup>-1</sup>	-6.31x10 <sup>-3</sup>	3.17x10 <sup>-3</sup>
	1.0	5.88x10 <sup>-1</sup>	2.53x10 <sup>-1</sup>	2.57x10 <sup>-1</sup>	2.9	-6.03x10 <sup>-1</sup>	2.56x10 <sup>-2</sup>	2.57x10 <sup>-2</sup>
	2.0	6.17x10 <sup>-1</sup>	1.64x10 <sup>-1</sup>	1.51x10 <sup>-1</sup>	2.9	-6.69x10 <sup>-1</sup>	-3.62x10 <sup>-2</sup>	4.26x10 <sup>-3</sup>
	5.0	1.39	8.52x10 <sup>-2</sup>	8.64x10 <sup>-2</sup>	2.1	-7.70x10 <sup>-1</sup>	-4.76x10 <sup>-2</sup>	2.05x10 <sup>-3</sup>
2x10 <sup>-2</sup>	0.0	6.01x10 <sup>-1</sup>	6.06x10 <sup>-1</sup>	5.70x10 <sup>-1</sup>	*	-2.70x10 <sup>-2</sup>	-1.06x10 <sup>-2</sup>	3.79x10 <sup>-3</sup>
	0.1	6.55x10 <sup>-1</sup>	5.83x10 <sup>-1</sup>	5.63x10 <sup>-1</sup>	*	-9.78x10 <sup>-2</sup>	-3.73x10 <sup>-2</sup>	9.41x10 <sup>-3</sup>
	0.2	6.75x10 <sup>-1</sup>	5.67x10 <sup>-1</sup>	5.51x10 <sup>-1</sup>	*	-1.41x10 <sup>-1</sup>	-1.44x10 <sup>-2</sup>	-6.63x10 <sup>-4</sup>
	0.5	6.67x10 <sup>-1</sup>	4.81x10 <sup>-1</sup>	4.68x10 <sup>-1</sup>	*	-2.68x10 <sup>-1</sup>	-8.38x10 <sup>-3</sup>	-2.73x10 <sup>-4</sup>
	1.0	6.07x10 <sup>-1</sup>	3.22x10 <sup>-1</sup>	2.90x10 <sup>-1</sup>	*	-4.43x10 <sup>-1</sup>	1.25x10 <sup>-2</sup>	-9.50x10 <sup>-4</sup>
	2.0	7.89x10 <sup>-1</sup>	1.89x10 <sup>-1</sup>	1.94x10 <sup>-1</sup>	*	-6.52x10 <sup>-1</sup>	-1.50x10 <sup>-2</sup>	-4.49x10 <sup>-3</sup>
	5.0	1.74	1.04x10 <sup>-1</sup>	1.04x10 <sup>-1</sup>	*	-7.66x10 <sup>-1</sup>	-4.71x10 <sup>-2</sup>	-6.27x10 <sup>-3</sup>
5x10 <sup>-2</sup>	1.0	7.89x10 <sup>-1</sup>	4.03x10 <sup>-1</sup>	3.65x10 <sup>-1</sup>	*	-4.68x10 <sup>-1</sup>	1.76x10 <sup>-2</sup>	-6.98x10 <sup>-3</sup>
10 <sup>-1</sup>	1.0	8.57x10 <sup>-1</sup>	4.68x10 <sup>-1</sup>	4.35x10 <sup>-1</sup>	*	-4.78x10 <sup>-1</sup>	-4.33x10 <sup>-2</sup>	-1.80x10 <sup>-2</sup>
-10 <sup>-4</sup>	0.0	6.04x10 <sup>-1</sup>	6.17x10 <sup>-1</sup>	5.99x10 <sup>-1</sup>	*	1.65x10 <sup>-2</sup>	-2.18x10 <sup>-2</sup>	6.95x10 <sup>-2</sup>
-10 <sup>-2</sup>	1.0	8.80x10 <sup>1</sup>	6.37x10 <sup>-1</sup>	8.91x10 <sup>1</sup>	*	-9.75x10 <sup>-1</sup>	-1.61x10 <sup>-2</sup>	9.87x10 <sup>-1</sup>

term in the particle turbulent energy balance. It appears that the observed cross products are no larger than the statistical error (indicated by the value at  $\Gamma = 0$ ) for moderate  $\Gamma$  but take on (statistically) significant negative values for larger  $\Gamma$ . These negative values would indicate that the buoyancy model is acting as a source of energy at these larger values of  $\Gamma$ , through the mathematics of the simulation. This unrealistic behavior is apparently the consequence of the model assumption that  $\rho'/\rho_0 \ll 1$  (or,  $\Gamma \ll g\Delta X_3$ ) and permits a fairly accurate estimate to be made on the upper limit to (physically reasonable) values for  $\Gamma$ . It appeared that potential temperature gradients of up to about  $0.02$  (time scales)<sup>-2</sup> could be considered in the simulation.

Shears in the horizontal mean winds again tended to result in mean square displacements varying as the cube of the time for the duration of the observations, but sufficiently stable temperature stratifications seemed ultimately to reduce the diffusion to a lower power law, bringing the displacements closer to an eddy diffusion at those times. Figure 10 illustrates a typical result for the mean square displacements, considering a moderate shear of the x-component of the mean wind ( $K_x = 1.0$  (time scale)<sup>-1</sup>) and a moderately stable temperature stratification ( $\Gamma = 0.01$  (time scale)<sup>-2</sup>). The Lagrangian velocity correlations appeared similar to those observed in the neutrally-stratified case, as shown in Figure 11. In fact, there did not appear to be any well-defined trends in the effects of mean shear and temperature stratification on the Lagrangian integral scale. An average over all of the single fluid point results gave a value of the Lagrangian integral scale of 3.1 Eulerian time scales. The effects of the buoyancy

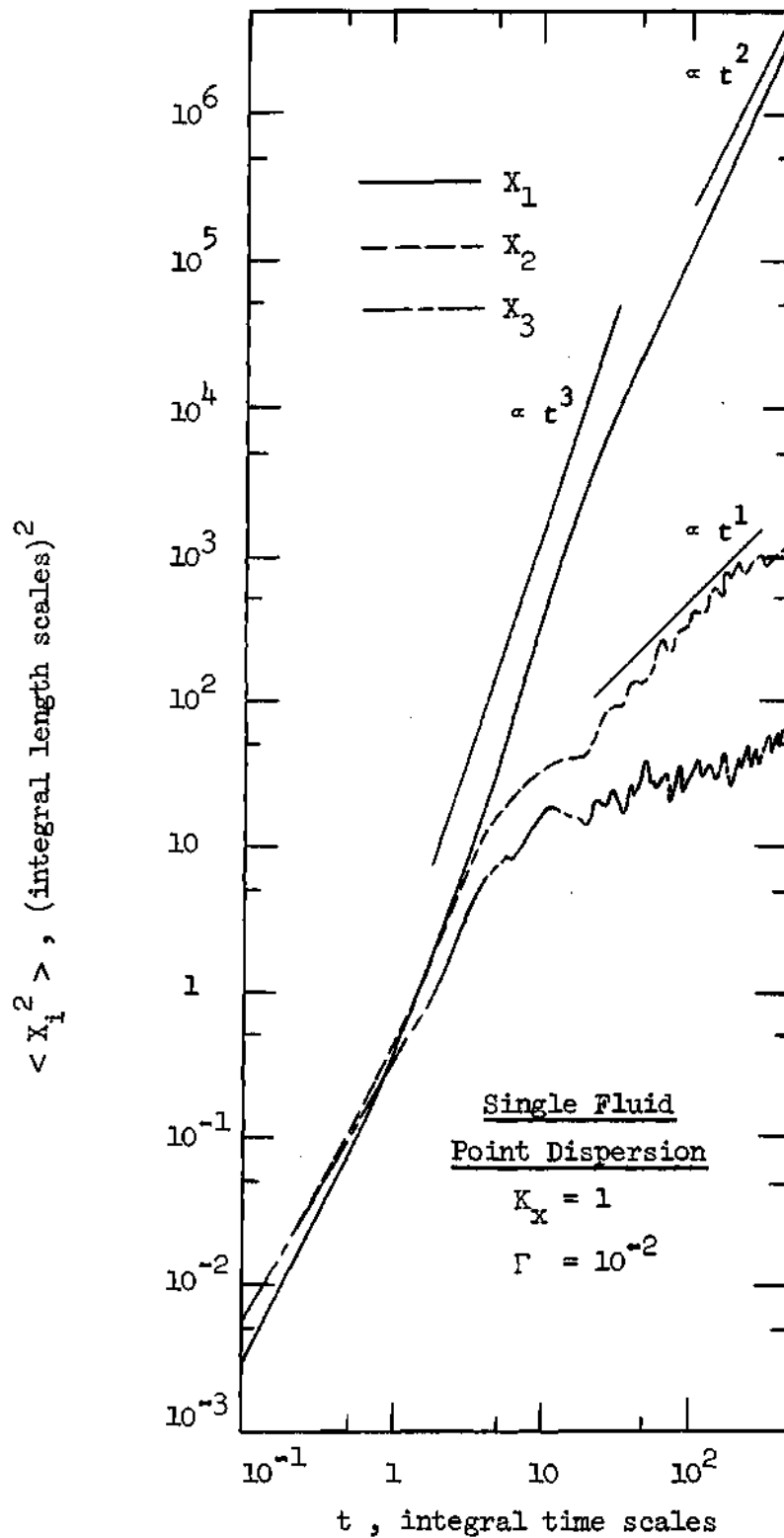


Figure 10. Fluid Point Dispersion Through a Field with Moderate Shear and Stable Temperature Stratification



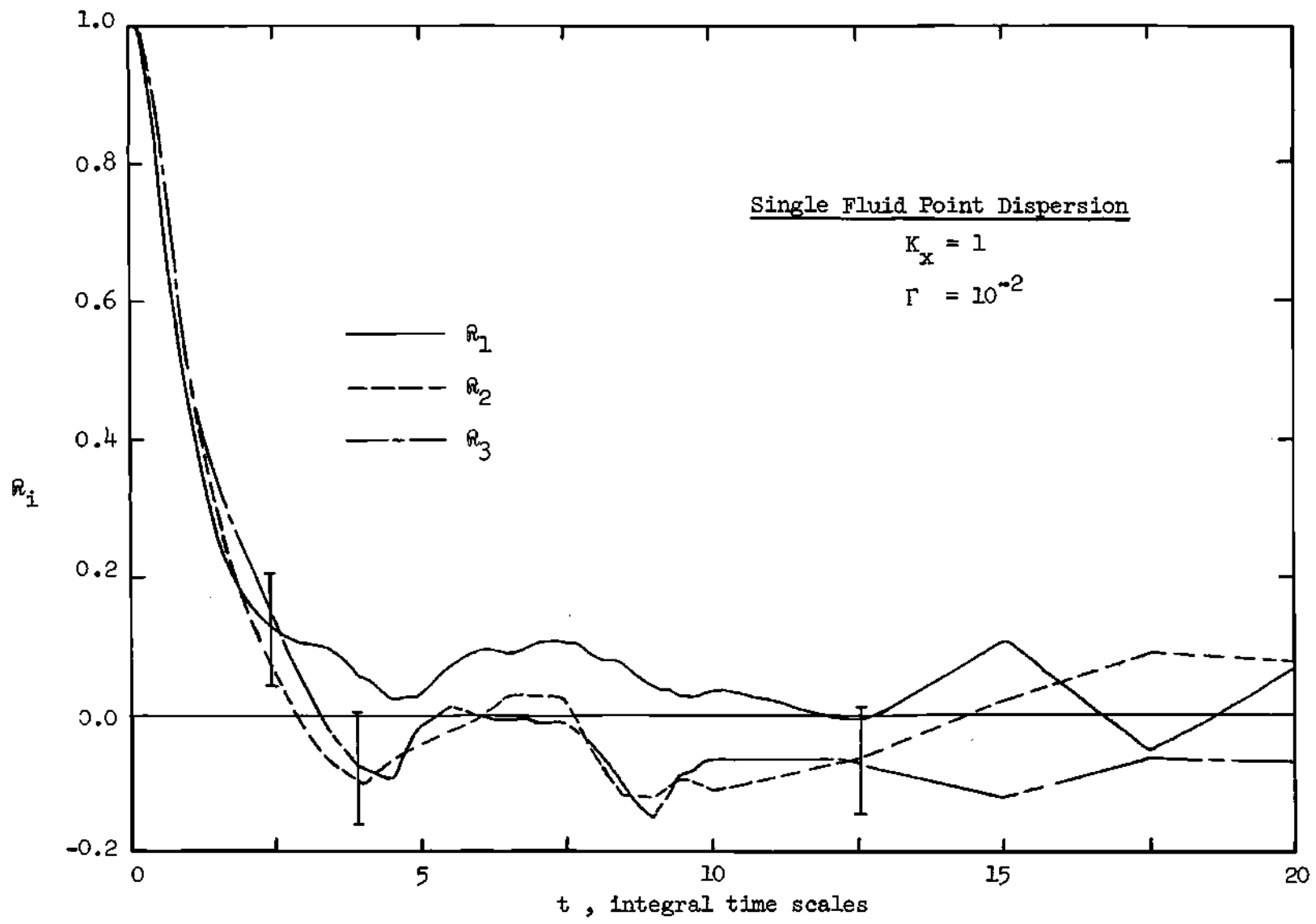


Figure 11. Lagrangian Velocity Time Correlations, Moderate Shear and Temperature Stratification 9

term were evident in the vertical component of the mean square turbulent velocity and appear to result in decreased diffusion in the direction dominated by shear from the  $t^3$  power law toward the eddy diffusion otherwise expected. The observation that the shear-dominated component does not obey any one power law for all intermediate values of  $\Gamma$  seems to be the result of continuous decreases in  $\langle w^2 \rangle$  with increasing stability. The shear-induced dispersion, which appears to obey

$$\langle X_1^2 \rangle \propto \langle w^2 \rangle \left( \frac{d\bar{u}_1}{dz} \right)^2 T_L t^3 \quad (t \rightarrow \infty) \quad (4.8)$$

as discussed previously, and which appears to completely over-shadow the eddy diffusion terms in the case of neutral stability, might decrease and possibly obey no one power law if the vertical velocity  $\langle w^2 \rangle$  were decreased by the use of intermediate values of stability. Slightly more stable temperature stratifications appear to cause a transition at intermediate times (approximately 10 time scales) from the shear-induced dispersion obeying the  $t^3$  power law to a dispersion obeying a  $t^2$  power law, which seems to be the result of the combined effects of mean wind shear and mean square vertical displacement (in contrast with the mean square vertical velocity of the  $t^3$  law). As shown in Figure 12 and Table 1, this dispersion appears to be given by

$$\langle X_1^2(t) \rangle \propto \left( \frac{d\bar{u}_1}{dz} \right) \langle z^2 \rangle_{\infty} t^2 \quad (t \rightarrow \infty) \quad (4.9)$$

where  $\langle z^2 \rangle_{\infty}$  is the value at which the mean square vertical

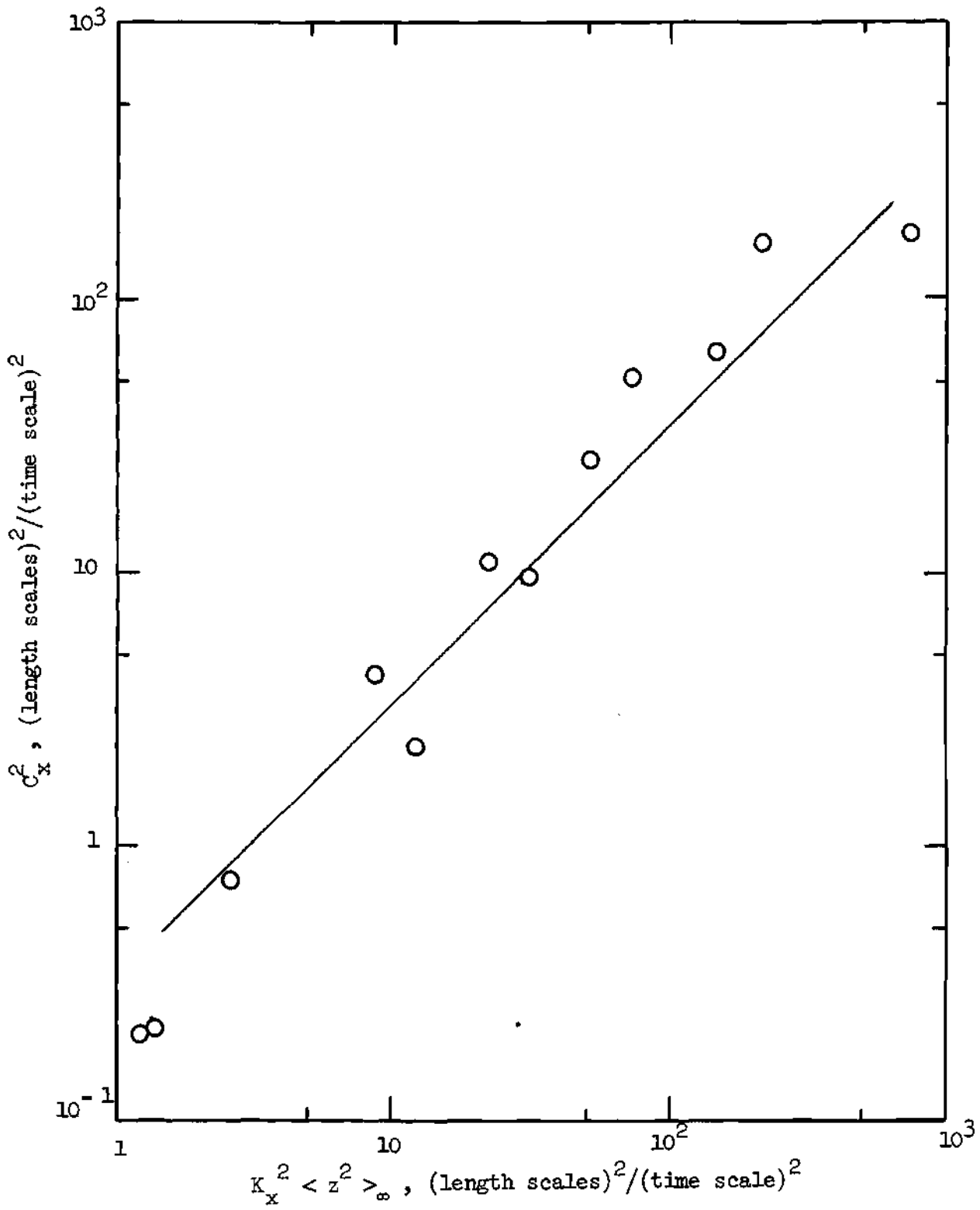


Figure 12. Variation of  $C_x^2$  with Shear

displacement levels off. This effect apparently completely overshadowed the eddy diffusion terms also.

Increasingly strong stable temperature stratifications resulted in the vertical diffusion leveling off at continually smaller mean square values. Quite large values of  $\Gamma$  appeared to result in values of the coefficient  $(d\bar{U}_1/dz)^2 < z^2 >_\infty$  which were sufficiently small that the eddy diffusion was no longer overshadowed. The particle dispersions at long times after release in these cases exhibited a linear variation with time. These cases, however, appeared to lie in the region where the buoyancy acceleration terms began to act as sources in the turbulent energy equations, as evidenced by the increasingly negative values observed for the temperature-velocity cross correlation  $\rho_{zw}$  discussed previously and shown in Table 2. Thus, insufficient information could be gathered here to formulate the results in complete generality.

Unstable Density Stratification ( $\Gamma < 0$ ). Consideration of negative potential temperature gradients resulted in an unstable behavior with respect to the vertical components of the particle displacement and mean square turbulent velocity magnitude. The vertical diffusion, as shown in Figure 13, appeared to be reasonably approximated at long times by an exponential increase, in agreement with Kao [1968].

In cases where a mean wind shear was also considered, the exponential increase in the vertical led to quite vigorous diffusion in the direction dominated by shear, with the mean square particle displacements varying with at least the cube of the time for long times after release.

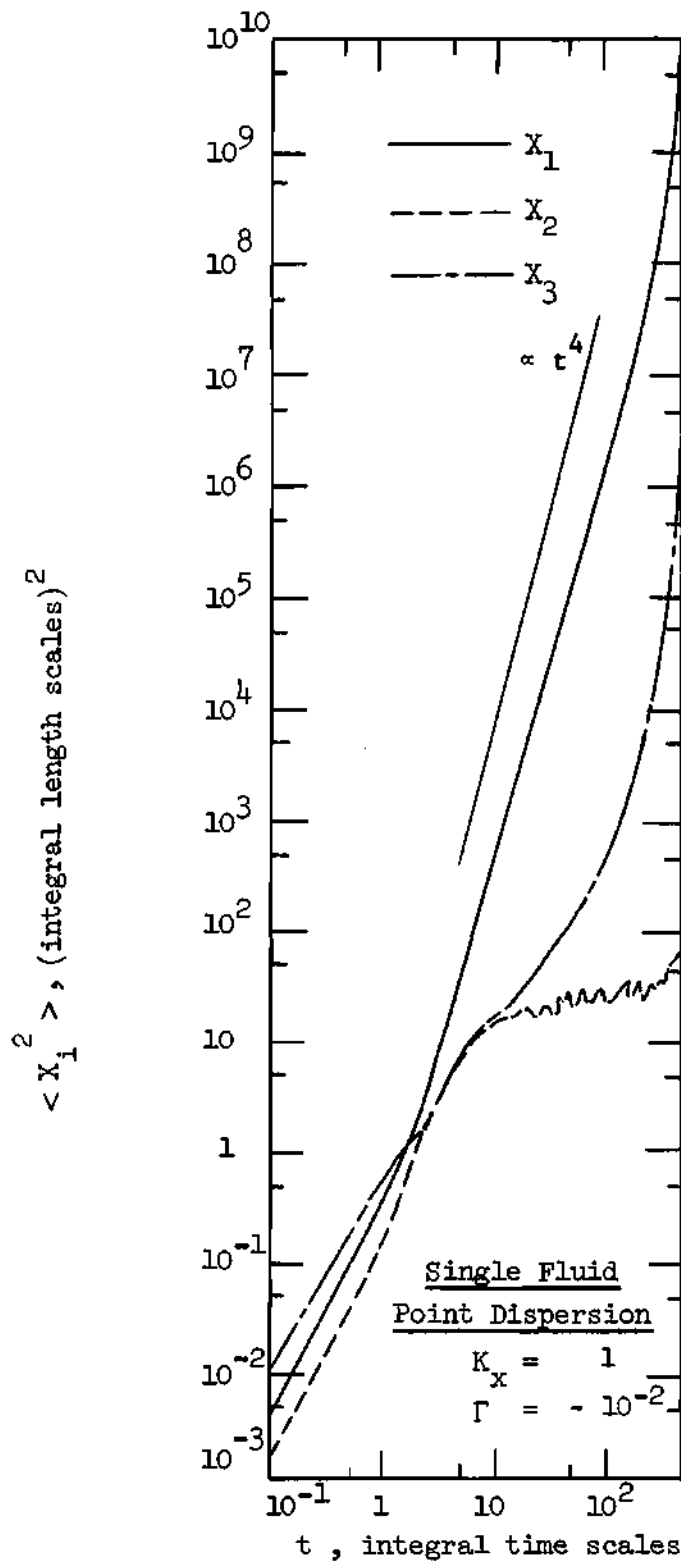


Figure 13. Fluid Point Dispersion Through an Unstably Stratified Field

Analysis Maintaining Explicit Eulerian Correlations Over Two Time Step Increments. No qualitative nor significant quantitative changes were observed in the diffusion when the time interval over which Eulerian acceleration correlations were maintained was increased to two time step increments from the single time step considered in the preceding discussions. Comparison of Figure 10 and 14 illustrates the similarity between the results of the two analyses for a typical set of parameters discussed above, with moderate shear and potential temperature gradient magnitudes. Table 3 illustrates the similarity in the results for the mean square turbulent velocity component magnitudes  $\langle u_i^2 \rangle$  and cross correlations  $\rho_{uw}$ ,  $\rho_{vw}$ , and  $\rho_{zw}$ . Comparison of Figures 11 and 15 illustrates the similarities in the Lagrangian time correlations for the turbulent velocity components of the two analyses. (Figure 15 also illustrates, by the smaller magnitude of the random fluctuations, the effects of including 500 realizations in the averages as compared with only 150 realizations in the other Lagrangian velocity correlation analyses).

These similarities in the two analyses seemed to indicate that the model which maintains Eulerian correlations over one time step simulated the pertinent characteristics of turbulent diffusion as successfully as the model which maintains the correlations over two time steps. Thus, it seemed more desirable to consider more variations in the set of input parameters using one or the other of the two analyses than to consider the same combinations of parameters with both analyses. Preliminary runs indicated that the two time step analysis required

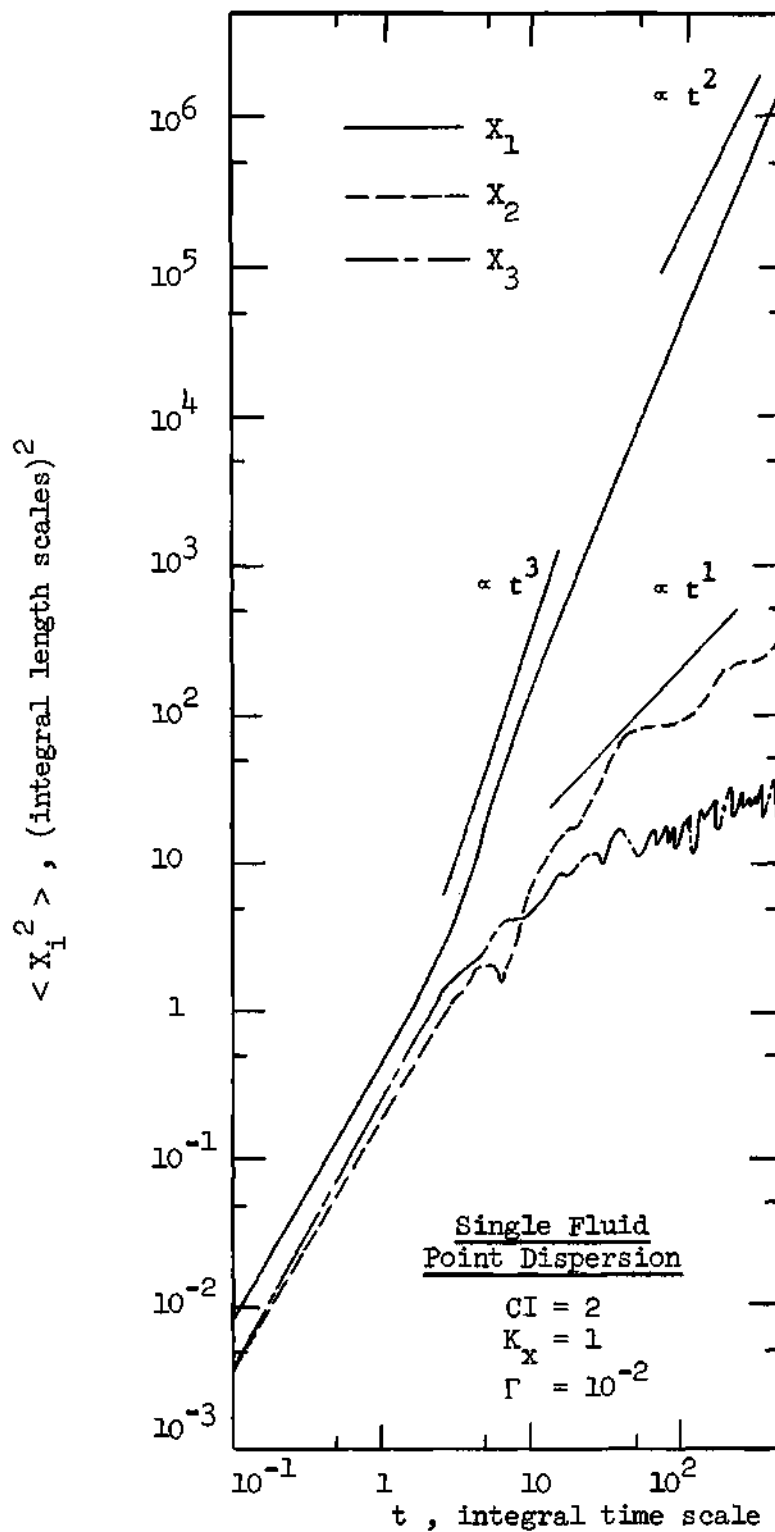


Figure 14. Fluid Point Dispersion Through Field with Moderate Shear and Stable Temperature Stratification, Maintaining Explicit Eulerian Correlations over 2 Time Steps

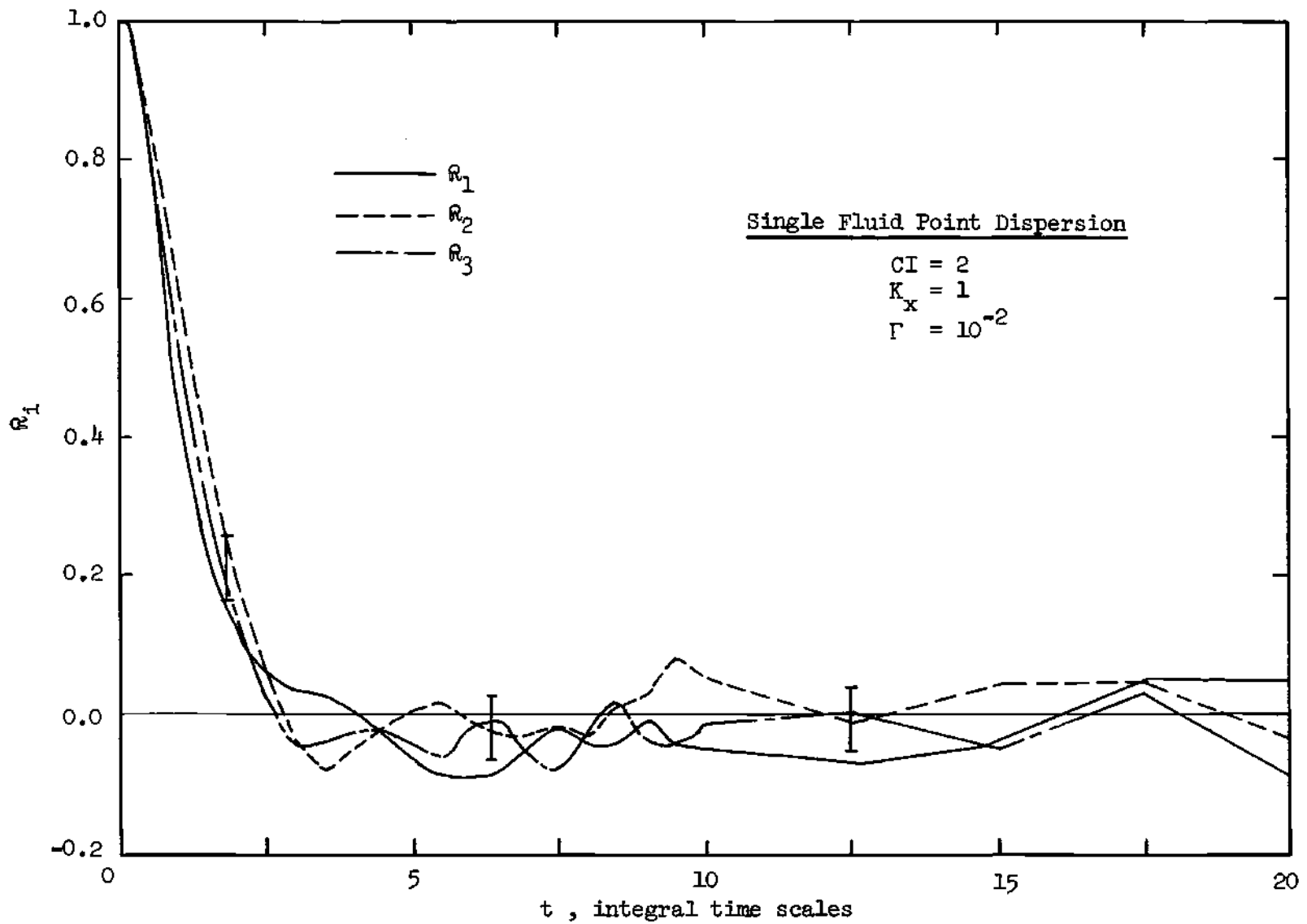


Figure 15. Lagrangian Time Correlations,  $CI = 2$



Table 3. Comparison of the Statistical Characteristics  
of the Diffusion of a Single Fluid Point for  
CI = 1 and CI = 2 ( $\Gamma = 10^{-2}$ ,  $K_x = 1$ )

Statistic	Result for CI = 1	Result for CI = 2
$P_x$	2	2
$C_x^P$	9.5	$1.0 \times 10^1$
$\langle X^2 \rangle_{500}$	$3.1 \times 10^6$	$1.9 \times 10^6$
$D_y$	1.1	$8.6 \times 10^{-1}$
$P_z$	0	0
$C_z^P$	$3.1 \times 10^1$	$2.4 \times 10^1$
$\langle u^2 \rangle$	$5.88 \times 10^{-1}$	$3.33 \times 10^{-1}$
$\langle v^2 \rangle$	$2.53 \times 10^{-1}$	$1.58 \times 10^{-1}$
$\langle w^2 \rangle$	$2.57 \times 10^{-1}$	$1.61 \times 10^{-1}$
$\rho_{uw}$	$-6.03 \times 10^{-1}$	$-3.65 \times 10^{-1}$
$\rho_{vw}$	$2.56 \times 10^{-2}$	$-2.07 \times 10^{-2}$
$\rho_{zw}$	$2.57 \times 10^{-1}$	$1.17 \times 10^{-2}$
T	2.9	2.5

approximately 75% more computing time than the single time step analysis, due to the required increases in storage requirements and numbers of operations. Thus it was deemed advisable to restrict the study to the single step analysis. This reasoning also was a justification for maintaining Eulerian acceleration correlations over only one time step increment in the particle pair analysis.

#### Point Pair Analysis

Several similarities were observed between the results of the single particle and particle pair analyses that were anticipated from physical considerations of the problem. For example, in cases where a uniform mean wind ( $K_x = 0$ ) and neutral density stratification ( $\Gamma = 0$ ) were considered, the space and time scales for transition to eddy diffusion in the particle pair analysis appeared to be the same as the corresponding scales in the single particle analysis and the observed particle separations for the relative dispersion of the two particles were about twice the particle displacements observed at long times in the single particle analysis. This result was anticipated since the two particles would be dispersing quite independently of each other at long times after release.

Other similarities were observed in the behavior of the vertical component of diffusion with variations in the temperature stratification. A "leveling-off" of the relative vertical dispersion was observed for approximately the same moderately stable stratifications which resulted in the inhibition of the vertical diffusion of the single fluid point previously discussed. Another physically reasonable observed characteristic was that the relative pair dispersion leveled off at approximately

twice the mean square single particle value.

Several differences were also anticipated and observed in the results of the two analyses. For example, the correlations between the initial velocity components of the particle pair led to a relatively small value for the relative velocity between the two particles. Thus the effects of a given value for the mean square turbulent velocity magnitude would be lessened in the two particle analysis and were not observed to extend to the space and time scales of the corresponding effects in the single particle analysis. As shown in Figure 16, this early decay of the influence of the initial velocity exposed an intermediate time scale behavior which may have been masked by the initial velocity influence in the single particle analysis and which was characterized by mean square particle separations varying with at least the cube of the time in this intermediate time range after release. This effect is evidently the result of the scale of the acceleration correlations being greater than the scale of the initial velocity effect in these studies. It is not completely clear what relationship this behavior has to the diffusion in an inertial scale of eddies which would follow the Richardson law of dispersion discussed previously, but it is interesting that the conditions necessary for the two phenomena to be observed are quite similar.

There were observed other differences in the results of the two analyses that could not have been anticipated in detail from the results of the single particle analysis. It is here that the justification for considering the two particle analysis actually lay, and it is these differences that form the interesting results of this analysis. The

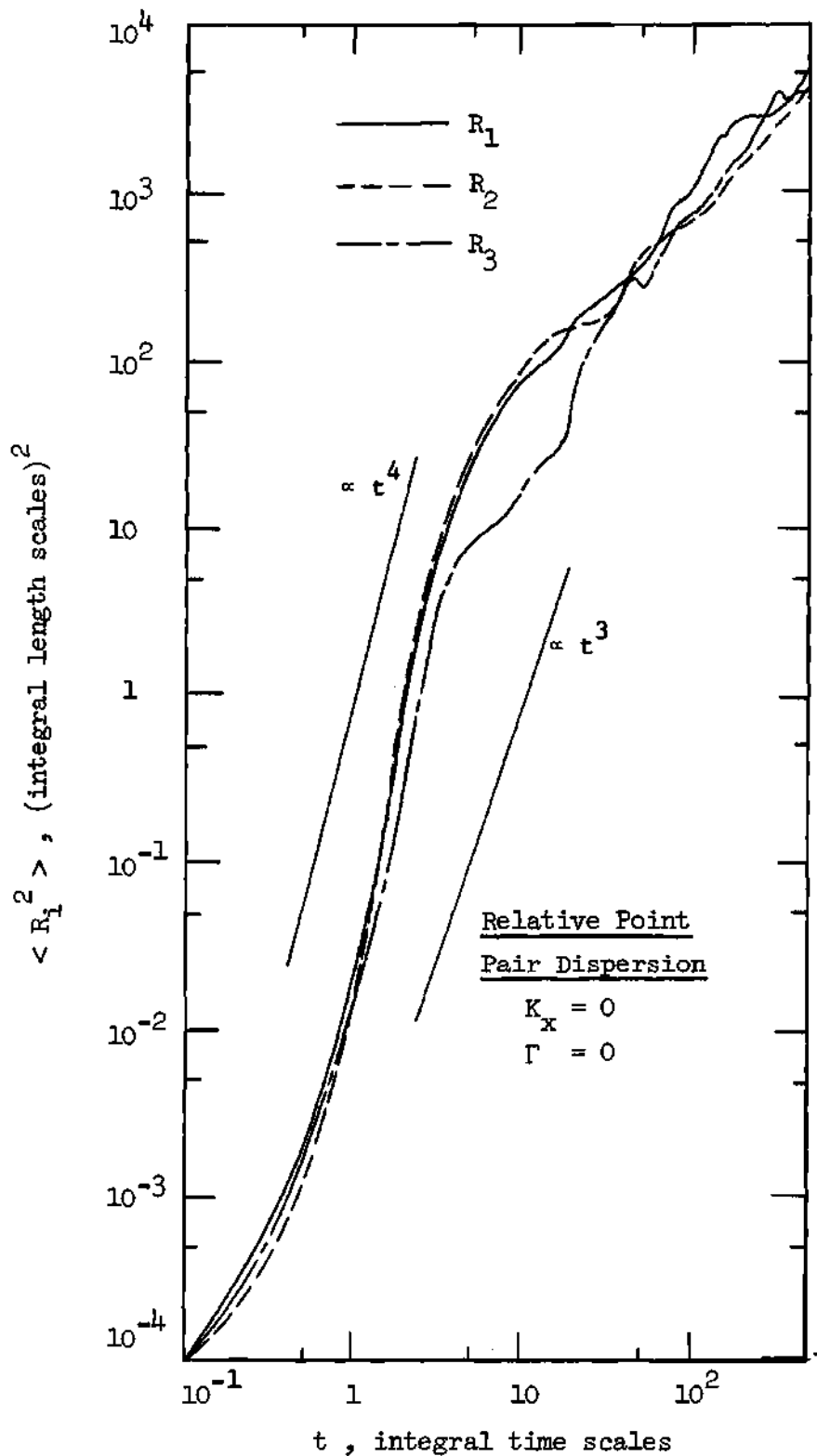


Figure 16. Point Pair Dispersion Through Acceleration Field with Finite Length and Time Correlation Scales

consequences of the lessened effects of the initial particle velocity discussed above might be put in this category. Other differences form the major part of the discussion following.

Neutrally Stratified Atmospheres. Consideration of the relative dispersion of two fluid points as each wandered through a neutrally stratified ( $\Gamma = 0$ ) uniform ( $K_x = 0$ ) field resulted in the mean-square relative particle separation versus time of Figure 16. Note that it is the separation components of the particles relative to their initial separation components that are plotted. Three time intervals with apparently distinct processes are evident in this graph, for each of the separation components. An initial time interval extends to times after release of the order of one-half of the integral time scale, in which is apparent the effects of the initial relative turbulent velocity components. In this interval, the displacements are well approximated by

$$\langle R_i^2(t) \rangle \propto t^2 \quad (4.10)$$

where the constant of proportionality is of the order of  $8 \times 10^{-5}$  for each of the three components. The slight decrease in the constant for the y-component relative to the other two is evidently the result of the initial (longitudinal) correlation in y (the direction of the initial separation vector) being slightly greater than the initial (transverse) correlations in x and z. The major conclusion to be drawn here is that the effects of the initial velocity are (correctly, as discussed above) simulated as having smaller space and time scales in the particle pair analysis than in the single particle analysis.

An intermediate time interval in which effects of the acceleration correlations are clearly felt is evident to times of the order of 5 to 10 integral time scales. The mean square separations vary with at least the cube of the time in this range; but this period is clearly one of transition and the separations do not actually follow any one power law here. The space and time scales of this behavior are similar to those of the Richardson diffusion; here, the particle separations and times are such that the influence of the initial conditions has been lost but the influence of the acceleration correlations is still evident. Particle displacements in an apparent inertial range have been noted by Byzova, et al. [1970] in observations of smoke plumes as having space and time scales in good agreement with those noted here. The particle trajectories in this time range appear to be influenced by both Lagrangian acceleration correlations (tending to result in  $\langle R_1^2(t) \rangle \propto t^4$ ) and a Richardson-type diffusion. The combining of these effects could result in the transition regime observed.

The final phase of particle dispersion is clearly an isotropic eddy diffusion extending from approximately 10 integral time scales to the limit of the time range considered. In this range, the influences of both the initial conditions and the Lagrangian correlations are negligible and the particles are dispersing independently. This is evidenced in the plot of the Lagrangian velocity correlations of Figure 17 and the measured eddy diffusivities of Table 4. There did not appear to be any well-defined influence of mean shear or temperature stratification on the Lagrangian velocity correlations. An average over

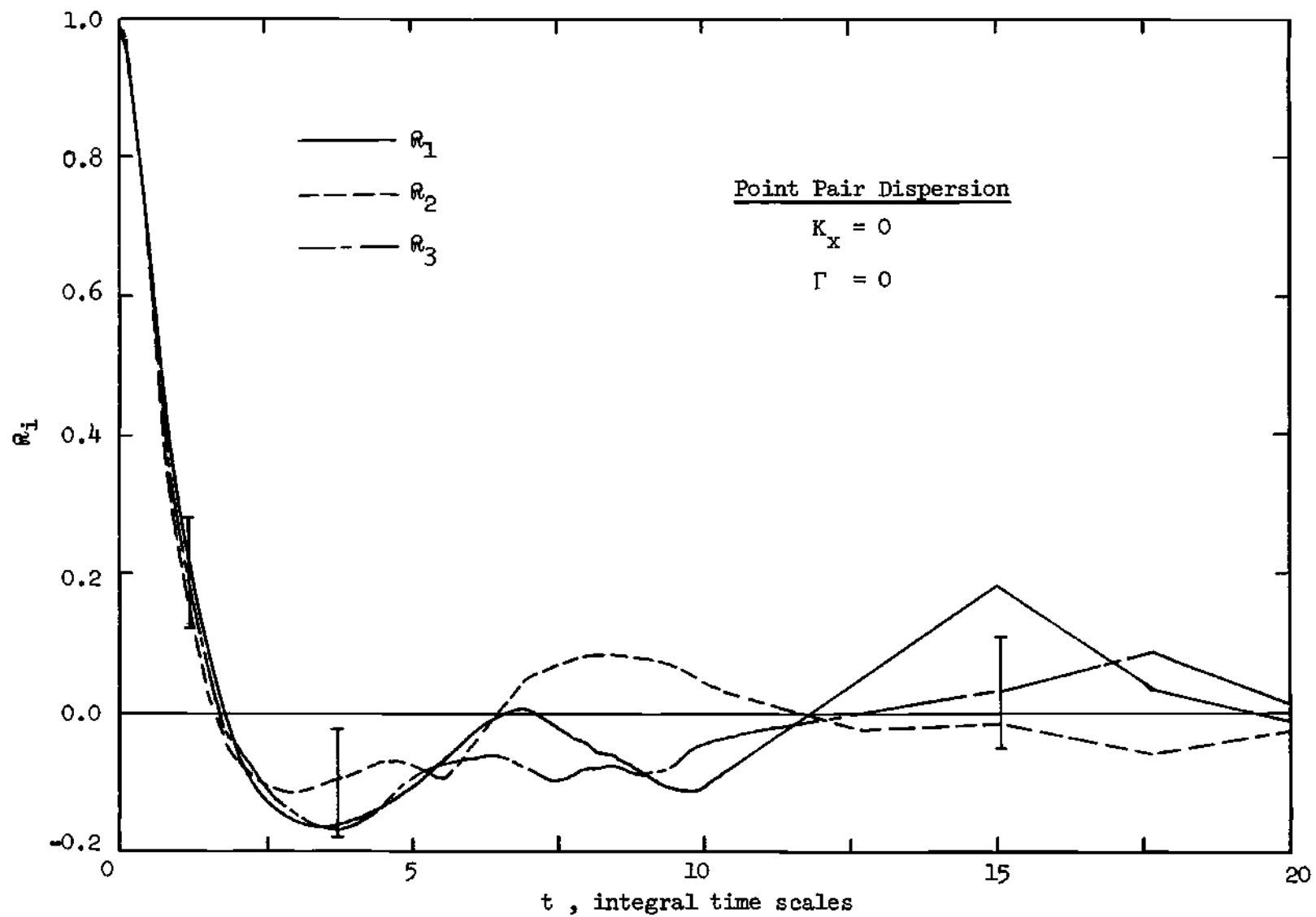


Figure 17. Lagrangian Space-Time Correlations ( $\tau = 0$ )

Table 4. Statistical Properties of the Relative Diffusion of Two Fluid Points

$$(L = 10, TL = 10, \omega = 1, u_I = 0.7, \underline{r}_0 = (0, 1, 0))$$

$\Gamma$ (TS <sup>-2</sup> )	$K_x$ (TS <sup>-1</sup> )	$P_x$	$C_x^P$ (LS <sup>2</sup> /TS <sup>P</sup> )	$\langle R^2 \rangle_{500}$ (LS <sup>2</sup> )	$D_y$ (LS <sup>2</sup> /TS)	$P_z$	$C_x^P$ (LS <sup>2</sup> /TS <sup>P</sup> )
0	0.0	1	$1.0 \times 10^1$	$4.5 \times 10^3$	1.9	1	7.5
	0.1	3	$1.8 \times 10^{-2}$	$3.0 \times 10^6$	2.0	1	8.1
	0.2	3	$4.7 \times 10^{-2}$	$7.6 \times 10^6$	2.5	1	3.5
	0.5	3	$2.3 \times 10^{-2}$	$1.9 \times 10^7$	$4.0 \times 10^{-1}$	1	1.6
	1.0	3	$3.8 \times 10^{-1}$	$3.0 \times 10^7$	$2.2 \times 10^{-1}$	1	$9.0 \times 10^{-1}$
	2.0	3	$8.4 \times 10^{-1}$	$8.1 \times 10^7$	$7.7 \times 10^{-2}$	1	$3.4 \times 10^{-1}$
	5.0	3	4.3	$5.7 \times 10^8$	$1.7 \times 10^{-1}$	1	$6.8 \times 10^{-1}$
$10^{-4}$	1.0	3	$5.0 \times 10^{-1}$	$2.9 \times 10^7$	$2.5 \times 10^{-1}$	1	1.0
$10^{-3}$	0.0	1	8.9	$5.1 \times 10^3$	2.2	1	8.7
	0.1	3	$1.3 \times 10^{-2}$	$1.4 \times 10^6$	2.5	1	5.0
	0.2	3	$3.4 \times 10^{-2}$	$5.0 \times 10^6$	$8.5 \times 10^{-1}$	1	3.4
	0.5	3	$1.1 \times 10^{-1}$	$1.3 \times 10^7$	$3.5 \times 10^{-1}$	1	1.4
	1.0	3	$5.0 \times 10^{-1}$	$2.7 \times 10^7$	$2.5 \times 10^{-1}$	1	$9.0 \times 10^{-1}$
	2.0	3	$9.0 \times 10^{-1}$	$4.4 \times 10^7$	$2.2 \times 10^{-1}$	1	$4.3 \times 10^{-1}$

TS = Integral Time Scales of the Eulerian Acceleration Correlations  
 LS = Integral Length Scales of the Eulerian Acceleration Correlations



Table 4. Continued

$\Gamma$ ( $\text{ms}^{-2}$ )	$K_x$ ( $\text{ms}^{-1}$ )	$P_x$	$C_x^P$ ( $\text{IS}^2/\text{ms}^P$ )	$\langle R^2 \rangle_{500}$ ( $\text{IS}^2$ )	$D_y$ ( $\text{IS}^2/\text{ms}$ )	$P_z$	$C_z^P$ ( $\text{IS}^2/\text{ms}^P$ )
$10^{-3}$	5.0	3	2.3	$2.2 \times 10^8$	$1.2 \times 10^{-1}$	1	$2.2 \times 10^{-1}$
$2 \times 10^{-3}$	0.0	1	7.4	$5.1 \times 10^3$	1.8	1	7.4
	0.1	3	$1.0 \times 10^{-2}$	$1.2 \times 10^6$	2.0	1	4.2
	0.2	3	$3.4 \times 10^{-2}$	$3.6 \times 10^6$	$8.5 \times 10^{-1}$	1	3.4
	0.5	3	$1.0 \times 10^{-1}$	$8.1 \times 10^6$	$8.5 \times 10^{-1}$	1	1.1
	1.0	2	$6.2 \times 10^{-1}$	$1.5 \times 10^7$	$4.5 \times 10^{-1}$	0	$1.1 \times 10^2$
	2.0	2	$1.2 \times 10^2$	$3.7 \times 10^7$	$1.4 \times 10^{-1}$	0	$5.5 \times 10^1$
	5.0	2	$2.0 \times 10^2$	$1.2 \times 10^8$	$9.5 \times 10^{-2}$	0	$4.0 \times 10^1$
$5 \times 10^{-3}$	0.0	1	$1.0 \times 10^1$	$5.7 \times 10^3$	2.5	1	4.0
	0.1	3	$1.8 \times 10^{-2}$	$1.3 \times 10^6$	2.5	1	2.4
	0.2	2	6.8	$1.6 \times 10^6$	2.1	0	$5.0 \times 10^2$
	0.5	2	$1.2 \times 10^1$	$4.7 \times 10^6$	$9.0 \times 10^{-1}$	0	$2.2 \times 10^2$
	1.0	2	$3.9 \times 10^1$	$1.1 \times 10^7$	$3.7 \times 10^{-1}$	0	$7.9 \times 10^1$
	2.0	2	$7.1 \times 10^1$	$2.7 \times 10^7$	$2.1 \times 10^{-1}$	0	$5.8 \times 10^1$
	5.0	2	$1.9 \times 10^2$	$6.8 \times 10^7$	$1.2 \times 10^{-1}$	0	$2.8 \times 10^1$
$10^{-2}$	0.0	1	7.4	$4.6 \times 10^3$	1.8	0	$5.0 \times 10^2$

Table 4. Continued

$\Gamma$ (TS <sup>-2</sup> )	$K_x$ (TS <sup>-1</sup> )	$P_x$	$C_x^P$ (LS <sup>2</sup> /TS <sup>P</sup> )	$\langle R^2 \rangle_{500}$ (LS <sup>2</sup> )	$D_y$ (LS <sup>2</sup> /TS)	$P_z$	$C_z^P$ (LS <sup>2</sup> /TS <sup>P</sup> )
10 <sup>-2</sup>	0.1	2	9.5 x 10 <sup>-1</sup>	1.9 x 10 <sup>5</sup>	2.5	0	4.0 x 10 <sup>2</sup>
	0.2	2	2.5	6.2 x 10 <sup>5</sup>	2.2	0	2.3 x 10 <sup>2</sup>
	0.5	2	9.0	2.2 x 10 <sup>6</sup>	1.2	0	1.4 x 10 <sup>2</sup>
	1.0	2	1.6 x 10 <sup>1</sup>	5.0 x 10 <sup>6</sup>	8.0 x 10 <sup>-1</sup>	0	6.3 x 10 <sup>1</sup>
	2.0	2	6.6 x 10 <sup>1</sup>	1.2 x 10 <sup>7</sup>	3.2 x 10 <sup>-1</sup>	0	3.5 x 10 <sup>1</sup>
	5.0	2	1.2 x 10 <sup>2</sup>	2.5 x 10 <sup>7</sup>	1.2 x 10 <sup>-1</sup>	0	1.5 x 10 <sup>1</sup>
2 x 10 <sup>-2</sup>	0.0	1	9.0	5.7 x 10 <sup>3</sup>	3.5	0	2.9 x 10 <sup>2</sup>
	0.1	2	4.4 x 10 <sup>-1</sup>	5.3 x 10 <sup>4</sup>	2.1	0	1.8 x 10 <sup>2</sup>
	0.2	2	1.6	2.0 x 10 <sup>5</sup>	1.9	0	1.3 x 10 <sup>2</sup>
	0.5	2	4.6	8.6 x 10 <sup>5</sup>	1.7	0	8.3 x 10 <sup>1</sup>
	1.0	2	1.1 x 10 <sup>1</sup>	2.2 x 10 <sup>6</sup>	8.0 x 10 <sup>-1</sup>	0	5.0 x 10 <sup>1</sup>
	2.0	2	3.3 x 10 <sup>1</sup>	5.3 x 10 <sup>6</sup>	4.2 x 10 <sup>-1</sup>	0	2.6 x 10 <sup>1</sup>
	5.0	2	6.3 x 10 <sup>1</sup>	1.4 x 10 <sup>7</sup>	1.6 x 10 <sup>-1</sup>	0	1.2 x 10 <sup>1</sup>
5 x 10 <sup>-2</sup>	1.0	2	4.2	4.4 x 10 <sup>5</sup>	1.6	0	2.5 x 10 <sup>1</sup>
10 <sup>-1</sup>	1.0	2	1.3	1.5 x 10 <sup>5</sup>	1.8	0	1.6 x 10 <sup>1</sup>
- 5 x 10 <sup>3</sup>	0.0	1	7.1	3.8 x 10 <sup>3</sup>	1.8	(exponential)	

all of the point pair results gave a value for the Lagrangian space-time correlation time scale of 2.7 Eulerian time scales.

The inclusion of a small vertical shear of the x-component of the mean wind ( $K_x = 1.0 \text{ (time scales)}^{-1}$ ) in the above analysis has the dramatic effect of replacing the eddy diffusion in the shear-dominated component by a more vigorous dispersion, varying as the cube of the time as shown in Figure 18. This effect has much the same space and time scales as the corresponding effect in the single particle analysis and has the same secondary effect of decreasing slightly the eddy diffusivities in the directions not controlled by shear. The variation of  $C_x^3$ , defined by

$$\langle R_x^2(t) \rangle = C_x^3 t^3 \quad (t \rightarrow \infty) \quad (4.11)$$

with the magnitude of the shear  $d\bar{U}/dx$  is shown in Figure 19 to be well approximated by

$$C_x^3 \propto \langle w^2 \rangle (d\bar{U}/dx)^2 T_L \quad (4.12)$$

as suggested by Deardorff [1970]. This shear-induced behavior was not restricted to intermediate times after release nor was it the result of eddies in any apparent inertial range. The coefficient  $C_x^3$  was not directly related to the viscous dissipation. As in the single particle analysis, relatively large negative values for the velocity cross correlation  $\rho_{uw}$  shown in Table 5, are indicated for increasing shear magnitudes and describe increasingly large contributions to the

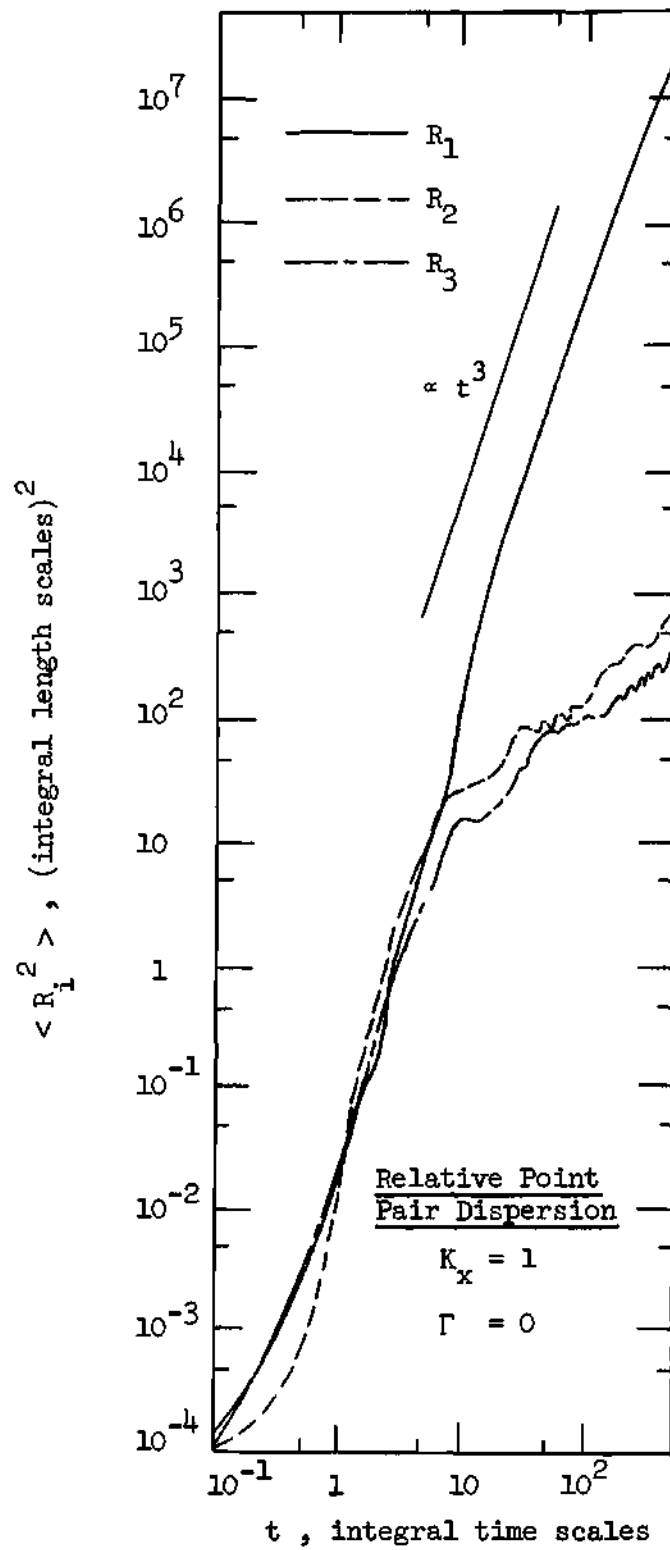


Figure 18. Point Pair Dispersion Through Field with Moderate Shear

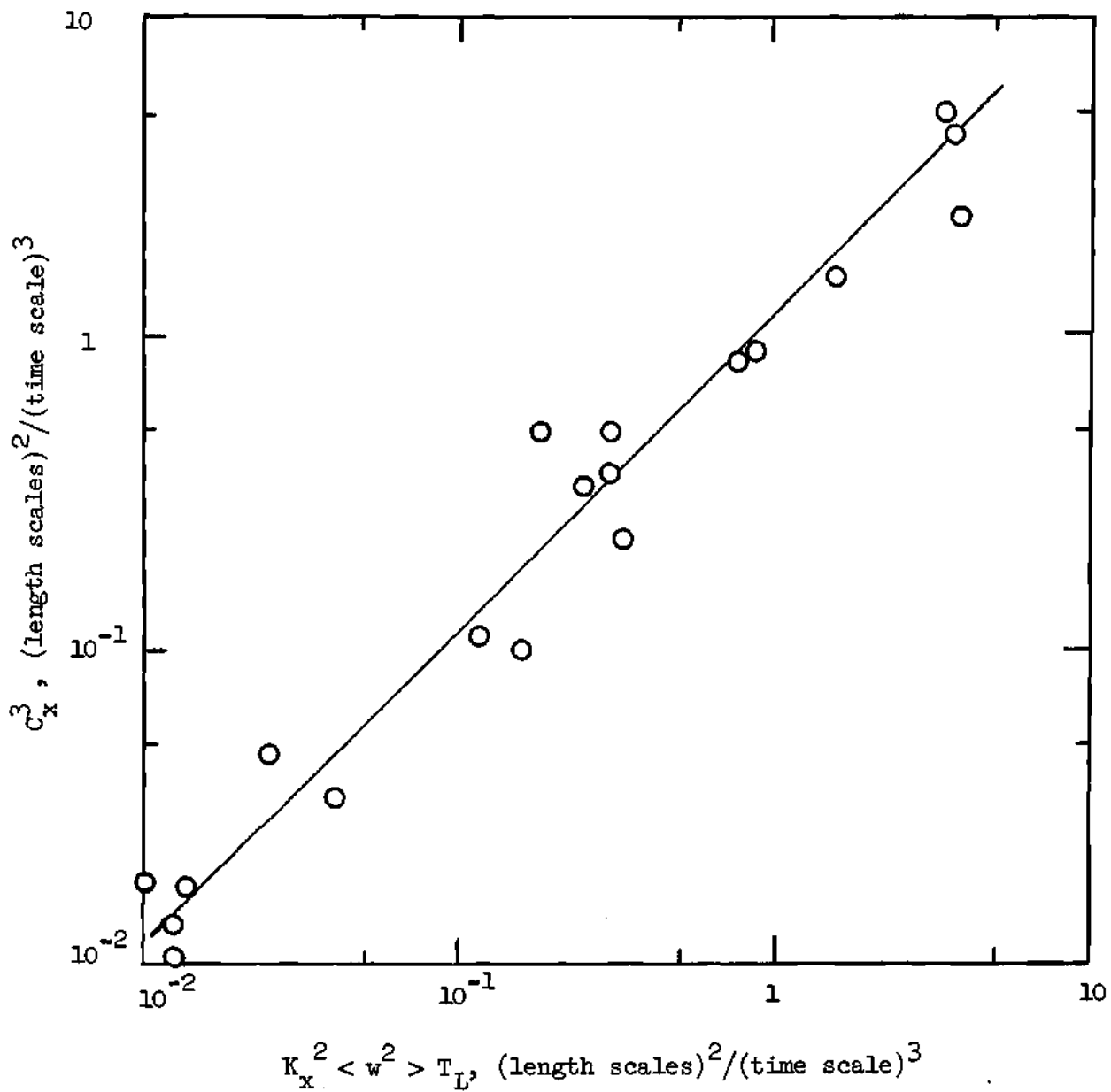


Figure 19. Variation of  $C_x^3$  with Shear, Point Pair Analysis

Table 5. Lagrangian Velocity Characteristics of the Relative Diffusion of Two Fluid Points

(L = 10, TL = 10,  $\omega = 1$ ,  $u_I = 0.7$ ,  $\tilde{r}_0 = (0, 1, 0)$ )

$\Gamma$ (TS <sup>-2</sup> )	$K_x$ (TS <sup>-1</sup> )	$\langle u^2 \rangle$ (IS <sup>2</sup> /TS <sup>2</sup> )	$\langle v^2 \rangle$ (IS <sup>2</sup> /TS <sup>2</sup> )	$\langle w^2 \rangle$ (IS <sup>2</sup> /TS <sup>2</sup> )	T (TS)	$\rho_{uw}$	$\rho_{vw}$	$\rho_{zw}$	
0	0.0	5.92x10 <sup>-1</sup>	5.95x10 <sup>-1</sup>	5.96x10 <sup>-1</sup>	1.6	4.41x10 <sup>-4</sup>	-2.26x10 <sup>-3</sup>	7.52x10 <sup>-2</sup>	
	0.1	6.23x10 <sup>-1</sup>	4.41x10 <sup>-1</sup>	4.51x10 <sup>-1</sup>	1.9	-1.02x10 <sup>-1</sup>	-6.17x10 <sup>-3</sup>	6.64x10 <sup>-2</sup>	
	0.2	5.44x10 <sup>-1</sup>	3.62x10 <sup>-1</sup>	3.62x10 <sup>-1</sup>	1.5	-1.67x10 <sup>-1</sup>	6.72x10 <sup>-3</sup>	6.21x10 <sup>-2</sup>	
	0.5	3.31x10 <sup>-1</sup>	1.73x10 <sup>-1</sup>	1.74x10 <sup>-1</sup>	6.9	-2.72x10 <sup>-1</sup>	-2.65x10 <sup>-2</sup>	4.84x10 <sup>-2</sup>	
	1.0	2.80x10 <sup>-1</sup>	1.28x10 <sup>-1</sup>	1.28x10 <sup>-1</sup>	2.2	-4.61x10 <sup>-1</sup>	2.24x10 <sup>-3</sup>	4.22x10 <sup>-2</sup>	
	2.0	3.24x10 <sup>-1</sup>	7.94x10 <sup>-2</sup>	7.73x10 <sup>-2</sup>	7.0	-6.54x10 <sup>-1</sup>	-2.29x10 <sup>-2</sup>	3.73x10 <sup>-2</sup>	
	5.0	8.66x10 <sup>-1</sup>	6.04x10 <sup>-2</sup>	5.91x10 <sup>-2</sup>	2.9	-7.73x10 <sup>-1</sup>	-1.76x10 <sup>-2</sup>	4.31x10 <sup>-2</sup>	
10 <sup>-4</sup>	1.0	2.22x10 <sup>-1</sup>	9.02x10 <sup>-2</sup>	9.51x10 <sup>-2</sup>	1.7	-6.63x10 <sup>-1</sup>	-1.68x10 <sup>-1</sup>	4.44x10 <sup>-2</sup>	
	10 <sup>-3</sup>	0.0	5.91x10 <sup>-1</sup>	5.92x10 <sup>-1</sup>	5.91x10 <sup>-1</sup>	2.0	2.87x10 <sup>-3</sup>	8.19x10 <sup>-4</sup>	5.24x10 <sup>-2</sup>
		0.1	6.59x10 <sup>-1</sup>	5.03x10 <sup>-1</sup>	5.04x10 <sup>-1</sup>	1.8	-9.40x10 <sup>-2</sup>	-1.20x10 <sup>-2</sup>	5.31x10 <sup>-2</sup>
		0.2	5.58x10 <sup>-1</sup>	3.57x10 <sup>-1</sup>	3.67x10 <sup>-1</sup>	1.5	3.09x10 <sup>-5</sup>	-6.43x10 <sup>-3</sup>	3.96x10 <sup>-2</sup>
		0.5	3.82x10 <sup>-1</sup>	2.05x10 <sup>-1</sup>	2.05x10 <sup>-1</sup>	2.3	5.00x10 <sup>-5</sup>	-1.57x10 <sup>-2</sup>	3.14x10 <sup>-2</sup>
		1.0	2.77x10 <sup>-1</sup>	1.17x10 <sup>-1</sup>	1.19x10 <sup>-1</sup>	2.2	-7.14x10 <sup>-1</sup>	2.05x10 <sup>-2</sup>	2.92x10 <sup>-2</sup>
		2.0	3.30x10 <sup>-1</sup>	8.71x10 <sup>-2</sup>	8.00x10 <sup>-2</sup>	2.4	-6.31x10 <sup>-1</sup>	-3.86x10 <sup>-4</sup>	2.78x10 <sup>-2</sup>
5.0	8.80x10 <sup>-1</sup>	6.33x10 <sup>-2</sup>	6.07x10 <sup>-2</sup>	3.0	-7.70x10 <sup>-1</sup>	1.93x10 <sup>-2</sup>	2.76x10 <sup>-2</sup>		

TS = Integral Time Scales of the Eulerian Acceleration Correlations  
 IS = Integral Length Scales of the Eulerian Acceleration Correlations

Table 5. Continued

$\Gamma$ (TS <sup>-2</sup> )	$K_x$ (TS <sup>-1</sup> )	$\langle u^2 \rangle$ (IS <sup>2</sup> /TS <sup>2</sup> )	$\langle v^2 \rangle$ (IS <sup>2</sup> /TS <sup>2</sup> )	$\langle w^2 \rangle$ (IS <sup>2</sup> /TS <sup>2</sup> )	T (TS)	$\rho_{uw}$	$\rho_{vw}$	$\rho_{zw}$
$2 \times 10^{-3}$	0.0	$5.91 \times 10^{-1}$	$5.92 \times 10^{-1}$	$5.89 \times 10^{-1}$	*	$2.97 \times 10^{-3}$	$1.70 \times 10^{-3}$	$4.14 \times 10^{-2}$
	0.1	$6.72 \times 10^{-1}$	$5.06 \times 10^{-1}$	$5.09 \times 10^{-1}$	*	$-9.08 \times 10^{-2}$	$-1.58 \times 10^{-2}$	$3.72 \times 10^{-2}$
	0.2	$5.94 \times 10^{-1}$	$3.85 \times 10^{-1}$	$3.97 \times 10^{-1}$	*	$-1.45 \times 10^{-1}$	$-6.63 \times 10^{-3}$	$3.19 \times 10^{-2}$
	0.5	$4.59 \times 10^{-1}$	$2.47 \times 10^{-1}$	$2.51 \times 10^{-1}$	*	$-2.84 \times 10^{-1}$	$-7.06 \times 10^{-3}$	$2.99 \times 10^{-2}$
	1.0	$3.39 \times 10^{-1}$	$1.52 \times 10^{-1}$	$1.41 \times 10^{-1}$	*	$-4.46 \times 10^{-1}$	$-3.96 \times 10^{-3}$	$2.40 \times 10^{-2}$
	2.0	$3.74 \times 10^{-1}$	$9.02 \times 10^{-2}$	$9.15 \times 10^{-2}$	*	$-6.53 \times 10^{-1}$	$-2.51 \times 10^{-2}$	$2.18 \times 10^{-2}$
	5.0	$9.42 \times 10^{-1}$	$6.47 \times 10^{-2}$	$6.26 \times 10^{-2}$	*	$-7.83 \times 10^{-1}$	$-2.31 \times 10^{-2}$	$1.93 \times 10^{-2}$
$5 \times 10^{-3}$	0.0	$5.89 \times 10^{-1}$	$5.90 \times 10^{-1}$	$5.80 \times 10^{-1}$	1.6	$1.67 \times 10^{-4}$	$-5.08 \times 10^{-3}$	$4.12 \times 10^{-2}$
	0.1	$6.67 \times 10^{-1}$	$5.44 \times 10^{-1}$	$5.42 \times 10^{-1}$	*	$1.43 \times 10^{-5}$	$-1.69 \times 10^{-2}$	$3.22 \times 10^{-2}$
	0.2	$6.49 \times 10^{-1}$	$4.33 \times 10^{-1}$	$4.48 \times 10^{-1}$	2.9	$-2.30 \times 10^{-5}$	$-2.59 \times 10^{-3}$	$1.88 \times 10^{-2}$
	0.5	$5.22 \times 10^{-1}$	$2.94 \times 10^{-1}$	$3.03 \times 10^{-1}$	*	$-2.78 \times 10^{-1}$	$-6.42 \times 10^{-3}$	$2.30 \times 10^{-2}$
	1.0	$4.17 \times 10^{-1}$	$1.74 \times 10^{-1}$	$1.76 \times 10^{-1}$	*	$-4.47 \times 10^{-1}$	$-2.36 \times 10^{-2}$	$1.48 \times 10^{-2}$
	2.0	$4.26 \times 10^{-1}$	$1.02 \times 10^{-1}$	$1.05 \times 10^{-1}$	*	$-6.72 \times 10^{-1}$	$-1.61 \times 10^{-2}$	$1.75 \times 10^{-2}$
	5.0	1.07	$7.10 \times 10^{-2}$	$6.96 \times 10^{-2}$	*	$-8.07 \times 10^{-1}$	$-3.85 \times 10^{-2}$	$1.82 \times 10^{-2}$

\* Value not computed

Table 5. Continued

$\Gamma$ ( $\text{TS}^{-2}$ )	$K_x$ ( $\text{TS}^{-1}$ )	$\langle u^2 \rangle$ ( $\text{JS}^2/\text{TS}^2$ )	$\langle v^2 \rangle$ ( $\text{IS}^2/\text{TS}^2$ )	$\langle w^2 \rangle$ ( $\text{JS}^2/\text{TS}^2$ )	$T$ ( $\text{TS}$ )	$\rho_{\text{uv}}$	$\rho_{\text{vw}}$	$\rho_{\text{zw}}$
$10^{-2}$	0.0	$5.87 \times 10^{-1}$	$5.89 \times 10^{-1}$	$5.76 \times 10^{-1}$	2.7	$-5.01 \times 10^{-3}$	$-1.65 \times 10^{-3}$	$1.87 \times 10^{-2}$
	0.1	$6.69 \times 10^{-1}$	$5.63 \times 10^{-1}$	$5.55 \times 10^{-1}$	3.5	$-8.86 \times 10^{-2}$	$-8.91 \times 10^{-3}$	$1.20 \times 10^{-2}$
	0.2	$6.87 \times 10^{-1}$	$5.08 \times 10^{-1}$	$5.02 \times 10^{-1}$	2.3	$-1.45 \times 10^{-1}$	$-4.35 \times 10^{-3}$	$1.87 \times 10^{-2}$
	0.5	$5.66 \times 10^{-1}$	$3.47 \times 10^{-1}$	$3.47 \times 10^{-1}$	1.8	$-2.77 \times 10^{-1}$	$-6.14 \times 10^{-3}$	$9.32 \times 10^{-3}$
	1.0	$4.93 \times 10^{-1}$	$2.33 \times 10^{-1}$	$2.28 \times 10^{-1}$	4.0	$-4.52 \times 10^{-1}$	$-1.37 \times 10^{-2}$	$1.28 \times 10^{-2}$
	2.0	$5.25 \times 10^{-1}$	$1.35 \times 10^{-1}$	$1.32 \times 10^{-1}$	2.0	$-6.25 \times 10^{-1}$	$-1.30 \times 10^{-2}$	$7.34 \times 10^{-3}$
	5.0	1.18	$7.67 \times 10^{-2}$	$7.44 \times 10^{-2}$	2.3	$-7.82 \times 10^{-1}$	$-2.00 \times 10^{-2}$	$7.09 \times 10^{-3}$
	0.0	$5.87 \times 10^{-1}$	$5.90 \times 10^{-1}$	$5.62 \times 10^{-1}$	*	$-9.35 \times 10^{-3}$	$-1.09 \times 10^{-2}$	$1.80 \times 10^{-2}$
	0.1	$6.46 \times 10^{-1}$	$5.80 \times 10^{-1}$	$5.59 \times 10^{-1}$	*	$-8.69 \times 10^{-2}$	$-1.14 \times 10^{-2}$	$3.58 \times 10^{-3}$
	0.2	$6.98 \times 10^{-1}$	$5.39 \times 10^{-1}$	$5.20 \times 10^{-1}$	*	$-1.47 \times 10^{-1}$	$-1.01 \times 10^{-2}$	$4.14 \times 10^{-3}$
0.5	$6.72 \times 10^{-1}$	$4.26 \times 10^{-1}$	$4.19 \times 10^{-1}$	*	$-3.00 \times 10^{-1}$	$2.77 \times 10^{-3}$	$7.29 \times 10^{-3}$	
1.0	$6.35 \times 10^{-1}$	$2.89 \times 10^{-1}$	$2.86 \times 10^{-1}$	*	$-4.69 \times 10^{-1}$	$3.15 \times 10^{-2}$	$3.37 \times 10^{-3}$	
2.0	$7.23 \times 10^{-1}$	$1.82 \times 10^{-1}$	$1.76 \times 10^{-1}$	*	$-6.42 \times 10^{-1}$	$3.93 \times 10^{-3}$	$4.39 \times 10^{-3}$	
5.0	1.51	$9.75 \times 10^{-2}$	$9.28 \times 10^{-2}$	*	$-7.72 \times 10^{-1}$	$1.97 \times 10^{-2}$	$2.86 \times 10^{-3}$	
$5 \times 10^{-2}$	1.0	$8.01 \times 10^{-1}$	$4.02 \times 10^{-1}$	$3.71 \times 10^{-1}$	*	$-4.88 \times 10^{-1}$	$-1.34 \times 10^{-2}$	$-9.24 \times 10^{-4}$
$10^{-1}$	1.0	$8.95 \times 10^{-1}$	$4.46 \times 10^{-1}$	$4.19 \times 10^{-1}$	*	$-5.67 \times 10^{-1}$	$3.05 \times 10^{-2}$	$-8.22 \times 10^{-3}$
$-5 \times 10^{-3}$	0.0	$5.84 \times 10^{-1}$	$5.90 \times 10^{-1}$	$6.93 \times 10^{-1}$	*	$-1.25 \times 10^{-2}$	$-2.09 \times 10^{-2}$	$3.67 \times 10^{-1}$



turbulent energy balance by shear production.

Stably Stratified Atmospheres. The effects of stable temperature stratifications ( $\Gamma > 0$ ) on the dispersion of the two particles were very similar to the corresponding effects in the single fluid point analysis. Slightly stable stratifications tended to reduce the vertical eddy diffusivity as shown in Table 4; at moderately large positive values for  $\Gamma$ , the vertical diffusion was completely inhibited and the mean square particle separation "leveled off." The value at which the vertical dispersion leveled off appeared to decrease with increasingly strong stable stratifications, as shown in Table 4. Very large values for  $\Gamma$ , however, led to unrealistic negative values for the cross product  $\langle zw \rangle$ , indicating the buoyancy accelerations were acting as a source of turbulent energy at these values of  $\Gamma$ . As in the single particle analysis, it appeared the buoyancy simulation was invalid for values of  $\Gamma$  much above  $0.03 (\text{time scales})^{-2}$ . Again, this appeared to be the consequence of the model assumption of small density fluctuations becoming unrealistic. Within the range of values for which the buoyancy acceleration model appears valid, the relative vertical dispersion of the two particles levels off at approximately the same stable stratifications as the vertical diffusion of the single particle and at a mean square value about twice the single particle result, as shown by a comparison of Tables 1 and 4.

Consideration of both stable temperature stratifications and vertical shears of the horizontal mean wind led to results that were qualitatively very similar to corresponding results of the single fluid point analysis. As illustrated in Figure 20, mean wind shears

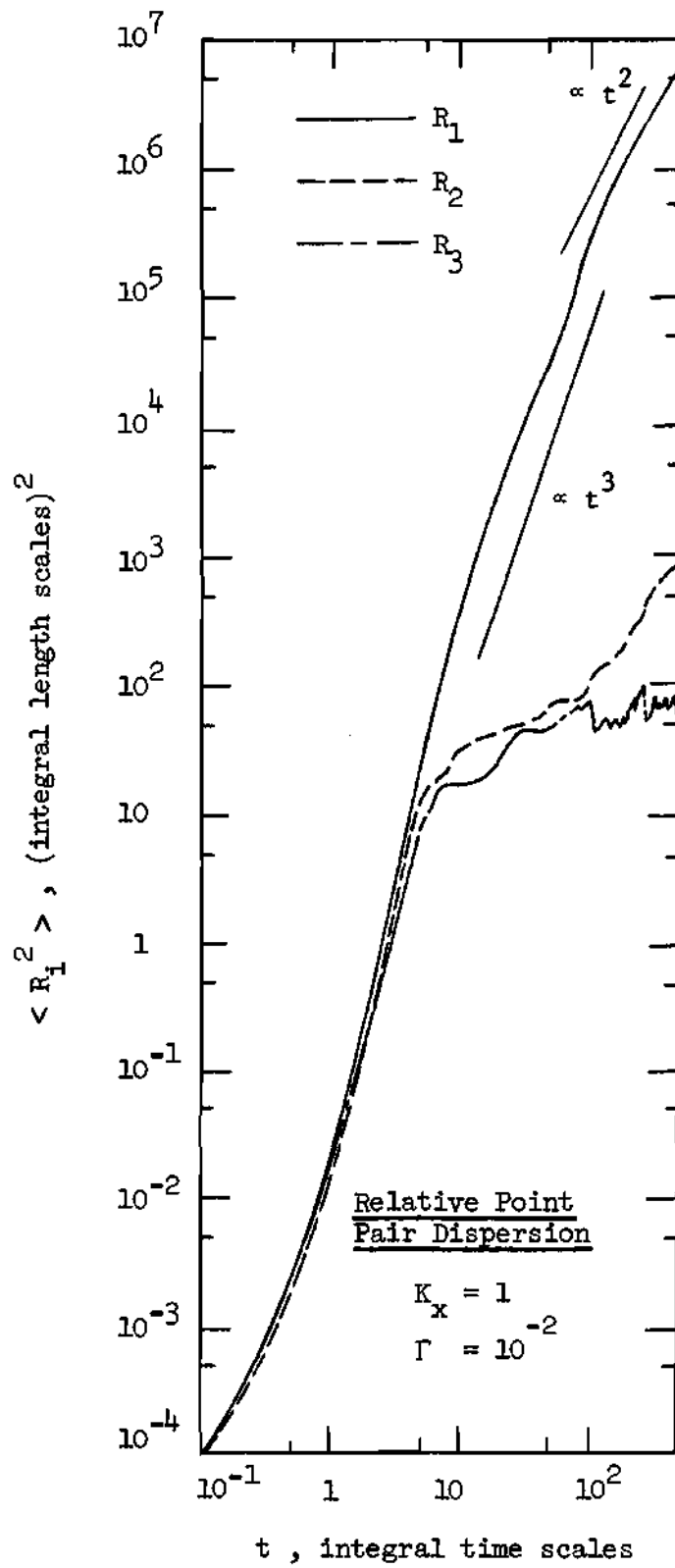


Figure 20. Point Pair Dispersion Through Field with Moderate Shear and Stable Temperature Stratification

tended to cause rapid particle dispersion in the direction controlled by shear at long times after release obeying a  $t^3$  power law (with coefficient  $C_x^3$  given in Table 4 and Figure 19) while increasingly stable temperature stratifications tended to reduce the dispersion back toward the eddy diffusion (linear in time) that would otherwise be expected. Moderately strong stratification tended to result in completely inhibited vertical dispersion and dispersion in the direction controlled by shear obeying

$$\langle R_x^2(t) \rangle \propto \left( \frac{\partial U}{\partial z} \right)^2 \langle z^2 \rangle_\infty t^2 \quad (4.13)$$

as shown in Table 4 and Figure 21. The same space and time scales were observed for this phenomenon in the particle pair and single particle analyses, and the same physical process appeared to be dominating the results.

The effects of varying the initial particle separation  $r_0$  are evident in the short time behavior of cases in which mean shears were considered. In particular, finite initial displacements in the vertical lead to slight increases in the coefficient of the  $t^2$  power law at short times for the component controlled by shear. This effect does not appear to be inconsistent with the relation proposed by Justus [1969],

$$\langle R_x^2(t) \rangle \propto \left( \frac{\partial \bar{U}}{\partial z} \right)^2 (\Delta z_0)^2 t^2 \quad (4.14)$$

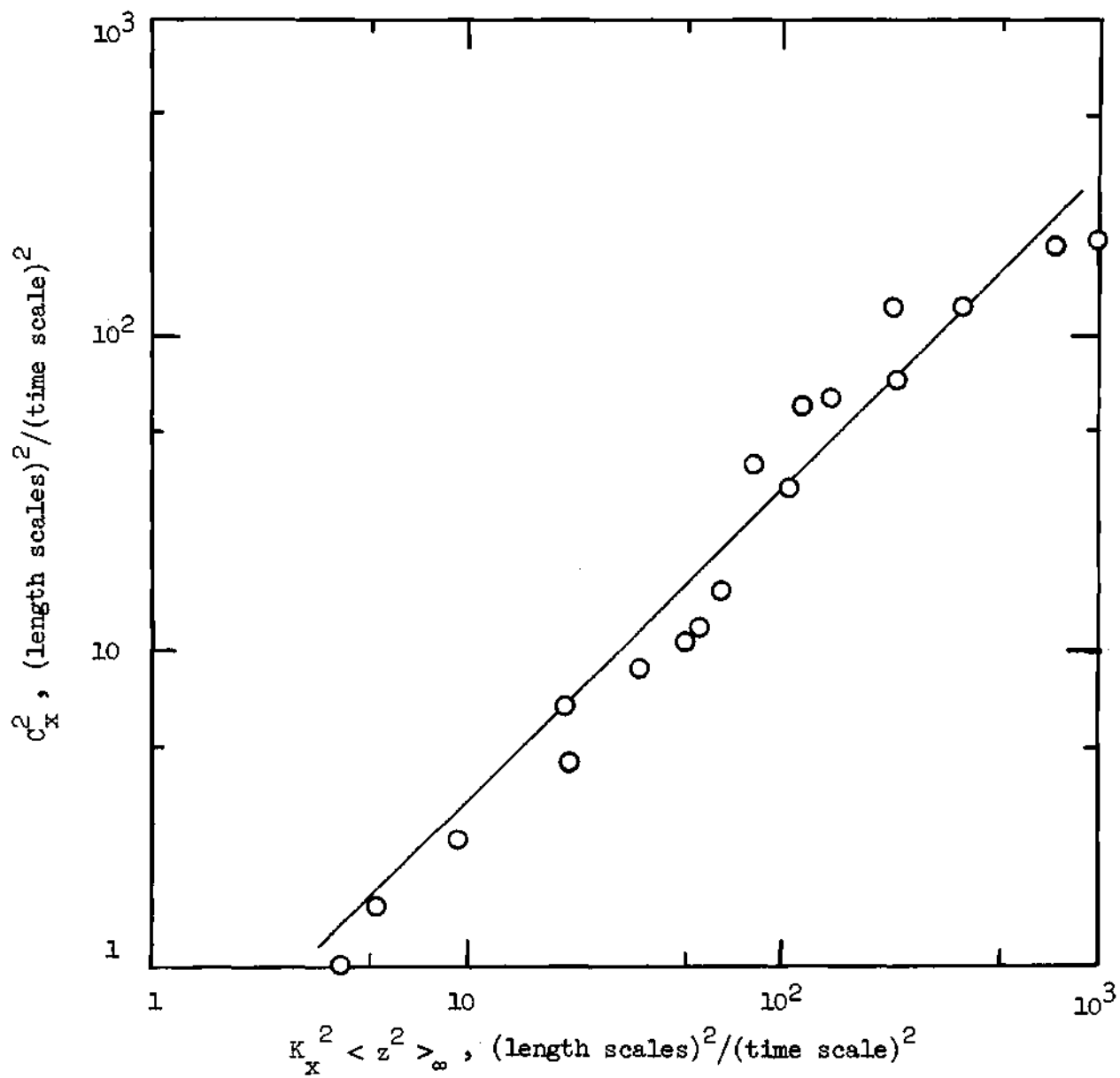


Figure 21. Variation of  $C_x^2$  with Shear, Point Pair Analysis

but is evident only during small times after release (out to approximately one time scale) and appears to be overshadowed by the intermediate time behavior discussed above thereafter, as illustrated by a comparison of Figures 20 and 22.

Unstably Stratified Atmospheres. The consideration of unstable temperature stratifications ( $\Gamma < 0$ ) in the two particle analysis led to results very similar to corresponding results in the single particle analysis. The vertical component of relative point separation appeared to increase rapidly, after an initial period, in an approximately exponential fashion. This increase was also evident in the vertical mean square turbulent velocity. These increases led to very rapid increases in the particle separation components which were controlled by shear.

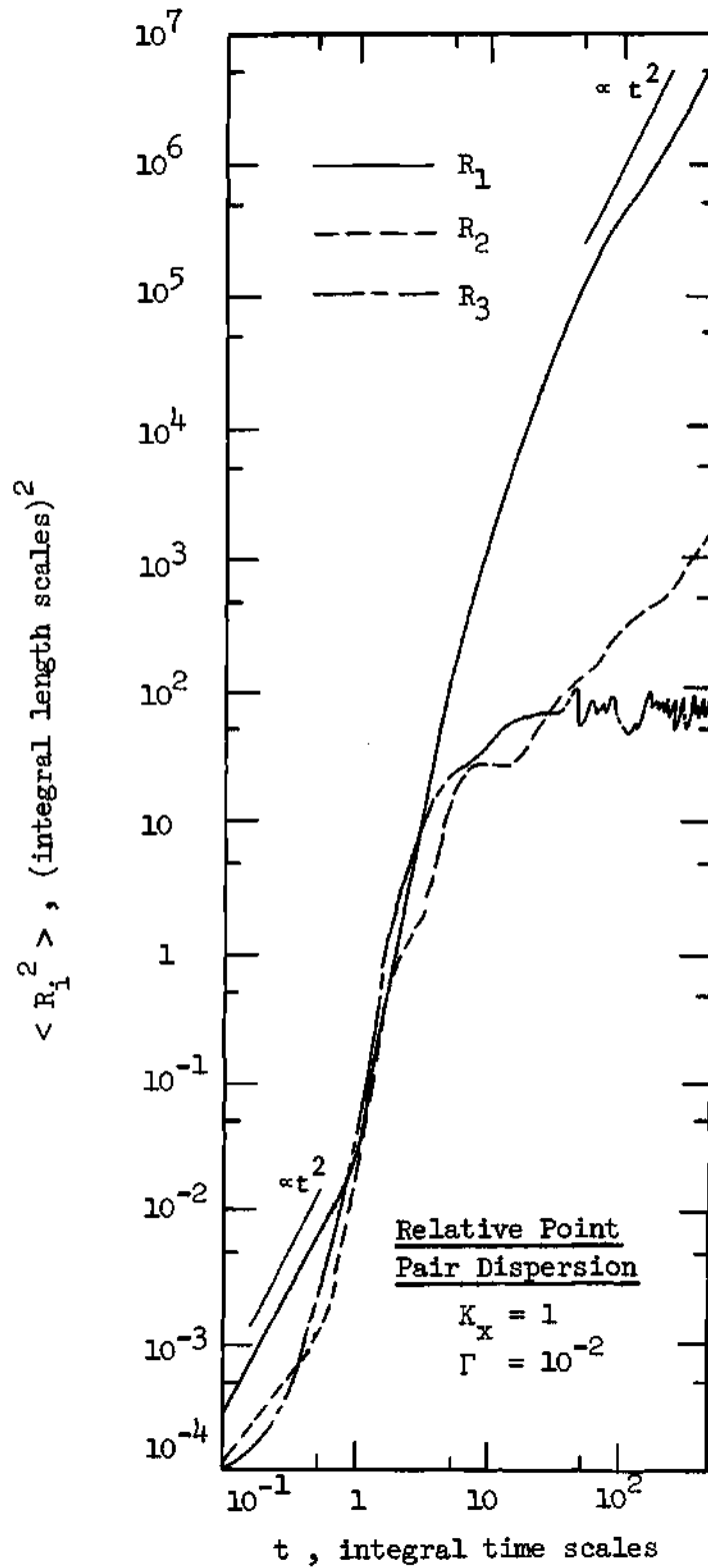


Figure 22. Point Pair Dispersion with Initial Separation in Direction of Shear

## CHAPTER V

## CONCLUSIONS AND RECOMMENDATIONS

The present study was an attempt to determine if a numerical model, based on a random walk process in a background space-time correlated acceleration field, could successfully simulate certain characteristics of atmospheric turbulent diffusion. Various statistical aspects of the resulting particle dispersion have been compared with corresponding features of turbulent diffusion as proposed by previous researchers.

The observed results indicate that the technique successfully simulates nearly incompressible, stably-stratified, shear dependent atmospheric turbulent diffusion and should prove to be a useful tool for studying the dispersal of pollutants in the earth's atmosphere as well as the general problem of the relation between Lagrangian and Eulerian statistics.

Both the short and the long time behavior of the fluid point displacements in a neutrally stratified atmosphere with uniform mean winds were successfully modeled. The turbulent velocity components were observed to have a Lagrangian time correlation scale somewhat greater than the Eulerian acceleration time correlation scale and to be stationary for appropriate choices for the viscous damping parameter and the mean square initial velocity component magnitude. The influence of the

initial conditions did not appear to extend as far in time in the study of the relative dispersal of two fluid points as in the study of the single fluid point, due to the influence of the initial correlation between the two fluid points. An intermediate time transition period was evident in these studies which appeared to be the result of the combination of the influences of Lagrangian acceleration correlations (tending to result in  $\langle R_1^2(t) \rangle \propto t^4$ ) and a Richardson-type diffusion (tending to result in  $\langle R_1^2(t) \rangle \propto t^3$ ).

Mean wind shears tended to increase the diffusion in the direction controlled by shear such that the mean square particle displacements in that direction varied as the cube of the time for times after release longer than the correlation time scale.

Stable temperature stratifications resulted in decreased diffusion in the vertical. Sufficiently stable stratifications were observed to completely inhibit the vertical diffusion and led to a "leveling-off" of the vertical mean square particle displacements at values which decreased with further increases in stability. This buoyancy-induced effect was also evident in the vertical component of the mean square turbulent velocity and appeared to result in decreased diffusion in the direction dominated by shear. Sufficiently stable temperature stratifications appeared to reduce the  $t^3$  dependence of these components back toward the eddy diffusion otherwise expected.

An unstable condition resulted, in which the vertical mean square displacement component increased exponentially, when negative potential temperature gradients were considered.

Thus, the model appears capable of simulating a number of



important aspects of highly anisotropic turbulent diffusion, in spite of the model assumption of an isotropic background acceleration field.

As is usually the case, several interesting possibilities for additional research were suggested by the preliminary results. One of the possibly more important areas where further work might be fruitful is that of modeling the density fluctuation  $\rho'$  of Equation (2.4). The present model includes essentially first order terms in  $\rho'/\rho_0 \ll 1$  and allows only fairly moderate vertical temperature gradients to be considered, as discussed above. A more sophisticated model for these density fluctuations might eliminate the unrealistically negative values for the cross product  $\langle zw \rangle$  observed for larger values of  $\Gamma$ , which again revealed that the buoyancy accelerations were acting as if they were a source of turbulent energy in that region.

Further investigation of the general problem of the turbulent energy balance of the diffusion model should also be interesting and useful. Turbulent energy equations may be derived from the turbulent momentum Equations, (2.28), as

$$\begin{aligned} \frac{D}{Dt} \frac{1}{2} \langle u_i^2 \rangle &= \langle u_i a_i \rangle - K_i \langle u_i u_3 \rangle \\ &\quad - \Gamma_i \langle u_i X_3 \rangle - \omega \langle u_i^2 \rangle \end{aligned} \quad (5.1)$$

where repeated indices do not imply summation. The first term on the

right is the turbulent pressure force term  $-1/\rho_0 \langle u_i \partial p' / \partial x_i \rangle$ .

The remaining terms on the right are the Reynolds stress, the buoyancy term and the viscous dissipation. Stationary turbulent velocity fields would require that the left hand side be zero. It should be straightforward to investigate the balance of the four terms on the right to determine the changes in the relative importances of the various contributions resulting from variations in the several input parameters, and to investigate in more detail the stationarity of the computed turbulent velocity. In this connection, values of  $\omega$  might be found which would improve any observed deviation from stationarity. These studies would also be important in simulating a decaying field of atmospheric turbulence.

Another topic in the area of more detailed simulation of some of the observed features of atmospheric turbulence would be additional research on the effects of more realistic mean wind and potential temperature profiles. These might be matched with observed characteristics of the earth's boundary layer or upper atmosphere.

Also, it would be interesting to see the effects of the inclusion of a Coriolis term in the particle equations of motion and the consideration of the geostrophic wind (which is a result of a balance between mean pressure gradient and Coriolis forces) as the mean wind of the discussion above. The Coriolis effects would become important in the large scale eddy diffusion of the general atmospheric circulation.

## BIBLIOGRAPHY\*

1. Amsden, A. A., and F. H. Harlow, Transport of turbulence in numerical fluid dynamics, Journal of Computational Physics, 3, 94, 1968.
2. Angell, J. K., D. H. Pack, W. H. Hoecker, and N. Delver, Lagrangian-Eulerian time-scale ratios estimated from constant volume balloon flights past a tall tower, Quarterly Journal of the Royal Meteorological Society, 97, 87, 1971.
3. Ball, F. K., Viscous dissipation in the atmosphere, Journal of Meteorology, 18, 553, 1961.
4. Batchelor, G. K., The application of the similarity theory of turbulence to atmospheric diffusion, Quarterly Journal of the Royal Meteorological Society, 76, 133, 1950.
5. Batchelor, G. K., The Theory of Homogeneous Turbulence, Cambridge University Press, London, 103, 1953.
6. Bell, J. R., Algorithm 334, Normal random deviates, Communications of the Association for Computing Machinery, 11, (7), 498, 1968.
7. Brier, G. W., The statistical theory of turbulence and the problem of diffusion in the atmosphere, Journal of Meteorology, 7, 283, 1950.
8. Byzova, N. L., V. N. Ivanov, E. K. Gargh, and Y. S. Osipov, Use of statistical wind characteristics for theoretical and experimental estimation of passive particle diffusion, Journal of Geophysical Research, 75, (18), 3605, 1970.
9. Deardorff, J. W., and R. L. Peskin, Lagrangian statistics from numerically integrated turbulent shear flow, Physics of Fluids, 13, (III), 584, 1970.
10. Dutton, J. A., and G. H. Fichtl, Approximate equations of motion for gases and liquids, Journal of the Atmospheric Sciences, 26, 241, 1969.

---

\* The reference form used herein follows that used by the American Geophysical Union.

11. Einstein, A., On the movement of small particles suspended in a stationary liquid demanded by the molecular-kinetic theory of heat, Annalen der Physik, 17, 549, 1905, reprinted in Investigations on the theory of the Brownian Movement, edited by R. Furth, translated by A. D. Cowper, Dover, New York, 1956.
12. Harlow, F. H., and A. A. Amsden, Numerical calculation of almost incompressible flow, Journal of Computational Physics, 3, 80, 1968.
13. Harlow, F. H., and P. Nakayama, Simulating fluid turbulence, Science Journal, 3, 74, 1967.
14. Hay, J. S., and F. Pasquill, Diffusion from a continuous source in relation to the spectrum and scale of turbulence, in Advances in Geophysics, 6, Edited by F. N. Frenkiel and P. A. Sheppard, Academic Press, New York, 345, 1959.
15. Justus, C. G., Dissipation and diffusion by turbulence and irregular winds near 100 km, Journal of the Atmospheric Sciences, 26, 1137, 1969.
16. Kao, S. K., Relative dispersion of particles in a stratified rotating atmosphere, Journal of the Atmospheric Sciences, 25, 481, 1968.
17. Knapp, A. W., Connection between Brownian motion and potential theory, The Journal of Mathematical Analysis and Applications, 12, (2), 328, 1965.
18. Kolmogorov, A. N., The local structure of turbulence on incompressible viscous fluid for very large Reynolds numbers, Comptes Rendus, Academy of Science, U.S.S.R., 30, 301, 1941.
19. Kraichnan, R. H., Diffusion by a random velocity field, Physics Fluids, 13 (I), 22, 1970.
20. Lilly, D. K., The representation of small-scale turbulence in numerical simulation experiments, Proceedings of the IBM Scientific Computing Machine Symposium on Environmental Sciences, The International Business Machine Corporation, White Plains, New York, 195, 1967.
21. Lin, C. C., On a theory of dispersion by continuous movements, Proceedings of the National Academy of Science, U. S., 46, 566, 1960a.
22. Lin, C. C., On a theory of dispersion by continuous movements, II. Stationary anisotropic processes, Proceedings of the National Academy of Science, U. S., 46, 1147, 1960b.

23. Lumley, J. L., and H. A. Panofsky, The Structure of Atmospheric Turbulence, John Wiley and Sons, New York, 1964.
24. Lumley, J. L., and S. Corrsin, A random walk with both Lagrangian and Eulerian statistics, in Advances in Geophysics, 6, 179, 1959.
25. Patterson, G. S., Jr., and S. Corrsin, Computer experiments on random walks with both Eulerian and Lagrangian statistics, Dynamics of Fluids and Plasmas, 275, 1965.
26. Prandtl, L., Uber die ausgebildete turbulenz, Proceedings of the 2nd International Congress on Applied Mechanics, Zurich, 92, 1926.
27. Richardson, L. F., Atmospheric diffusion shown on a distance-neighbour graph, Proceedings of the Royal Society, (A100), 709, 1926.
28. Riley, J., and S. Corrsin, Simulation and computation of dispersion in turbulent shear flow, Proceedings of a Conference on Air Pollution Meteorology, Raleigh, North Carolina, April, 1971.
29. Taylor, G. I., Diffusion by continuous movements, Proceedings of the London Mathematical Society II, 20, (3), 1, 1920.
30. Thompson, R., Numeric calculation of turbulent diffusion, Quarterly Journal of the Royal Meteorological Society, 97, (411) 93, 1971.
31. von Karman, Th., The fundamentals of the statistical theory of turbulence, Journal of the Aeronautical Sciences, 4, 131, 1937.

## VITA

James Edward Hicks, son of Mr. and Mrs. Frank Jefferson Hicks, was born August 18, 1945 in Atlanta, Georgia. He attended the public schools of Decatur, Georgia and was graduated from Decatur High School in 1963.

In September, 1963, Mr. Hicks entered the Georgia Institute of Technology and received the degree of Bachelor of Aerospace Engineering in June, 1967. Continuing his education there, he received the degree Master of Science in Aerospace Engineering in June, 1969.

He married the former Juanita Elizabeth Norman of Decatur in December, 1969.

His publications include:

"Response of Winds in the 90- to 140-km Altitude Region to Variations in Solar Activity," Journal of Geophysical Research, 75, (28), 5560, 1970, (Co-author C. G. Justus).

"Computer Modeled Diffusion in Stratified Shear Turbulence," presented at 52nd Annual Meeting of the American Geophysical Union, Washington, D. C., April, 1971, (Co-author C. G. Justus).

He is a member of the Sigma Gamma Tau, Phi Eta Sigma, Tau Beta Pi and Phi Kappa Phi Honor Societies, and the Sigma Xi professional research society.